Characterization of acid phase anaerobic digestion of municipal sludges to improve biological nutrient removal processes

by

Antonio Albornoz

A thesis

presented to the University of Waterloo

in fulfillment of the

thesis requirement for the degree of

Master of Applied Science

in

Civil Engineering (Water)

Waterloo, Ontario, Canada, 2017

AUTHOR'S DECLARATION

I hereby declare that I am the sole author of this thesis. This is a true copy of the thesis, including any required final revisions, as accepted by my examiners.

I understand that my thesis may be made electronically available to the public.

Abstract

Enhanced biological phosphorus removal (EBPR) can improve the balance sheet for waste water treatment plants. However, for phosphate accumulating organisms (PAOs) to work efficiently, there needs to be a readily biodegradable carbon source as their substrate for growth. Side stream hydrolysis and acid-phase fermentation of the sludge can generate readily available carbon in the form of volatile fatty acids (VFAs). The VFAs are subsequently consumed by PAOs to support the phosphorus removal process. Phosphorus is then recovered from the waste activated sludge using various dewatering and sorting methods.

This study evaluated modeling of side-stream acid-phase digestion of primary sludge to support consistent production of VFAs and thereby stabilize and optimize phosphorus removal processes. In this regard, hydrolysis processes were focused on since they are typically the rate-limiting step in anaerobic digestion. It was found that the literature fails to provide consistent information to aid in the modeling of this process, particularly with regards to the values of the hydrolysis rate constants and the sensitivity of these constants to environmental factors such as temperature, pH, and sludge composition.

An experimental set up consisting of three semi-batch reactors provided data that was subsequently employed in the model evaluation. The reactors were fed with either primary sludge (PS), waste activated sludge (WAS), or a mixture of both (mixed liquor (ML)). The ML set up received 62% PS and 38% WAS by volume. The reactors were fed with sludge from the Elmira WWTP and were operated at an SRT of 6 days. Water quality parameters such as pH, NH_3, COD, SS, TKN, VFA, PO_4 were monitored using standard analytical methods. It was found that adding WAS to PS increased the hydrolysis of PS solids by 19% based on VFA produced by influent Total COD.

BioWin model simulations employed this data to calibrate a baseline model that described the observed VFA production. It was found that traditional anaerobic hydrolysis rate expressions could not describe all data sets consistently. In an effort to improve the universality of the hydrolysis expression, two extensions for the model were considered. The product inhibition extension considered reduced hydrolysis at high VFA concentrations. This model performed well but improved with the second extension regarding enzyme concentration. It was found that including the effect of hydrolytic enzymes in the model can improve the ability of the model to predict results and it is suggested that the follow up research expands in this area to consider more specific enzymes.

Acknowledgements

I would like to thank Dr. Wayne Parker for his patient guidance, support and advice throughout this project. His expertise was the key to understanding and overcoming many of the difficulties I encountered during my research.

I would also like to extend my gratitude to Qirong Dong, Weiwei Du, Daniela Conidi, and the rest of the staff at EnviroSim Associates Ltd for providing timely and accurate software support that was paramount to the modelling portion of this thesis.

I am grateful to Mark Merlau and Mark Sobon, the laboratory technologists at the University of Waterloo, and to undergraduate research assistant Sharon He, for the invaluable help with my experimental set up and their insights for the analytical methods used in this study.

Also, I thank Amy Green and the staff at the writing and communications centre at the University of Waterloo for their editing advice and patience through the revision stages.

I would also like to acknowledge Dr. Peter Huck and Dr. Adil Al-Mayah, from the University of Waterloo Civil and Environmental Engineering Department, for being part of my review committee and second reading this thesis.

Finally, to my family and friends, thank you for sharing this journey with me. You are the source of all inspiration.

Table of contents

List of Figures

List of tables

1. Introduction

Enhanced biological phosphorus removal (EBPR) processes remove phosphorus (P) from wastewater to prevent eutrophication in freshwater systems. These processes can be carried without chemical additives, and the form of removed P can be amenable for recovery technologies as an added value product for the wastewater treatment plant (Barnard et al., 2014). In an EBPR process, phosphate accumulating organisms (PAOs) store P in a two-stage anaerobic-aerobic process. Under anaerobic conditions, PAOs use an internal reserve of polyphosphates as energy to uptake volatile fatty acids (VFA) and store the carbon as poly-B-hydroxy-alkanoates (PHA). Subsequently, in an aerobic environment, the PAOs consume the stored PHAs and uptake intracellular P. PAOs typically accumulate 4 to 8% of dry biomass as P, and in full-scale plants, this process can remove over 85% of P from domestic wastewaters (Gebremariam et al., 2011). The successful operation of EBPR processes is dependent upon the availability of VFAs in the anaerobic stage (Yuan et al., 2011). EBPR systems have been widely accepted and mostly operated empirically to achieve low P effluent levels, but ever since the technology was implemented process instability to achieve consistent treatment has been a critical weakness (Gebremariam et al., 2011).

The availability of VFAs in wastewaters differs between locations and with the time of year depending upon the extent of hydrolysis and fermentation that occurs in the sewer system (Ucisik & Henze, 2008). In systems that have low VFA concentrations in the raw wastewater, fermentation of primary sludge to generate VFAs has been employed to sustain EBPR processes (Banister & Pretorius, 1998). Historically, few studies have researched the acid-phase step of the anaerobic digestion process as most researchers have focused on the production of methane (Elefsiniotis & Oldham, 1994). However, there has been an increased interest in VFA production in the last three decades. The idea of using an activated primary sedimentation tank to build up a fermenting sludge blanket as

VFA source was first proposed by Barnard in 1984. Later on, Maharaj & Elefsiniotis (2001) confirmed sludge fermentation as a feasible way of supplementing VFAs for downstream BNR. Shortly after, Ferreiro & Soto (2003) reported that operation at an SS concentration between 2-6 g/L showed the most VFA production and that the VFA yields produced at 20°C and 35°C were practically the same. Then, Ucisik & Henze (2008) concluded that PS always has a higher VFA yield than WAS, but that WAS could still be a possible source of VFA for BNR processes because of its potential to produce soluble organic matter. Also, Yuan et al., (2011) found the process is inhibited at temperatures lower than 4°C, and with the lack of mixing. Throughout the literature review, the focus has been towards characterizing the kinetics of the hydrolysis process as it is believed to be rate-limiting. The reported hydrolysis rates were found to vary widely depending on various parameters such as temperature, origin, composition, mixing, and residence times. This variability makes it difficult to reliably predict VFA yields via modeling and thus posing challenges to improve EBPR operation and design.

Preceding studies have revealed that the VFA yield in primary sludge anaerobic fermenters is commonly 10% of the total influent COD when six days of fermentation is employed (Banister & Pretorius, 1998) although it has been reported to be as high as 17% (Ristow et al., 2005). Additionally, the composition of VFAs might play a significant role in providing PAOs with a competitive advantage over other biomass. There is a general agreement that acetate and propionate are beneficial for BNR, although there is an ongoing discussion as to whether which acid is superior (Chen et al., 2013; Gebremariam et al., 2011; Thomas et al., 2003).

The outset hypothesis of this project was that the low yields of VFAs might happen due to low concentrations of active fermentative biomass in raw wastewaters. Influent ordinary heterotrophic organisms (OHOs) are commonly low, although reported values range from 7 to 25% of total influent COD (Dold et

al., 2010). Hence, a portion of this study sought to investigate the potential to enhance VFA production from primary sludge by supplementing the feed to the fermenter with waste activated sludge (WAS). The studies by Ucisik & Henze (2008) have shown that fermentation of PS produced a higher amount of VFAs than WAS from the same origin. However, adding WAS to PS might improve the hydrolysis of particulate substrates. Saturating the fermentative biomass in the primary sludge with substrate high in carbohydrates and protein, as well as adding more biomass from WAS might enhance VFA production and process stability via anaerobic fermentation (Chen et al., 2013). In fact, when Ji et al., (2010) mixed PS and WAS at a VSS ratio of 1:1, the VFA yield increased from 85 to 118 mg COD/g VSS, an effective 40% increase in yield.

Prior studies have employed first order reactions to describe the fermentation of primary sludges when fermented on their own (e.g. Banister & Pretorius, 1998). However, the reported range of hydrolysis rate constants is extensive. Ferreiro & Soto (2003) found them to be 0.095 and 0.169 d^{-1} for 20 and 35˚C respectively while Ristow et al., (2005) found it to be of 0.992 d^{-1} at 35˚C. Experimental data from anaerobic digesters was fit to Monod kinetics and surface reaction kinetics (Contois kinetics), but it was found that below an SRT of 8 days the models failed to predict the rates accurately. WAS fermentation has also been fitted to a first-order reaction with hydrolysis constants ranging from 0.11 to 0.17 at ambient temperatures of 20 to 24˚C (Yuan et al., 2011), 0.14 to 0.16 d^{-1} (Pavlostathis & Giraldo-Gomez, 1991), and 0.168 to 0.6 d^{-1} (Ghosh, 1981). Additionally, Pavlosthathis & Giraldo-Gomez (1991) concluded that protein hydrolysis was the rate-limiting step in the anaerobic digestion of organics. Because of the variable nature of these rates, it is challenging to select appropriate rate constants for predictive simulation. Further, few studies have simulated fermenters that received a mixture of PS and WAS. Hence, the role of WAS organisms in model simulations has not yet been elucidated. Therefore, this study aimed to evaluate the performance of existing models of hydrolysis and acidogenic processes in the context of acid phase anaerobic digestion of PS and WAS.

Objectives

Using data collected in bench scale fermentation reactors receiving Primary Sludge (PS), Waste Activated Sludge (WAS) and a mix of PS and WAS (ML) respectively the objectives of the study were to:

1. Characterize sludges obtained from the Elmira WWTP and assess their fermentation to produce VFAs
2. Investigate whether the addition of WAS could improve the fermentability of the Elmira primary sludge
3. Evaluate and enhance models of acid-phase anaerobic digestion to simulate sludge fermentation in support of EBPR processes

Scope

This project investigated acid-phase anaerobic digestion of PS and WAS at ambient temperature in three bench-scale digesters operated for 40-days. The raw and digested sludges were characterized across a range of standard responses including pH, suspended solids, COD, VFA, nitrogen, and phosphorus species and VFA yields were determined for systems operated with PS, WAS and ML as feeds. The data generated from the experimental work was also employed to evaluate the default hydrolysis models within the BioWin simulator. Alternate hydrolysis rate expressions that can describe the digestion results were subsequently evaluated by testing them against the bench-scale data.

2. Literature review

2.1 Biological nutrient removal and anaerobic digestion

Phosphorus (P) removal from wastewater can prevent eutrophication in freshwater systems and recovering P as an added value product can translate into gains for the treatment plant. Conventional treatment methods such as chemical precipitation use iron salts or alum to achieve low effluent phosphorus concentrations in the range of 0.1 to 1.0 mg/l (Metcalf & Eddy, 2003). Iron salts have relatively small cost in comparison to other chemicals, and the sludge it produces has excellent dewatering properties. However, iron is not the most efficient precipitant and can cause corrosion, staining and metal carry over (Yeoman et al., 1988). On the other hand, alum is a better precipitant because it will not release P during recycling, storage, or digestion. Furthermore, alum produces small sludge volumes, no pH adjustment, and can have flexible points of addition and improves clarifier performance. However, alum dosage can be expensive and has been shown to inhibit nitrification in some systems with short sludge age (Yeoman et al., 1988). Overall, the main disadvantage of chemical P removal is the additional cost that the consumption of chemicals represents to the plant's operational budget.

Enhanced biological phosphorus removal (EBPR) processes can remove P from wastewater without chemical additives, and the form of removed P can be amenable for P recovery technologies (Barnard et al., 2014). Rabinowitz & Fries (2010) did a 20-year net present value analysis on the 100 ML/d Pine Creek WWTP (Alberta) that has an EBPR process with a target of <0.3 mg P/L. They found that primary sludge fermentation was 8% cheaper than mechanical primary sludge thickening combined with chemical P removal, and 22% cheaper than gravity thickening of primary and chemical P removal.

In an EBPR process, phosphate accumulating organisms (PAOs) store P in a two-stage anaerobic-aerobic process. PAOs are heterotrophic organisms, and several species have shown phosphate accumulating ability. To date, no microbial isolate exhibiting all the physiological characteristics given to PAOs has been cultured. The different studies that aim to classify PAOs via molecular techniques have found that the proportion of bacterial populations varied with the origin of sludge (Gebremariam et al. 2011).

It has been hypothesized that PAOs are comprised of two main groups, aerobic PAOs (APAO) which use oxygen as the electron acceptor, and denitrifying PAOs, capable of nitrogen reduction and denitrification (Comeau et al., 1986; Hu et al., 2002). When nitrate loading has exceeded the denitrification of OHOs, the PAOs have been found to use nitrate as the electron acceptor and remove P from a system at approximately 80% efficiency when compared to aerobic conditions (Hu et al., 2002).

Various species have been proposed to be responsible for PAO behavior, mainly *b-proteobacteria*-affiliated organisms belonging primarily to the genus *Rhodocyclus* and have been named *Accumulibacter*. They form approximately 20% of the bacterial population and are responsible for 70% of the P-accumulating activity (Gebremariam et al., 2011). Another species also exhibiting PAO behavior is *Actinobacter* where various organisms have been shown to exhibit certain P-accumulating behavior. Due to their many detections both in a laboratory and full-scale analysis, the genus *Tetrashphaera* is also attributed to PAOs (Gebremariam et al., 2011). Last, the *y-proteobacteria* from the genus *Acinetobacter* was assumed as the primary organism responsible for P accumulation; however, it represents less than 10% of the bacterial population and often did not stain positive for polyphosphate; consequently, its role in EBPR systems is still widely debated (Gebremariam et al., 2011). For modeling purposes, PAOs have been lumped together as one putative species with the

ability to store polyphosphate and carbon in anaerobic and aerobic conditions respectively (Comeau et al., 1986).

Under anaerobic conditions, PAOs use an internal reserve of polyphosphates as energy to uptake volatile fatty acids (VFA) and store the carbon as poly-B-hydroxy-alkanoates (PHA). This ability to thrive in anaerobic conditions yields a competitive advantage for the PAOs over other heterotrophs because of the absence of nitrates and oxygen. These conditions also favor some fermentation of readily biodegradable COD (rbCOD) to VFA supporting the process even further. It has been suggested that when the ratio of rbCOD/P in the plant influent is more than 15, acceptable P removal is possible (Barnard et al., 2014). Two primary processes happen in this stage, VFA uptake and phosphate release (Smolders et al., 1995). PAOs uptake VFA via facilitated diffusion across the membrane and store it as an insoluble lipid PHA, the energy to carry on this process comes from the hydrolysis of previously accumulated polyphosphate which causes phosphate release into the medium (Yeoman et al., 1988).

The polyphosphate has been suggested to be a source of energy for both the transport and storage of substrate (Comeau et al.,1986). There is a consensus in the literature that PHA has the chemical composition of poly-B-hydroxybutyrate $(C_4H_6O_2)_n$ or PHB and this is why these two acronyms are used interchangeably in modeling studies (Henze et al., 2000). Meanwhile, the role of the anaerobic zone is to maximize the storage of organic substrates in the bio-p bacteria via minimizing the presence of electron acceptors and optimizing the supply of readily available carbon (Comeau et al.,1986).

Subsequently, in an aerobic environment, the PAOs consume the stored PHAs and uptake intracellular P. Four main processes play a role in this stage: P uptake, PHA consumption, glycogen production and ammonia (NH_3) is used for cell growth (Smolders et al., 1995). In aerobic conditions, the first-order growth kinetics of PAOs are dependent on the PHA content of the cells since it is the only substrate available for growth in these circumstances (Smolders et al., 1995). A

fraction of PHA is used to synthesize new cells while the remainder is used to take up and store P (Wentzel et al., 1989). This uptake has been described in the literature as "luxury uptake" since the previously starved cells (in anaerobic conditions) will uptake more phosphate than is strictly necessary for cell metabolism (Deinema et al., 1980). PAOs typically accumulate 4 to 8% of dry biomass as P, and in full-scale plants, this process can remove over 85% of P from domestic wastewaters (Gebremariam et al. 2011). The maximal reported P content of PAOs is in the range of 0.35 mg P/mg VSS (Smolders et al., 1995).

The main assumptions for PAO growth are:

(1) Polyphosphate provides a unique energy reserve exclusively used by PAOs to take up acetate anaerobically

(2) OHOs are limited to fermentative processes and hence are out-competed by PAOs

(3) the anaerobic-aerobic sequence serves as a unique ecological niche for PAOs (Gebremariam et al., 2011)

EBPR systems have been mostly operated empirically to achieve low P effluent levels, but ever since the technology was implemented process instability has been a critical weakness for achieving consistent and stricter treatment goals (Gebremariam et al., 2011). Most studies that have tried to address this instability have focused on identifying which PAO species play a larger role in EBPR. However, this approach has failed from a practical approach to identify said species and their interactions in this process (Chen et al., 2017; Gebremariam et al., 2011). Therefore, instead of using an isolated and specialized organism, the approach that has been suggested by Gebremariam et al. (2011) is to induce an ecological condition that favors functional richness of the bacterial population. It is however evident that the successful operation of EBPR processes is dependent upon the availability of VFAs in the anaerobic stage since this will drive the PHA concentration and the subsequent P uptake rates (Yuan et al., 2011).

2.2 Acid-phase anaerobic digestion

Conventional treatment processes use anaerobic digestion of organic wastes as an energy-conservative process that produces biogas, reduces sludge generation, and has a simple process configuration (Ferreiro & Soto, 2003). Metcalf & Eddy (2003), describe anaerobic digestion as consisting of four main processes:

1) Hydrolysis of particulate organics into soluble polymers

2) Acidification of these soluble polymers into VFAs

3) Acetogenesis or acetic acid generation from VFAs

4) Methanogenesis of acetic acid and hydrogen

The following section describes how BioWin has implemented anaerobic digestion in their comprehensive Activated Sludge Anaerobic Digestion (ASDM) Reference to Figure 2.1 for the conceptual schematic of the process. Anaerobic Digestion is typically assumed to start with the decay of influent biomass which produces un-biodegradable organic matter, biodegradable organics the release of NH3, PO4, Mg and Ca. Ordinary Heterotrophic Organisms (OHOs) mediate the hydrolysis of the biodegradable particulate matter and produce soluble organic nitrogen (NOS), phosphate (PO4-P) and readily biodegradable COD (Sbsc). The NOS will undergo ammonification by OHOs and PAOs to produce NH3. PO4-P and NH3 may be removed from solution by precipitation of struvite and calcium phosphate. OHOs will then ferment Sbsc to VFAs, mainly acetic acid (Sbsa), propionic acid (Sbsp), and hydrogen (H2) and carbon dioxide (CO2). The model includes a provision for scenarios with high and low dissolved hydrogen concentrations. Further, the dissolved hydrogen and the carbon dioxide strip from solution at a rate proportional to the saturation in solution. Acetogens convert Sbsp to Sbsa which produces hydrogen; however, high hydrogen concentrations inhibit this process. The process reaches completion when the acetoclastic methanogens consume acetic acid, and the hydrogenotrophic

methanogens consume dissolved hydrogen and CO2 to generate methane and CO2 gas. High and low pH level limits control the growth of OHOs, acetogens, and methanogens.

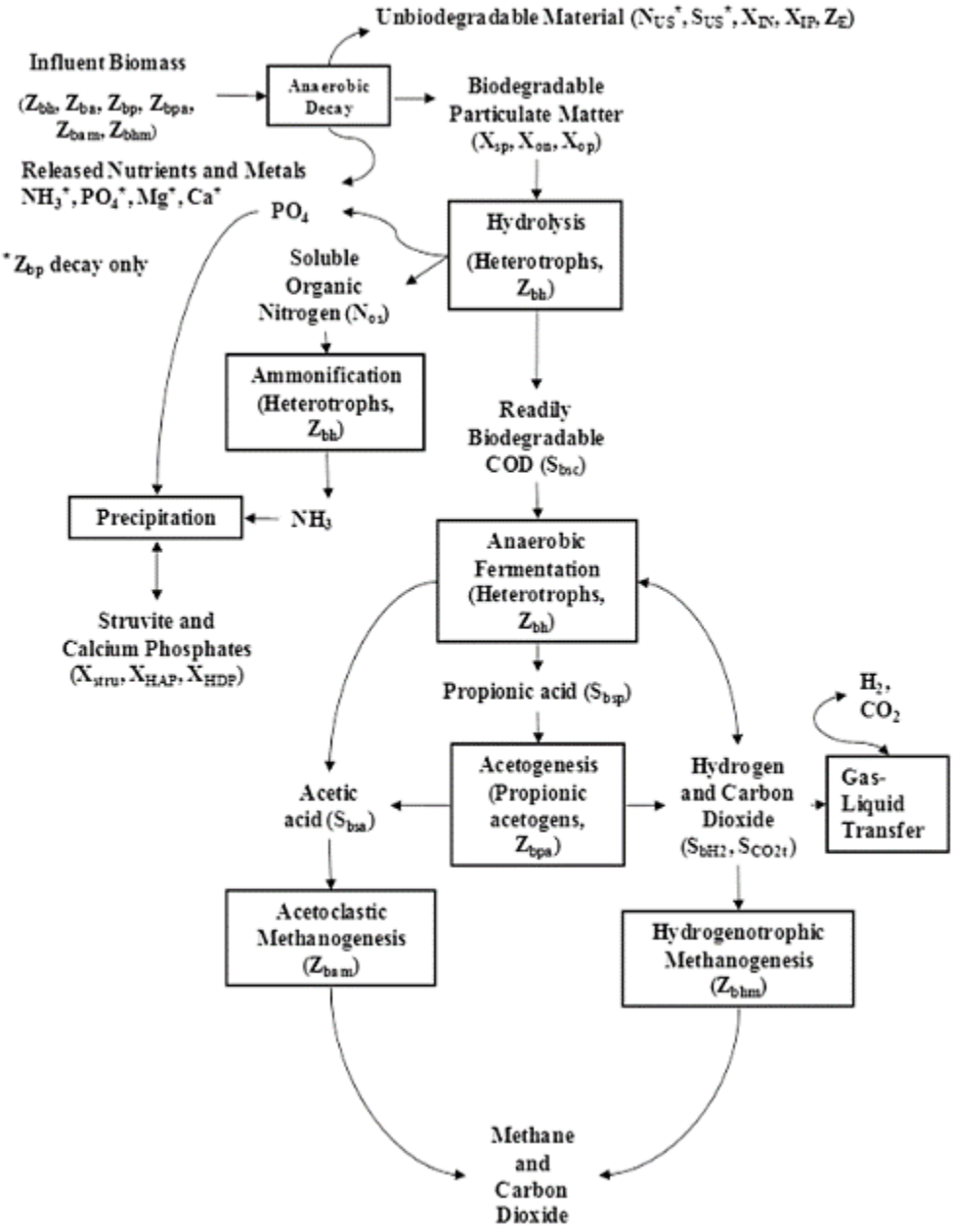

Figure 2.1: Schematic of Anaerobic Digestion process in BioWin 5.1

By inhibiting the methanogenesis stage and directing the reaction towards the acid-phase, the anaerobic digestion model can be operated to produce VFAs. These acids have a broad range of applications such as in the production of biodegradable plastics (PHA), electricity, hydrogen gas and the biological removal of nutrients (P and N) from wastewater (Lee et al., 2014). It is of importance for any of these applications, particularly for BNR, to generate VFAs consistently. The acid-phase anaerobic digestion is a reliable process, and it can apply to many organic substrates. Lee et al., (2014) presented a compendium of different VFA sources, among these the most commonly studied are Primary Sludge (PS), Waste Activated Sludge (WAS), and Food Waste (FW). Additionally, fewer studies have focused on ambient temperatures or in co-fermentation of combined wastes.

Using sludge produced at the treatment plant as a source for VFAs can have many benefits. Treatment plants already generate large quantities of sludge, which is rich in organics making them good candidates for VFA production (Lee et al., 2014). The advantages of using waste-derived VFAs can translate to cost savings by avoiding the use of chemical additives, reducing the amount of sludge produced by the treatment process, and potentially creating an additional revenue stream if P is recovered and sold.

The availability of VFAs in incoming wastewaters differs between locations and with the time of year depending upon the extent of hydrolysis and fermentation that occurs in the sewer system (Ucisik & Henze, 2008). In systems that have low VFA concentrations in the raw wastewater, fermentation of primary sludge to generate VFAs has been employed to sustain downstream EBPR processes (Banister & Pretorius, 1998). Historically, few studies have researched the acid-phase step of the anaerobic digestion process as most researchers have focused on the production of methane (Elefsiniotis & Oldham, 1994). However, there has been an increased interest in VFA production in the last three decades.

Various studies have demonstrated that using primary sludge is a feasible alternative for the production of VFAs, but operational conditions can affect their

yields. Maharaj & Elefsiniotis (2001) showed that VFA and sCOD production was highest at a 30h HRT, at 25˚C with a VFA: COD ratio of 0.8 to 1. Yuan et al. (2011) found peak production values similarly around 25˚C where 84% of the overall VFA production happened within the first five days. Also, temperatures lower than 4˚C as well as the lack of mixing were found to inhibit VFA production. Ferreiro & Soto (2003) reported that operation with Suspended Solids concentrations between 2-6 g/L showed the most VFA production and that the VFA yields at 20˚C and 35˚C were similar. Ucisik & Henze, (2008) concluded that PS always has a higher VFA yield than WAS, but that WAS could still be a possible source of VFA for BNR processes because of its potential to produce soluble organic matter.

The previous studies have revealed that the yield of VFAs in primary sludge anaerobic fermenters is relatively modest, commonly 10% of the total influent COD at six days fermentation (Banister & Pretorius, 1998) although it has been reported to be as high as 17% (Ristow et al. 2005). The larger fraction of biodegradable organics in PS yields more VFAs per gram of solids compared to AS or a mixture of PS and AS. Additionally, the composition of VFAs is a factor affecting process stability, several studies have shown that a larger fraction of propionate will give PAOs a competitive advantage over other biomass (Chen et al. 2013; Gebremariam et al., 2011; Thomas et al. 2003). Hydrolysis rates vary widely depending on various parameters such as temperature, the origin of sludge, composition, mixing, and residence times. This variability makes it difficult to predict VFA yields via modeling reliably.

The outset hypothesis of this project was that the low yields of VFAs that have been reported for fermentation of PS might occur due to low concentrations of active fermentative biomass in raw wastewaters. Influent Ordinary Heterotrophic Organisms (OHOs) are commonly found in small quantities, although reported values range from 7 to 25% of total influent COD (Dold et al., 2010). Hence, a portion of this study sought to investigate the potential to enhance VFA production from primary sludges by supplementing the feed to the fermenter

with waste activated sludge (WAS). Studies have shown that fermentation of primary sludge always produced a higher amount of VFAs than activated sludge from the same origin (Ucisik & Henze, 2008). However, by saturating the fermentative biomass in the primary sludge with substrate rich in carbohydrates and protein, as well as adding more biomass, from WAS might enhance VFA production and process stability in the acid-phase anaerobic fermentation (Chen et al., 2013). In fact, when Ji et al. (2010) mixed PS and WAS at a VSS ratio of 1:1, it increased VFA yield from 85 to 118 mg COD/g VSS an effective 40% increase in yield. However, the reasoning behind such phenomenon is not well understood and discussed in the analysis section.

2.3 Models for VFA production

There have been multiple attempts to model the acid-phase anaerobic digestion with the aim of describing solubilization of particulate organic matter and VFA production. Computer models have been found to be useful in this regard because they allow operators to test a process under different operational settings in a no-risk environment. With this information, treatment plant operators can optimize the performance of the methods to generate desired products. This section will briefly describe some of the models that were developed before the activated sludge digestion model (ASDM) used for simulation in BioWin. These models will serve as a basis for understanding how other researchers have characterized the operational factors affecting the hydrolysis process. The reviewed models include:

- First Order Models
    - Steady-state acid fermentation model (Lilley et al., 1990)
    - First order with respect to initial bVSS (Ferreiro & Soto, 2003)
    - First order with respect to initial bpCOD (Ristow et al., 2005)
    - Anaerobic Digestion Model No.1(ADM1) (Batstone et al., 2002).
- Surface-limiting models

- Dynamic pre-fermenter model (Münch et al., 1999)
- IAWQ ASM2d (Henze et al., 2000)

2.3.1 First-order models

It has been the most common practice to describe the fermentation of primary sludges using first-order reactions with respect to an initial concentration (e.g., VSS, COD, potential VFA). Experimentally, the production of VFAs in batch studies has been observed to start immediately, increasing at a rate that continually declines until it approaches a maximum VFA concentration after approximately 8 days (Banister & Pretorius, 1998). Furthermore, protein hydrolysis was the rate-limiting step in the anaerobic digestion of organics while carbohydrates and lipids will degrade slightly faster (Pavlostathis & Giraldo-Gomez, 1991). The reported range of hydrolysis rate constants is extensive, and the variety of conditions that the different studies have been carried out in makes it difficult to compare across the literature. However, the various conditions for the studies on sludge fermentability can also elucidate the factors to which hydrolysis is most sensitive.

2.3.1.1 Steady-state acid fermentation model (Lilley et al., 1990)

Lilley et al. (1990) studied the effect of solids concentration on the fermentation of primary sludge from a treatment plant in Cape Town, South Africa. The batch experiments were performed across a range of influent VSS from 11 g VSS/L to 42 g VSS/L. No concentration effect could be detected, and thus it would appear that fermentation kinetics per unit initial VSS is independent of VSS concentration. Instead, this study reported that for the batch experiments, VFAs formation is a first-order reaction with respect to potential VFAs remaining per initial VSS (Eq.2.1). In this expression, VFA'_{tvo} is the concentration in mg of VFA as COD per mg of initial VSS at any time t. k is the first order reaction constant, and VFA'_{pvo} is the potential mg of VFA as COD per mg of initial VSS:

$$\frac{d(VFA'_{tvo})}{dt} = -k * VFA'_{pvo} \quad \text{Eq. 2.1}$$

This expression can be solved to a more simplified equation (Eq 2.2) to calculate the yield, where VFA'_{ovo} is the initial mg of VFA as COD per mg of initial VSS:

$$VFA'_{tvo} = \left(VFA'_{pvo} - VFA'_{ovo}\right)\left(1 - e^{-kt}\right) + VFA'_{ovo} \quad \text{Eq. 2.2}$$

To solve the above expression VFA'_{pvo} and K must be determined from experimental results. The process to obtain these starts with a trial value of VFA'_{pvo}. Then the Log (VFA'_{pvo}- VFA'_{tvo}) for all values of VFA_{tvo} is calculated and plotted versus time. The best value for VFA'_{pvo} is the one that yields a straight line. k is determined by the slope of this line via Eq. 2.3:

$$m = -k * log_{10}e \quad \text{Eq. 2.3}$$

Lilley et al. (1990) reported values for VFA'_{pvo} of 0.14 mg VFA as COD per mg of initial VSS and K of 0.16 d^{-1} at 20 ˚C for PS. A maximum potential conversion of influent COD to VFA of 17%, at 20˚C, at retention times of less than 10 d was found for PS. It was recommended that acid fermentation systems should not exceed six days of retention time to avoid a reduced VFA yield due to methanogenic activity. Another finding was that besides generating VFA, the acid fermentation also produces non-VFA soluble COD at a very similar rate also following a first-order rate not influenced by sludge concentration.

2.3.1.2 First order with respect to initial bVSS (Ferreiro & Soto, 2003)

Ferreiro & Soto (2003) studied batch fermentation of primary sludge across temperatures of 10, 20 and 35 C and initial concentrations ranging from 0.7 g VSS/L to 10 g VSS/L. The substrate used in this study came from a municipal water treatment plant in Santiago de Compostela, Northwest Spain.

They found that a first-order hydrolysis expression with respect to the initial biodegradable VSS concentration could predict their results. By plotting the progression of biodegradable VSS over time in a semi-log plot, Ferreiro and Soto

(2003) could determine the hydrolysis coefficients from VSS data and found the first order constants (k_h) to be 0.038, 0.095 and 0.169 d^{-1} for 10, 20 and 35°C respectively. Regarding specific VFA production, this study found ranging values from 0.17 to 0.34 g VFA (as COD)/g of VSS depending mainly on sludge concentration and to a lesser extent with process temperature.

2.3.1.3 First order with respect to initial bpCOD (Ristow et al., 2005)

Ristow et al., (2005) collected experimental data from anaerobic digesters operating at acidogenic conditions at varying feed COD concentrations of 2, 13, and 40 g COD/L with a retention time of 10, 5 and 3.33 days at constant temperature of 35°C. The sludge was originated at the Athlone Wastewater treatment works (Cape Town, South Africa). This plant treats municipal wastewater mostly of domestic origin but with a significant mixed industrial component.

Ristow et al., (2005) tested a first-order response regarding the initial biodegradable particulate COD (Sbpi) according to Eq. 2.4. Their calculated constant (k_h) has a mean of 0.054 d^{-1} (±0.027 d^{-1}).

$$r_{hydr} = k_h \times S_{bp} \qquad \text{Eq. 2.4}$$

However, they found that a first-order rate equation with a single value for the specific rate constant could not accurately predict the rate of PS hydrolysis for each of the COD feed concentrations and retention times. Hence, Ristow et al. (2005) tried using alternative formulations for the kinetics. They evaluated fitting experimental data from anaerobic digesters to Monod kinetics and surface reaction kinetics (Contois kinetics) but found that below an SRT of 8 days these forms for the hydrolysis expression also failed to predict the rates accurately. In fact, it was found that using an empirical relationship where k_h is linearly dependent on hydraulic retention time (R_h) following Eq. 2.5; the model could reasonably predict the rate of PS hydrolysis in this study. An Upper pH limit (pH_{UL}) of 8 and a lower pH limit (pH_{LL}) of 6.04 were determined appropriate for the

acidogenic biomass. However, due to the empirical nature of this expression, it is challenging to apply it to other PS fermentation systems.

$$k_h = 0.0883 - 0.0055R_h + 0.06\left(\frac{pH - pH_{LL}}{pH_{UL} - pH_{LL}}\right) \quad \text{Eq. 2.5}$$

2.3.1.4 ADM1 (Batstone et al., 2002)

The Anaerobic Digestion Model No. 1 employs a broad basis, and its concepts have been considered to be compatible with previously released models in the ASM series (Batstone et al., 2015). It builds on other models and has been deemed to provide a basis for integration of plant-wide modeling (Batstone et al., 2015). The task group recommended using first-order kinetics for hydrolysis because it is the most fundamental approach that can capture the diversity of disintegration processes (Batstone et al., 2002). Also, it is assumed that composite waste (i.e., WAS and PS) first disintegrates into carbohydrate, protein and lipid particulate substrate and then undergoes hydrolysis. The disintegration step is also first-order with respect to the amount of composite waste material according to Eq. 2.6, and it accounts for lysis, non-enzymatic decay, phase separation and physical breakdown.

$$r_{dis} = k_{dis} X_{composite} \quad \text{Eq. 2.6}$$

Once the composite material has been disintegrated into carbohydrates, proteins, and lipids, three parallel hydrolysis pathways happen to each species. This separation is necessary since each hydrolysis pathway will yield different products. Eq. 2.7 describes the first-order rate of carbohydrate hydrolysis carbohydrate with respect to particulate carbohydrate concentration. The products of this reaction produce monosaccharides, followed by the uptake of sugars (Eq. 2.8) to produce VFAs. This uptake contains a Monod-type function on the sugar substrate and an inhibition factor (I_1) for pH limits and low or no substrate concentrations.

$$r_{hyd,ch} = k_{hyd,ch} X_{ch}$$ Eq. 2.7

$$r_{su} = k_{m,su} \frac{S_{su}}{K_s + S_{su}} X_{su} * I_1$$ Eq. 2.8

Eq. 2.9 describes the first-order rate of hydrolysis of proteins with respect to particulate protein concentration. The products of this reaction produce amino acids, whose uptake also produces various VFAs. The uptake of amino acids occurs at the rate described in Eq. 2.10.

$$r_{hyd,pr} = k_{hyd,pr} X_{pr}$$ Eq. 2.9

$$r_{aa} = k_{m,aa} \frac{S_{aa}}{K_s + S_{aa}} X_{aa} * I_1$$ Eq. 2.10

Eq. 2.11 describes the first-order rate of hydrolysis of lipids with respect to particulate lipid concentration. The products of this reaction produce long chain fatty acids (LCFA) whose uptake will produce acetate and hydrogen gas according to the rate in Eq. 2.12. The hydrolysis of lipids also produces some monosaccharides which will undergo the previously described sugar uptake. Note that the inhibition factor is different for lipids, it still contains pH limits but has a non-competitive product inhibition instead of low substrate inhibition as the previously discussed processes.

$$r_{hyd,li} = k_{hyd,li} X_{li}$$ Eq. 2.11

$$r_{fa} = k_{m,fa} \frac{S_{fa}}{K_s + S_{fa}} X_{fa} * I_2 \quad \text{Eq. 2.12}$$

The main disadvantage of this approach is that the substrate fraction of carbohydrate, protein and lipid content must be characterized which is not a common practice yet in these types of studies. This specific characterization makes it challenging to cross-compare with the other first order models. Another criticism, for all first order models, is that theoretically there is no limit for a maximum rate since the expressions suggest that increasing the species (i.e., VFA_{pvo}, bVSS, bpCOD) would increase the rate infinitely. Lastly, it would seem logical to link the concentration of active biomass to the expression in some form since biomass mediates the hydrolysis.

2.3.2 Surface-limiting models

An alternative to quantifying the hydrolysis as a function of the biodegradable particulate substrate is to use a surface-limiting model. Vavilin et al. (1996) described the kinetics of hydrolysis as a surface colonization of particles by hydrolytic bacteria followed by enzyme secretion and surface degradation. It is believed that the bacteria will use the products of this reaction for growth. Since the growth step was assumed to be rapid and therefore not rate-limiting, Dold and Marais (1986) proposed a formulation for this concept based on Levenspiels surface reaction theory for planar surfaces and a hydrolysis rate that was subject to the concentration of active bacteria (Z_{ad}) and the biodegradable particulate organics (S_{bp}) to active bacteria ratio shown in Eq. 2.13. Hence, when either the ratio or the bacteria are low, the rate of reaction is limited. Moreover, when the ratio is high, the reaction rate will reach a maximum.

$$r_{hydr} = \frac{k_{max}\left(\frac{S_{bp}}{Z_{ad}}\right) Z_{ad}}{K_s + \left(\frac{S_{bp}}{Z_{ad}}\right)} \quad \text{Eq. 2.13}$$

2.3.2.1 Dynamic pre-fermenter model (Münch et al., 1999)

Munch et al. (1999) employed a dynamic mathematical modeling approach that accounted for the effects of substrate type, and the possibility of VFA consumption by methanogens. In this model, the kinetics of the degradation of the particulate substrate are described via Eq. 2.14. Instead of a first-order model, hydrolysis is described using a surface-limiting model because they found that the hydrolysis rate reduced when the biomass concentration was above a certain level. Hence, this formulation has the acidogenic biomass concentration (C_a) in the denominator. This causes the rate of hydrolysis to reduce at high bacterial concentrations, possibly due to a limited surface area of the substrate particles. It also includes the hydrolysis rate constant (k_{hydr}), and concentration of the hydrolytic enzymes (C_e) that will catalyze the particulate substrate (C_p) breakdown:

$$\boldsymbol{r_{hydr,p} = k_{hydr,p} \frac{C_p * C_e}{C_a}} \qquad \textbf{Eq. 2.14}$$

The aim of this model was to reduce the number of state variables while still describing VFA production in prefermenters. In the model, the sum of VFAs is considered instead of distinguishing individual VFAs, which is a practical approach if VFAs speciation is constant over time as in the case with the prefermenters. Eq. 2.15 describes the mass balance equation for VFAs in the model where HRT is the hydraulic retention time, Y_a is the yield of acidogenic biomass, $r_{x,a}$ is the growth of acidogens, and $r_{x,m}$ is the growth of methanogens:

$$\boldsymbol{\frac{dC_{VFA}}{dt} = \frac{1}{HRT}(C^{in}_{VFA} - C_{VFA}) + (1 - Y_a) * r_{x,a} - r_{x,m}} \qquad \textbf{Eq. 2.15}$$

Organism growth for acidogenic and methanogenic bacteria is carried via Monod kinetics with Eq. 2.16 and Eq. 2.17:

$$\boldsymbol{r_{X,a} = U_{max,a} \frac{C_{mo}}{(K_a + C_{mo})} \frac{C_{NH4-N}}{(K_n + C_{NH4-N})} C_{X,a}} \qquad \textbf{Eq. 2.16}$$

$$r_{X,m} = U_{max,m} \frac{C_{VFA}}{(K_m + C_{VFA})} \frac{C_{NH4-N}}{(K_n + C_{NH4-N})} C_{X,m} \quad \text{Eq. 2.17}$$

The hydrolytic enzyme production links with the hydrolysis rate via the yield coefficient and it was assumed to be non-growth associated. The mass balance for the enzyme concentration follows Eq. 2.18. Additionally, hydrolytic enzymes undergo denaturation (they become soluble) via Eq. 2.19 following first-order kinetics. These enzymes hydrolyze the soluble and particulate substrates as well as participate in the ammonification of proteins.

$$\frac{dC_e}{dt} = \frac{1}{HRT}(C^{in}{}_e - C_e) + Y_e(r_{hydr,p} - r_{hydr}) - r_{d,e} \quad \text{Eq. 2.18}$$

$$r_{d,e} = d_e C_e \quad \text{Eq. 2.19}$$

The model does not consider hydrogen-utilizing methanogens, or the effects of mixing intensity, temperature, and chemical inhibitors on the rate of VFA production (Münch et al., 1999). However, they found that this model was able to reasonably describe and explain the steady-state results reported by Elefsiniotis (1993) with respect to the effect of retention times over 3.5 days on effluent VFA, sCOD, and ammonia concentrations. The data was obtained in a bench-scale up-flow anaerobic sludge blanket prefermenters fed with primary sludge from a wastewater treatment plant in British Columbia, Canada.

2.3.2.2 IAWQ Activated Sludge Model 2d (Henze et al., 2000)

The task group developed the activated sludge models with the aim of providing the international community with a reliable model that could describe the activated sludge treatment process. As a result, the Activated Sludge Model No. 1 (ASM1) was developed and since has been proven to be an accurate tool to model nitrification-denitrification processes. As nutrient removal gained momentum in the research and treatment community, the task group revised

ASM1to include biological phosphorus removal processes. This new model called ASM2 presents a concept for the dynamic simulation of combined biological processes for the removal of COD, nitrogen, and phosphorus. The model known as ASM2d was developed shortly after as another extension to address unresolved issues with ASM2, specifically the need to include denitrifying PAOs in the model as a fraction of the PAOs that can grow in anaerobic conditions.

At the time it was deemed that the least researched processes in ASM2d were related to anaerobic hydrolysis and fermentation (Henze et al., 2000). The task group identified surface reactions as the typical way that hydrolysis processes happen. It was concluded that when there is close contact between the organisms that produce the hydrolytic enzymes and the slowly biodegradable substrate hydrolysis will be enhanced. In ASM2d, hydrolysis is described by three different processes that are dependent on electron acceptor: aerobic, anoxic and anaerobic hydrolysis. Out of these, anoxic and anaerobic were considered to be the least understood. However, there was a consensus that both processes have reduced rates when compared to aerobic hydrolysis so in the model a reducing factor is used. The main criticism of this approach is that the reducing factor (η_{fe}) was determined empirically and so far, no theoretical explanation has been found. The formulation of the hydrolysis processes consists of hyperbolic switching functions for oxygen and nitrate to describe environmental conditions, and hydrolysis is assumed to be a surface-limited reaction as per Eq 2.20:

$$\boldsymbol{r_{hydr,an} = k_h * \eta_{fe} * \frac{K_{o2}}{K_{o2}+S_{o2}} * \frac{K_{NO3}}{K_{NO3}+S_{NO3}} * \frac{X_s/X_h}{K_x+X_s/X_h} * X_h} \qquad \textbf{Eq. 2.20}$$

In ASM2d the hydrolysis process transforms particulate substrate (X_S) into fermentable readily biodegradable COD (S_f). Consequently, S_f is transformed into fermentation products (S_A) (i.e., Acetate) in a simple transformation process following Eq. 2.21. As it can be observed the fermentation process is not associated with the growth of heterotrophic organisms because doing so would increase the complexity of the model by increasing the number of variables and

processes. However, ASM2d does account for the growth of heterotrophic organisms on a fermentable substrate (S_F) following Monod kinetics via Eq. 2.22.

$$r_{fe} = q_{fe} \frac{K_{o2}}{K_{o2}+S_{o2}} * \frac{K_{NO3}}{K_{NO3}+S_{NO3}} * \frac{S_F}{K_{fe}+S_F} * \frac{S_{ALK}}{K_{ALK}+S_{ALK}} X_h \quad \text{Eq. 2.21}$$

$$r_{Xh,growth} = U_h \frac{S_{o2}}{K_{o2}+S_{o2}} * \frac{S_F}{K_F+S_F} * \frac{S_F}{S_A+S_F} * \frac{S_{NH4}}{K_{NH4}+S_{NH4}} * \frac{S_{po4}}{K_P+S_{po4}} * \frac{S_{ALK}}{K_{ALK}+S_{ALK}} X_h \quad \text{Eq. 2.22}$$

2.3.3 Potential areas for model improvement

Extensions to existing models have been considered as a response to the inconsistency in rate constants across different studies. Inhibitory effects of this process have appeared in the literature and are a feasible extension of our understanding (Pratt et al., 2012; Zoetemeyer et al., 1982). Product inhibition seems to be the most common effect whereby the concentration of the reaction's products decreases the rate of the reaction. Because of the assumption that this process is surface-based, the more product there is, the less likely that there will be contact between substrate and organism.

Another factor to consider with respect to its impact on hydrolysis is the role that enzymes play in the breakdown of organics. Hydrolytic enzymes such as those generated by *Cellulomonoas uda, C. biazotea, Aspergullus awamori*, mature compost, and activated sludge from municipal WWTP have been employed to improve the solubilization of solid waste (Lee et al., 2014). Humphrey (1979) pointed out for hydrolysis of cellulose, but also applicable for all particulate substrates; one must account for the generation of enzymes as the organism grows and the repression of the enzyme production due to product inhibition. Therefore, the reaction rate for enzyme production must link to bacteria growth, and the rate of production of the soluble substrate should be associated with the

rate of enzyme production, adding to the product inhibition considerations previously discussed.

It is challenging to measure and identify all the enzymes produced during this process. As previously discussed, the specific organisms responsible for hydrolysis have not been identified, and therefore there is not a single enzyme that is responsible for surface degradation. An alternative to characterizing the myriad of enzymes produced in this process is to use a lump enzyme term to describe the overall effect of all enzymes. However, to do this, we need an understanding of what types of enzymes will be produced.

Commonly, organic wastes consist of a mixture of carbohydrates, lipids, and proteins. Carbohydrates are hydrolyzed to monosaccharides and then degraded by glycolysis via the Embden Meyerhof pathway (Jones, 1992). Fats or lipids are hydrolyzed to glycerol and long chain fatty acids and then degraded by beta-oxidation (Jones, 1992). Proteins hydrolyze into amino acids which undergo deamination (Jones, 1992). The model developed by (Batstone et al. 2000) considers ten generic biological groups and three enzymatic groups with different kinetic parameters. In the case of lipids, the enzymes are called Lipolytic while for proteins there are proteolytic enzymes and carbohydrates are addressed by cellulolytic enzymes. In this study, a focus will be given to cellulolytic enzymes because they are widely understood and are the most applicable to the experimental sludge. Table 2.3 summarises common kinetic parameters for these types of enzymes:

Table 2.1: Enzyme parameters for model (Humphrey, 1979)

Parameter	Model	Magnitude	Units
Enzyme yield	$Y_{E/X}$	0.01	g/g
Substrate IC50 in enzyme growth	$K_{E/S}$	0.01	g/l
Enzyme half-saturation constant	α_Q	0.3	g/l
Half-saturation	K_s	0.1	g/l
Max specific growth rate	U_{max}	0.25	l/hr

It should be evident that there have been multiple attempts to describe hydrolysis and acid fermentation for primary sludges mathematically. Because most of these studies have reported conflicting results and a wide range of parameter values, it is challenging to select appropriate rate constants for predictive simulation. Further, few studies have simulated fermenters that received a mixture of PS and WAS. Hence, there is an opportunity to elucidate the role of WAS organisms in model simulations. The key challenges as summarized by Batstone et al.(2015) are influent characterization and parameter identification with regards to the hydrolysis coefficient, energy density and degradable fraction which define performance in most systems.

3. Materials and methods

This section describes the apparatus and methods that were employed to experimentally study the fermentation of sludges that were obtained from the Elmira WWTP. Two types of sludge (PS and WAS) were retrieved from the facility approximately three times a week and were transported in separate plastic jerry cans. The sludge was stored separately in a refrigerator that kept the samples at 4˚C when needed. The PS came from the primary clarifier underflow and was sampled before the morning desludging. The WAS came from the secondary underflow and sampling was done before its recycle into the process train. The physical and biochemical properties of the reactors and their feeds were assessed using standard laboratory analyses. Table 3.1 shows the average properties of these sludges as measured in the dynamic run of this study.

Table 3.1: Average properties of the feed PS and WAS

Parameter	Primary Sludge(PS)	Waste Activated Sludge (WAS)
	g/l	g/l
pH	6.3±0.31	6.92±0.06
TSS	10.10±1.16	6.70±0.19
VSS	8.71±1.00	5.15±0.14
sCOD	0.86±0.16	0.06±0.01
TCOD	16.17±2.07	7.89±0.55
Ammonium (mg/L)	35.06±3.69	6.69±1.91

* ± average standard error of the mean, n = 14

3.1 Reactor design and operation

3.1.1 Reactor design

The reactors employed in this study received either PS, WAS, or ML as a mixture of 38% WAS and 62% PS by volume. Figure 3.1 displays the experimental set up of the PS and ML reactors that had a volume of 5L. The WAS reactor was setup similarly, except in a 1L container. The temperature was maintained at 21˚C which

was the environmental temperature of the lab. The reactors were equipped with Bodine Model 0158 DC Gear mixers to maintain homogeneity at 160 rpm. There was also a Tedlar gas bag connected to the reactors to check for methane production.

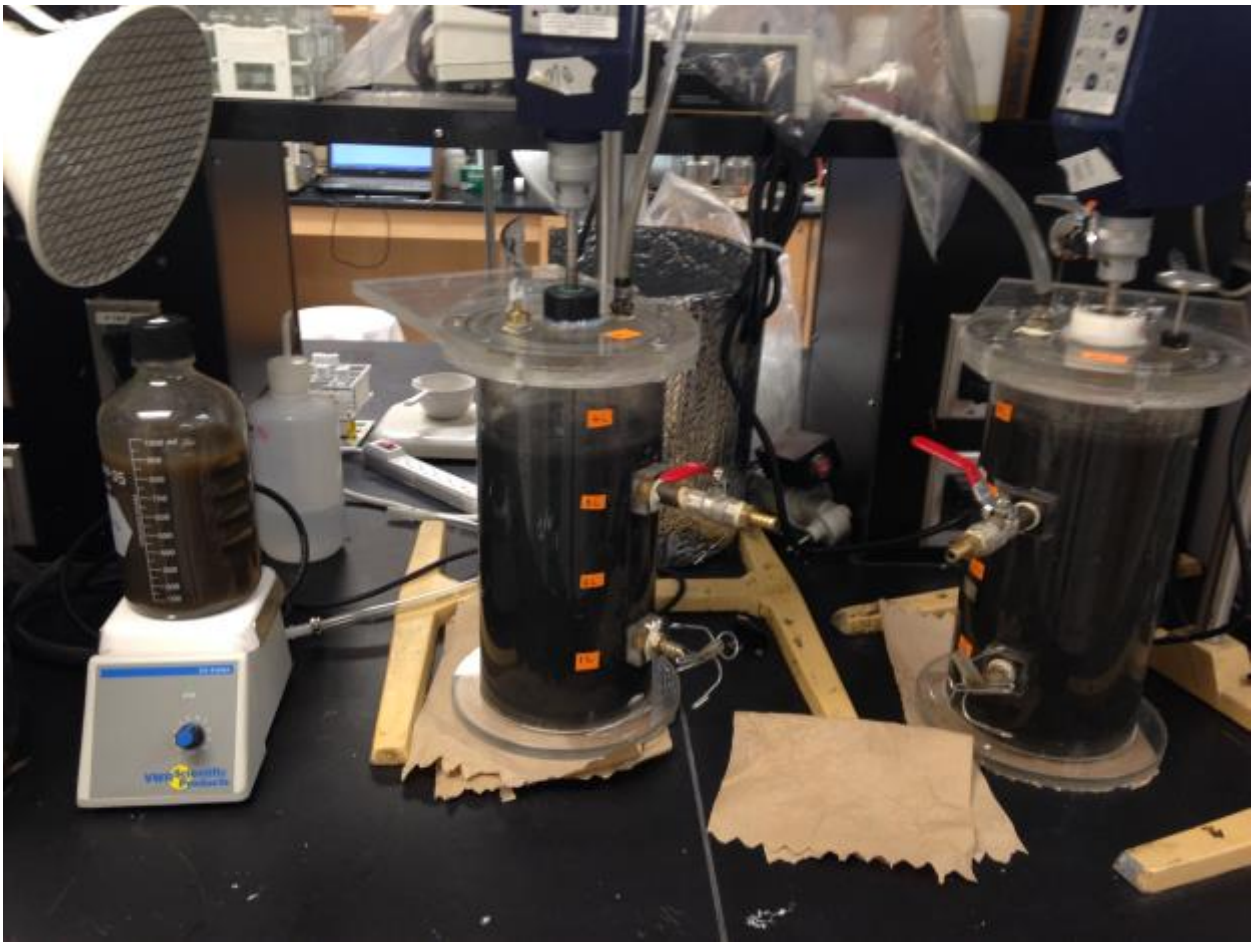

Figure 3.1: Experimental Acid-phase anaerobic digester set up. From left to right WAS, PS, and ML reactors are shown.

During sampling, the reactors headspace was purged with nitrogen gas. Each digester had two valves, an upper one for feeding and a lower one for sampling. Sampling was performed by manually retrieving the sample volume (Approximately 100 ml) from the lower valve of the reactor. Since the reactor had to be emptied by 1.66 L every feeding, sampling was done approximately half way through the emptying cycle. The valve was then closed, and the reactors were fed. For PS, the reactor was fed with 1.66 L of Primary Sludge. For ML, it was 1.03

primary sludge, and 0.63 waste activated sludge, an effective 62% PS and 38% WAS. Lastly, since the WAS reactor was significantly smaller (1L), the feeding volume was only 0.66 L every time. Additionally, because there was no valve in the WAS container, the samples were collected using a peristaltic pump to drain the required volume and perform sampling.

3.1.2 Reactor operation

The reactor was operated in two main stages, start-up and experimental run. During the start-up phase, the objective was to identify baseline scenarios and to gain knowledge about how to carry the experimental run. These different fermentation batches are summarized in table 3. 2. The reactors were emptied and cleaned in between runs and sludge stored at 4˚C when needed.

Table 3.2 Reactor trial runs schedule

Test No.	Dates	Activity	Notes
1	May 25-29	PS (x2) Star up run	Startup batch run meant to provide a practice run of the reactor setup and analytical methods. The two reactors were filled using PS and fermentation was allowed for 5 days.
2	Jun 2-6	PS (x2) Baseline run	Sampled twice daily, morning and afternoon for the first two days. Morning sample only for the remaining three days. The reactor was fed on the morning of the 3rd day to maintain an SRT of 6 days.
3	Jun 15-19	PS (x2) Baseline run	Same schedule as the previous week
4	Jun 22-26	PS and ML Baseline run	Same schedule as the previous week. ML = 3.3 L of PS + 0.7 L of WAS resulting in a 5:1 ratio of PS VSS to WAS VSS.
5	Jul 6-10	PS, ML, WAS Baseline run	Same schedule as the previous week. ML = of 2.4 L of PS + 1.6 L of WAS a 6:1 ratio of PS VSS to WAS VSS.
6	Jul 13-17	PS, ML, WAS Baseline run	Same schedule as the previous week. ML = of 3.1 L of PS + 0.9 L of WAS a 27:1 ratio of PS VSS to WAS VSS.
7	Jul 20-24	PS, ML, WAS Baseline run	Same schedule as the previous week. ML = 2.4 L of PS + 1.6 L of WAS a 5:1 ratio of PS VSS to WAS VSS.

During the experimental run, the three reactors were tested for an extended fermentation time of 40 days while keeping an SRT of 6 days. The feeding schedule was the same for all reactors and was performed every 2 days for the duration of the study according to the schedule in table 3.3 below, with fresh sludge from the plant collected in the morning of the test.

Table 3.3 Reactor dynamic run

Test No.	Dates	Activity	Notes
8	Jul 27- Sep 4	PS, ML, WAS Experimental run Extended time (40 days)	The reactors were fed every two days to maintain an SRT of 6 days. Sampling was performed before feeding. However some days only feeding happened without sampling.

3.2 Sample analysis

3.2.1 pH

An ion selective electrode (Model 420A, Orion Research Inc., USA) was employed to measure pH for all samples.

3.2.2 COD

The COD analysis was conducted using Hach's USEPA-approved dichromate COD method by Standard Method 5220 D (APHA, 1998). The reagents were prepared in-house according to the mentioned methods. For sample analysis, the tests were conducted in triplicates. For soluble COD (sCOD) and filtered and flocculated COD (ffCOD), the samples were centrifuged at 5000 rpm for 10 minutes. Consequently, the supernatant was filtered using, first, a 1.5 um Whatman filter for sCOD and a further filtration with a 0.45 um Whatman filter for ffCOD. TCOD, sCOD, and ffCOD samples were diluted using an appropriate factor for the Hach vials (Range 0-1500 mg COD/L). Then, 2 ml of diluted sample was added to each vial. The samples were run with a blank and a standard vial.

The blank was made of 2ml of DI water, while the standard solution had a value of 1000 mg COD/L. The vials were inverted 10 times before digestion in the HACH COD reactor (Model DRB 200) for 2 hours at 150˚C. Once at room temperature; the samples were measured using a HACH DR 2000 Spectrophotometer.

3.2.3 Suspended solids

Standard methods 2540D, E (APHA, 1998) was employed to measure TSS and VSS with filtration using a 1.5 um Whatman Glass Microfiber filter paper (934-AH) and then drying in the oven at 105˚C for 24 for hours for TSS. The mass of the samples plates was then measured, and the increase in weight represented TSS. Samples were then placed in an oven for at least one hour at 550˚C. After combustion, the plates were measured; the weight loss represented VSS.

3.2.4 Ammonia

An ion selective electrode (Orion 9512HPBBNWP model 720A) measured ammonia in solution for all samples. While the electrode performed the readings, the samples were mixed using a Scholar 171 magnetic stirrer to maintain homogeneity in the sample.

3.2.4 Total Kjeldahl nitrogen

The method employed for TKN analysis was the ammonia salicylate colorimetric assay. It involved adding 1.5 ml of a digestion solution to 1 ml of prepared sample in a digestion flask. The digestion solution was prepared by dissolving 40 g of potassium sulfate and 2 ml of selenium oxychloride in 250 ml of sulfuric acid. The sample was then digested in a Bran and Luebbe BD-40 block digester at 220˚C for 1.5 hours followed by digestion at 380˚C for 2.5 hours. This process converted all the organic nitrogen to ammonia. After the samples had been cooled overnight, the samples were adjusted to a neutral pH before analysis of ammonia in a Bran and Luebbe Auto Analyser 3. This analyzer measures the

concentration of ammonia in the samples colorimetrically. The sample reacts with sodium hypochlorite, a sodium hydroxide buffer solution, and phenol to produce indophenol. The color is intensified using sodium nitroprusside prior to the colorimetric analysis at 660 nm.

3.2.5 Volatile fatty acids

Flame-ionization detector (FID) Gas chromatography (GC) was employed to quantify the VFA content of samples. The chromatograph (Model: Hewlett Packard HP 5890 Series II) was equipped with a Nukol fused-silica capillary column and used helium as carrier gas. The GC was calibrated using a standard Volatile Free Acid Mix provided by Supelco (No. CRM 46975). The VFA concentrations in the 10mM standard mixture were 590 mg/L of Acetate, 730 mg/L of Propionate, 870 mg/L of Butyrate, and 1010 mg/L of Valerate respectively. Samples were prepared using a 1.5 ml glass vial with septa cap (Sigma-Aldrich). A volume of 1.3 ml from the sCOD samples was added to the vial with 0.2 ml of phosphoric acid. The vials were shaken for 30 seconds using a shaker to ensure homogeneity.

3.2.6 Orthophosphate

Orthophosphate or reactive phosphorus was measured using a standard Ascorbic Acid Total Phosphate Hach test kit. Samples were run in triplicates and diluted according to Hach specifications and limits for the test (6 to 60 mg PO4). The method consists in adding 0.4 ml of sample and 0.5 ml of solution B to a Hach test vial. Then, the vial is closed using a gray DosiCap C that contains the final reactant. The vials were inverted 2-3 times before letting a 10-minute reaction start. Once finished, the vials were inverted again and cleaned prior to reading with the Hach spectrophotometer. The reactive or orthophosphate ions react with molybdate and antimony ions in an acidic solution to form an antimonyl phosphomolybdate complex, which is reduced by ascorbic acid to phosphomolybdenum blue. The measurement wavelength was 880 nm.

4. Analysis of results

The objectives of this study were to assess the fermentability of Elmira's sludge, investigate whether the addition of WAS could improve VFA production, and evaluate how existing models for anaerobic digestion simulate sludge fermentation; all these in support of EBPR process implementation. The following results describe the operation of the semi-continuous batch reactors in the context of these objectives. The following analysis will contain:

- A description of the operating conditions of the reactors
- An analysis of the materials produced in fermentation experiments,
- A critical evaluation of the ability of the BioWin ASDM model to predict the experimental results
- A description of alternatives to improve model predictions and reduce errors

4.1 Baseline sludge fermentability

This section describes the performance of the bioreactors that were operated to hydrolyze and ferment the three different waste streams. The inputs and operating conditions of the bioreactors are described and then, the performance of the reactors regarding solubilization of COD and production of volatile fatty acids is assessed. The data generated in this portion of the study was employed in subsequent model assessment and development activities.

4.1.1 Suspended solids loading

The sludges used in this study originated from a full-scale WWTP, with the expectation that they may vary in composition with time. Hence, the solids concentrations of the sludges were regularly monitored to characterize the loading of organics into the bioreactors. Total Suspended Solids (TSS) are commonly determined via filtration and describe all solid material in the influent

solution. Within these solids, the organic fraction represents the Volatile Suspended Solids (VSS) and the inorganic portion, the remainder, called Fixed Suspended Solids (FSS). The VSS can then be further divided into biodegradable (bVSS) and non-bio degradable (nbVSS) fractions. The bVSS is the fraction that will be hydrolyzed contributing to bCOD and active biomass; whereas the nbVSS fraction contributes to sludge production. Hence this study was particularly interested in observing the reduction in VSS and how the organic fraction changed as the fermentation experiment progressed. A time series plot of the VSS loading to the three reactors shows that there was considerable variability in the organic solids that were fed to the bioreactors in Figure 4.1. This variability is especially prominent in the PS feed solids. This was attributed to variability in the plant's influent and primary clarifier operation and represents one of the operational challenges for EBPR. On the other hand, the WAS samples showed more stability than the PS samples. On average PS contained 1.3% TSS, ML 1% TSS and WAS 0.6% TSS. The variability in feed concentrations translated throughout this study, and it is important to consider the PS trend that had a stable operation until day 20 when the loadings increase.

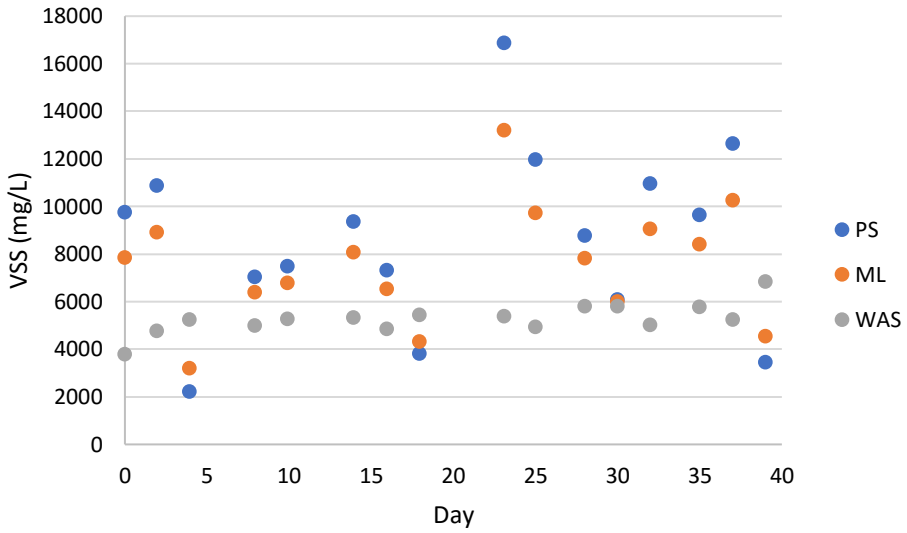

Figure 4.1:Time series of VSS loading to the reactors

To further characterize the variability, the organic fraction of solids, regarding the ratio of VSS to TSS was analyzed. This ratio serves as an indicator of the solid organic matter in the sludge which is available to undergo hydrolysis (bVSS). North American sludges commonly have values of approximately 85% for this characteristic and this value is a default in BioWin. The VSS to TSS ratios for the feeds were on average 0.86 ±0.02 for the PS, 0.83 ±0.02 for ML and 0.77 ±0.02 for the WAS. There was less organic matter in the WAS when compared to PS and ML, which was attributed to the fact that the WAS had already undergone biological processes that would have degraded some of the original organic matter. A time series plot (Figure 4.2) shows that these ratios had modest variability with time in the influent of the Elmira plant:

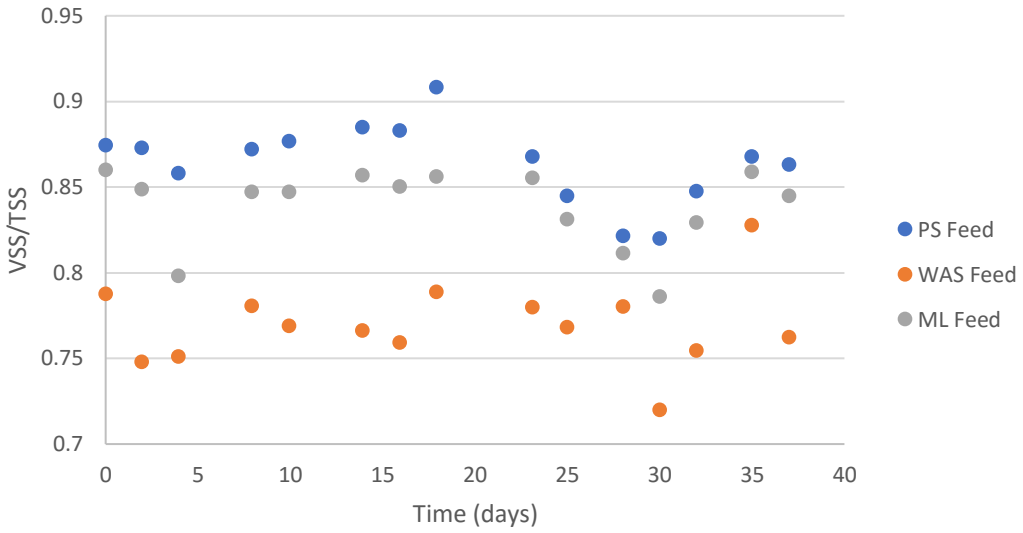

Figure 4.2: VSS/TSS ratio for feed samples to the reactors

4.1.2 Reactor pH

Characterization of the reactor pH was deemed to be important because hydrolysis is carried out by biological groups whose growth is impacted by pH values. The ideal pH range for hydrolysis and fermentation has been reported to

be between 5 and 6 (Elefsiniotis, 1993; Zoetemeyer et al. 1982). OHOs that act as acidogens can thrive at this pH. On the other hand, the growth of methanogens is inhibited under acidic conditions. Therefore, maintaining acidic conditions to prevent methanogenic growth and avoid the consumption of VFAs is important when producing VFAs. The pH results for the three reactors as well as the feed streams are shown in Figure 4.3 as time series plots to describe these conditions. From Figure 4.3 it can be observed that there was more variability in the PS values than in the WAS values. This was attributed to the variability in feed solids concentrations that was previously discussed.

Figure 4.3 also demonstrates that the pH for the PS and ML reactors decreased until day 20 by about 1.5 pH units and after day 20 the pH increased somewhat. When compared to the previous figures, it appears that solids and pH were inversely correlated. The lower the pH of the feed corresponded to the higher the VSS/TSS ratio, suggesting that the larger organic fraction of the sludge allowed for some pre-fermentation in the clarifier, generating a more acidic sludge.

Overall, the pH of the reactors averaged 5.1±0.5 for PS, 5.5±0.4 for ML, and 6.7±0.2 for the WAS which except for the WAS reactor were below the reported limit for growth of methanogens (pH= 6.0 to 6.5). The results indicate that for PS and ML the environment was appropriate for enhanced fermentation by the OHO population. The WAS pH values were in the range where some loss of VFAs to methanogenesis was possible and hence additional analysis was carried out to confirm whether methane production took place.

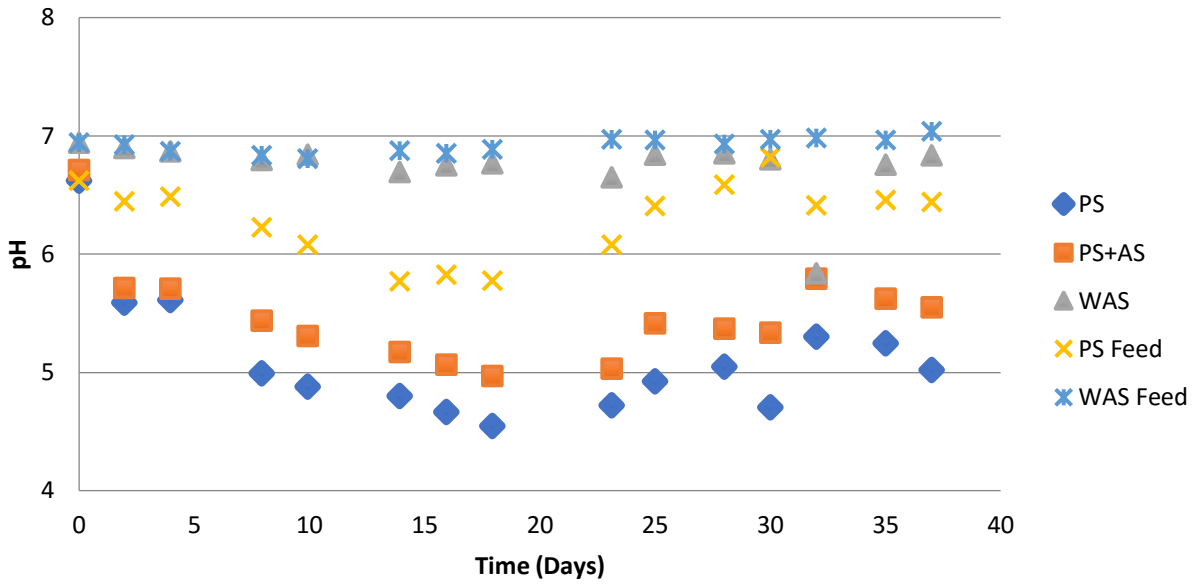

Figure 4.3: Experimental pH values versus time

4.1.3 COD Mass Balances

To further assess whether the observed acidogenic conditions were preventing methanogenesis, a set of cumulative mass balances on the total COD in the influent and effluent streams were conducted to assess if COD loss to methane production was occurring. Total COD should be conserved in fermenters because the hydrolysis process only converts particulate COD into soluble COD.

To calculate the mass balance, the cumulative COD mass entering and leaving the reactors was calculated from the measured concentrations in the feed and effluent streams and the corresponding flows. Figure 4.4 presents the calculated values for the three reactors. In Figure 4.4 for the case of PS, the influent and effluent mass flows were similar before day 26 after which some COD loss happened. This loss could be due to the increased solids loadings that happened before that day in the small gap after day 20 and shown previously in Figure 4.1. Perhaps this sudden change in solid concentrations enabled a small amount of

methanogenic activity. Another reason for the origin of methanogenic activity could be the extended retention time that happened within those days. For the WAS and ML reactors, the COD balance closed almost perfectly which was a good indication that there was minimal COD loss to methanogenesis and that VFAs were not consumed in these reactors.

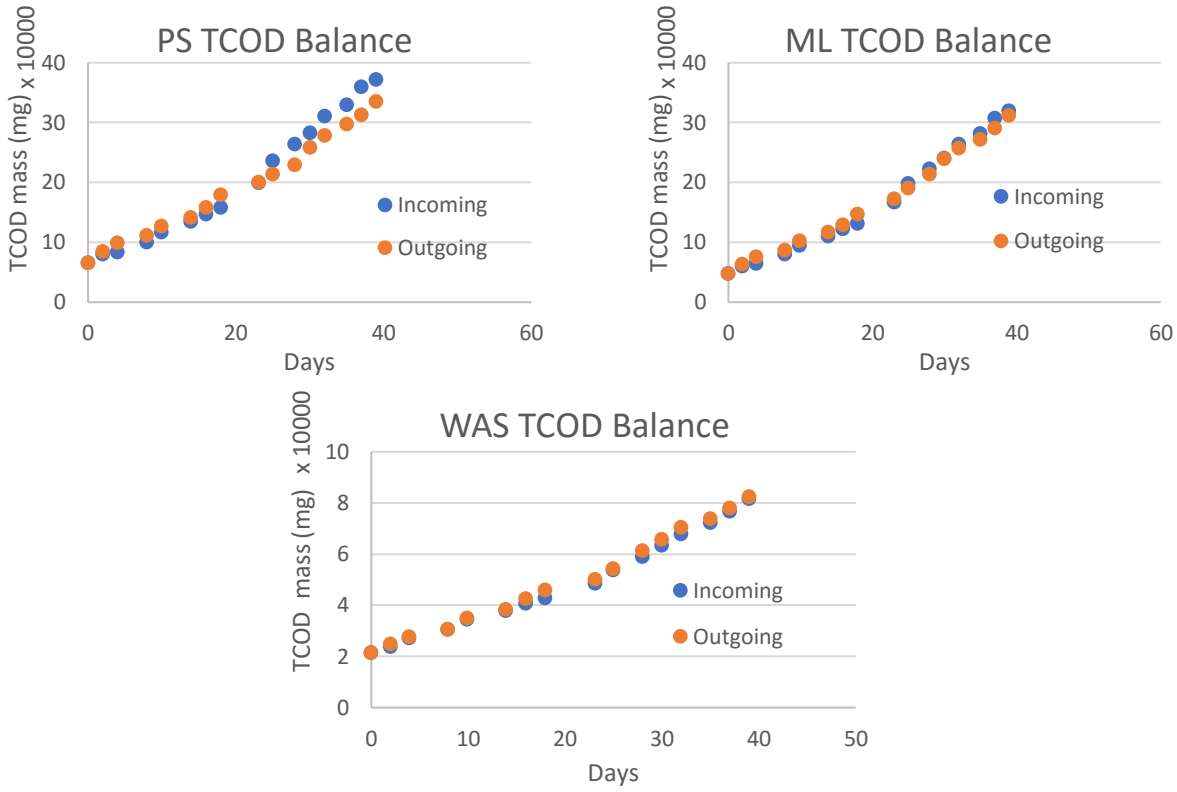

Figure 4.4: Total COD mass balances for all three reactors in the study period.

4.1.4 Degree of solubilization

Viewed collectively, the pH and COD mass balance results indicated that the conditions for hydrolysis and fermentation were favorable and hence the production of soluble substrates was examined. The degree of solubilization or yield of organic material by hydrolysis and fermentation were calculated using

the ratio of sCOD to total COD in the sludge samples (Ucisik & Henze, 2008) as per Eq. 4.1:

$$sCOD_{Yield} = \frac{sCOD_{Effluent}}{tCOD_{Influent}} \quad \text{Eq. 4.1}$$

Moreover, since the produced sCOD is typically not entirely made of VFAs, but also a non-VFA fraction, the VFA yield was calculated as the ratio of the VFA concentration in the effluent to the influent tCOD concentration as per Eq. 4.2:

$$VFA_{Yield} = \frac{VFA_{Effluent}}{tCOD_{Influent}} \quad \text{Eq. 4.2}$$

The estimated yield values are presented in Table 4.1. To compare with the literature, the yields from the influent COD as well as the influent VSS were calculated, and the results are summarized in Table 4.1. It can be observed that the yields of both sCOD and VFA were found to be within the ranges reported for similar studies. Although these studies were carried out in various conditions, they are somewhat relatable. Banister & Pretorius (1998) used batch reactors at room temperature with primary sludge from four Johannesburg plants with total solids ranging from 0.5 to 5.5% in an 8-day fermentation experiment. Even though this study's PS would be in the lower range of %TS, it appears that the yield was in the upper range. This would hint at excellent fermentability based on VFA yield per influent COD.

In the case of WAS, Ucisik & Henze (2008) evaluated sludges from six Denmark plants in a semi-continuous reactor setup to analyze acid fermentation at an SRT of 5 days and VSS of 30 g/l and 8.5 g/L. When compared to these values, the WAS used in the current study showed poor fermentability and fell in the lower range of soluble substrate production. For ML, there was no relatable literature at the studied ratio, but the yield was found to be effectively somewhere between PS and WAS closer to the PS yield. There is no evidence in Table 4.1 that adding WAS to PS improved the net yield of either sCOD or VFAs. Moreover, the standard deviation values for most yields were quite significant suggesting high variability

in yield values obtained in this study, possibly due to the variability in the loadings.

Table 4.1: sCOD and VFA yields summary

Process	PS	WAS	ML	Literature	Units
sCOD Yield	0.23±0.21	0.03±0.03	0.18±0.10	0.09-0.16 (PS)[3,1] 0.02- 0.05 (WAS)[3,1]	mg COD/mg CODi
	0.39±0.27	0.05±0.03	0.29±0.13	0.17-0.34 (PS)[4]	mg COD/mg VSSi
VFA Yield	0.23±0.22	0.01±0.01	0.19±0.15	0.10 (PS)[1]	mg COD/mg CODi
	0.36±0.24	0.01±0.02	0.28±0.19	0.25 (PS)[2] .07-0.18 (PS)[1] 0.011-0.023 (WAS)[2]	mg COD/mg VSSi

1. (Banister & Pretorious, 1998), 2. (Ucisik, 2008), 3. (Andreasen et al. 1997), 4. (Ferreiro & Soto, 2003)

It was decided that direct estimation of the net yield of VFA production from the feed sludges was not sufficient to assess the effect of WAS on PS fermentation since, for the ML reactor, the loading of PS into the reactor was less than that of the PS reactor. In the ML reactor, 38% of the feed solids were WAS, while 62% were PS. Hence, the yields of sCOD and VFA from the PS solids alone in the ML tests were calculated to assess whether adding WAS to the PS increased the production of sCOD and VFAs from PS solids. To determine the amount of effluent VFAs (or sCOD) due to WAS, the product of the yield and the solids fraction of WAS were calculated. Then, this amount was subtracted from the total effluent concentrations, and a revised yield was calculated for the PS solids with the previously described methodology for Eq. 4.1-2. Table 4.2 summarizes the estimated yields from PS alone in the ML reactor and compares them to the yields observed in the PS reactor. From Table 4.2 it can be observed that the PS yields increased by at least 10% in the ML reactor as compared to the PS reactor,

suggesting that there was a moderate increase in hydrolysis due to the presence of WAS. However, the standard deviation values were large in the context of the increment in yield signifying that the increment in yield had a significant variability and therefore reduced confidence. This variability was largely due to the variability in feed TCOD and VSS values. It is suggested that for a more accurate calculation of the effect of WAS on PS fermentability these values would need to be controlled more closely.

Table 4.2: PS yields in ML from only PS

	PS in ML	PS alone	% increment in yield		
sCOD Yield	0.25±0.13	0.23±0.21	22±22	mg COD/mg CODi	
	0.42±0.17	0.39±0.27	13±20	mg COD/mg VSSi	
VFA yield	0.28±0.21	0.23±0.22	19±29	mg COD/mg CODi	
	0.41±0.27	0.36±0.24	10±27	mg COD/mg VSSi	

4.1.5 VFA composition

The distribution of the individual volatile fatty acids was also characterized to obtain additional insight into the nature of the fermentation processes that were active. The dominant acids that were produced provide insight into the metabolic pathways for each reactor. It should be noted that this approach does not allow for inferences on population composition because organisms that produce a single acid (e.g., Propionate) have not yet been identified (Batstone et al., 2002).

Figures 4.5-4.7 summarize the VFAs that were measured in this study versus time. From these figures, it can be observed that the VFA speciation differed between reactors. The PS reactor had approximately 60% of acetate and propionate with the rest being higher order VFAs, the ML reactor had mostly

acetate and propionate, and the WAS reactor had mostly acetate with smaller fractions of other fatty acids.

Eastman and Ferguson (1981) reported that the production of different acid mixtures indicated differences in the metabolic pathways utilized by the organisms but not necessarily a change in the degree of solubilization. For example, one molecule of glucose will break down into two molecules of pyruvate, which is a key intermediate for different fermentation pathways. Then the different pathways convert pyruvate to a range of products including acetate, propionate, butyrate, ethanol, propanol, butanol, H2, and CO2 (Chen et al., 2017). In Figure 4.5, it can be seen that the PS reactor had a considerable amount of butyrate, (on average 30%), which is typical of a carbohydrate-rich substrate and food waste (Zoetemeyer et al., 1982). Also, the dominant species produced (propionate and acetate) suggest that PS fermentation followed a propionate type metabolic pathway (Chen et al., 2017). In this pathway, propionate can be produced either by the reduction of pyruvate with lactate as an intermediary or via the transcarboxylase cycle.

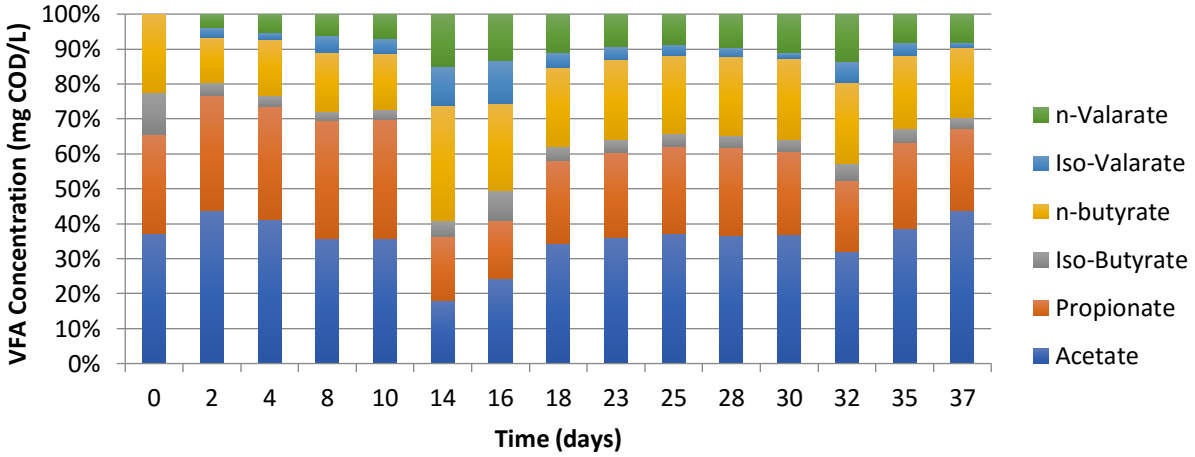

Figure 4.5:PS VFA composition

From Figure 4.6 it can be observed that VFA production in the ML reactor had a similar profile to the PS reactor with a high fraction of acetate and propionate.

This blend has been reported to be beneficial in the context of BNR since acetate will favor denitrification and propionate is taken up for P removal (Lee et al., 2014). On average, there was an increase of 5% in the overall fraction of acetate produced in the ML reactor when compared to the PS reactor. These results suggest that ML fermentation followed an acetate dominant metabolic pathway and this type of sludge could have increased potential in treatment plants. However, there was some variability over time in the fraction of propionate produced and this could present some stability challenges if the process is fine-tuned to a certain ratio.

It seems that the addition of WAS shifted the fermentation from a propionate type metabolic pathway to an acetate-ethanol one. This change could be due to the higher pH in the ML reactor. Fang & Liu (2002) reported that an elevated pH could increase the generation of acetate while decreasing butyrate production. The abundance of acetate is strongly associated with the functional enzymes in the acetyl-CoA pathway and syntrophic oxidation of ethanol or other long chain fatty acids and suggests that the sludge contained a large proportion of carbohydrates (Chen et al., 2017).

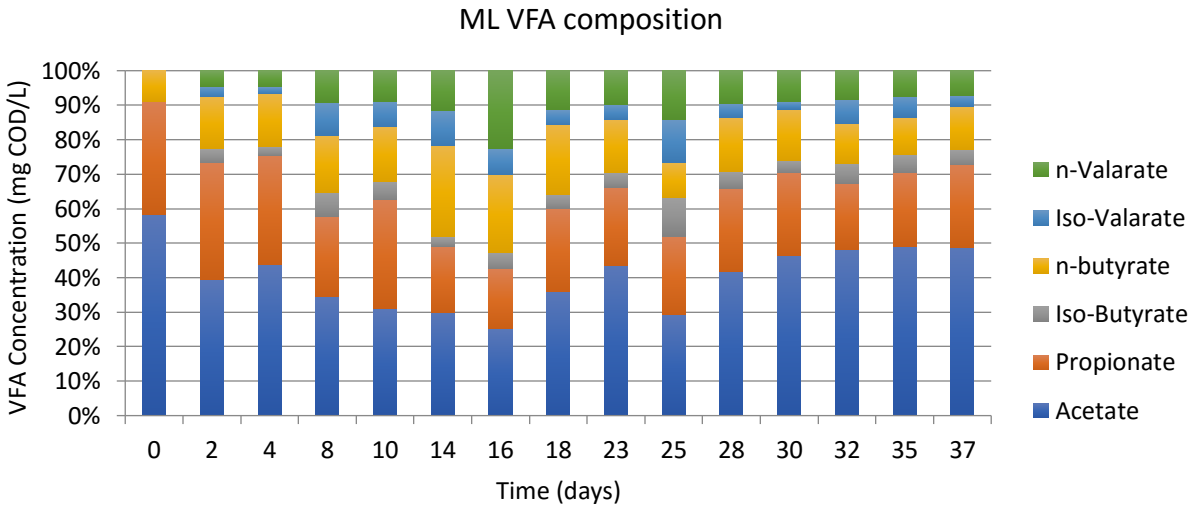

Figure 4.6: ML VFA composition

Figure 4.7 presents VFA production in the WAS reactor, and from this figure, it can be observed that there was a gap in the VFA composition data for a period of time due to analytical challenges. However, for the period when data was available it can be observed that WAS fermentation produced acetate exclusively during the first week, but then the fraction of acetate decreased quite rapidly. After the gap in data availability, acetate again became prominent but then followed a similar declining trend. While it was somewhat difficult to interpret these results, it appears that fermentation in this reactor followed the acetate-ethanol pathway (Chen et al., 2017).

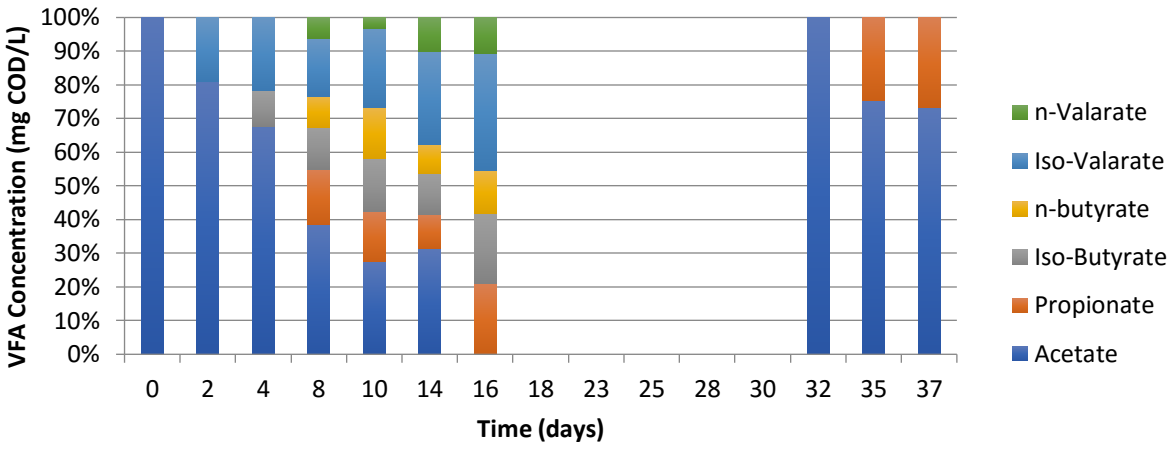

Figure 4.7: WAS VFA composition

4.1.6 Nitrogen and Phosphorus species

The responses of nitrogen (N) and phosphorus (P) species were also examined in this study as they can provide additional insight into the fate of N and P –bearing organic compounds in hydrolysis and fermentation. Banister et al., (1998) found that the amount of soluble P and N depended on retention time and solids, reaching maximum levels within 3 to 6 days with a 5.5% TS sludge. According to Banister et al., (1998), higher COD concentrations and the lower TKN/COD (0.05) and TP/COD (0.01) ratios are preferred in BNR processes. When these ratios are

too high, there is a risk of overloading the system with nutrients through the recycle streams.

One of the products of protein hydrolysis was soluble organic nitrogen. Furthermore, heterotrophs perform ammonification on soluble organic nitrogen to produce ammonia nitrogen. Hence, it was expected that ammonia levels would increase as the fermentation takes place. Table 4.3 present the yields of soluble nitrogen species compared across the three reactors and with reference literature values. In these tables, the ratios of TKN/COD the soluble fraction of all three bioreactors are below the ratios suggested by Bannister et al. (1998). This is particularly useful to maintain the nitrification-denitrification process further downstream and to avoid overloading the wastewater treatment system. Note that the effluent ammonia based on initial COD fell in the lower range when compared to similar studies, the main difference being the %TS of the sludge which the sludge from the literature (i.e., 5.5%) seems to have more when compared to the experimental values (0.6-1.6%). This agrees with the findings of Banister et al. (1998) who reported that the highest levels of nutrient release happened at higher suspended solids concentrations. Additionally, the pH for these systems averaged at 5.1±0.5 for PS, 5.5±0.4 for ML, and 6.7±0.2 for the WAS which was within the ideal pH for ammonia release (i.e., pH 5 to 7) as reported by Wu et al. (2009). This suggests that even though on the lower side when compared to literature, the ammonia released was reasonable.

Table 4.3: Soluble Nitrogen Species yields

Parameter	PS	WAS	ML	Lit.
TKN/COD ratio	0.009±0.002	0.025±0.006	0.012±0.002	0.05[1]
Ammonia-N (mg N/mg TCODin)	0.004 ±0.001	0.005 ±0.0007	0.004 ±0.0005	0.005 – 0.018[1]

[1](Banister et al., 1998)

In the BNR process, the concentration of phosphorus in the form of orthophosphate, reactive phosphorus, is a substrate that the PAOs will use to

grow. Since the effluent of the digester mixes into the anaerobic zone which also is the zone that contains most soluble P since PAOs use their internal reserves to metabolize VFAs. Therefore, effluent orthophosphate was also measured, and the results are summarized as follows. Table 4.4 presents the yields of soluble P species in the three reactors and compares them with reference literature values. A good TP/COD ratio is considered to be below 0.01, and the current results agree with this value. However, note that the production of soluble P, as opposed to nitrogen, falls in the upper range of the literature values suggesting a sludge with high P content. It is important to exercise caution with sludges that release high P content to avoid additional loading to downstream BNR. In full-scale plants, this will depend on process configuration and primary sludge composition, but supernatant pre-treatment has been suggested to avoid overloading the system when nutrient levels are too high (Banister et al., 1998). This was not considered to be the case for this study.

Table 4.4: Soluble Phosphorus yields

Parameter	PS	WAS	ML	Lit.
TP/COD	0.005±0.001	0.002±0.0003	0.003±0.0005	0.01[1]
O-PO4 (mg P/mg of initial COD)	0.013±0.002	0.007±0.0008	0.013±0.001	0.002-0.008[1]

[1](Banister et al., 1998)

4.1.7 Experimental hydrolysis rates

Lastly, hydrolysis rates were calculated for the experimental results. The complete enzymatic hydrolysis process described by Batstone et al. (2002) involves a multi-step process that reflects enzyme production, diffusion, adsorption, reaction and enzyme deactivation steps. It is assumed that acidogenic organisms (Z_{ad}) secrete an enzyme that hydrolyzes the biodegradable particulate substrate (S_{bp}), and then they benefit from the products of the reaction. A surface reaction kinetics formulation (Eq. 4.3) was used to determine initial rates of hydrolysis as per Dold et al. (1986) and the subsequent

methodology to calculate the rate from experimental data as presented by Ristow et al. (2005). In this formulation, k_{max} is the maximum specific substrate utilization rate constant for stored particulate substrate (S_{bp}) and K_s is the half-saturation coefficient. In addition to including the acidogenic biomass (Z_{ad}), this formulation also considers a maximum rate of hydrolysis under conditions of high substrate to biomass, which was hypothesized to be present in the current study since low VFA yields were attributed to low OHO concentrations in the influent. Additionally, the ratio $\left(\frac{S_{bp}}{Z_{ad}}\right)$ represents a food to organism ratio whereby the rate of hydrolysis will be reduced when there is food scarcity (i.e. not enough active sites to perform hydrolysis).

$$\boldsymbol{rate_{hydrolysis}} = \frac{\boldsymbol{k_{max}}\left(\frac{\boldsymbol{S_{bp}}}{\boldsymbol{Z_{ad}}}\right)}{\left(\boldsymbol{k_s}+\frac{\boldsymbol{S_{bp}}}{\boldsymbol{Z_{ad}}}\right)}\boldsymbol{Z_{ad}} \qquad \textbf{Eq. 4.3}$$

To calculate the rate of hydrolysis with this expression an estimation of the acidogenic biomass concentration (Z_{ad}) is needed using Eq 4.4. Assuming that the Yield constant of acidogenic biomass (Y_{ad}) is 0.22 and that b_{ad}, the acidogens endogenous respiration constant, taken as 0.2 d^{-1},as per Ristow et al. (2005), and an HRT (R_h) of 6 days, the only unknown is the rate of acidogenesis.

$$\boldsymbol{Z_{ad}} = \frac{\boldsymbol{Y_{ad}}\times\boldsymbol{rate_{acidogenesis}}\times\boldsymbol{R_h}}{(\mathbf{1}+\boldsymbol{b_{ad}}\times\boldsymbol{R_h})} \qquad \textbf{Eq. 4.4}$$

The rate of acidogenesis was initially suggested by Ristow et al. (2005) to be half of the rate of hydrolysis. However, when the ratio of effluent VFA to effluent sCOD was taken for the experimental data it was found that most of the sCOD was present as VFA. Therefore, the rate of acidogenesis was practically the same as the one determined for hydrolysis, see Appendix A for the calculation of this ratio. To estimate an initial first-order hydrolysis rate, Eq. 4.5 can be used. For this initial estimate, the term (b_{ad}*Z_{ad}) was neglected because it typically only accounts for 1% of the total value and because it was assumed that the feed did not include any acidogenic biomass. To use Eq. 4.5, the biodegradable particulate

fractions for the influent and the effluent were determined under steady-state conditions. The particulate COD for the feed was determined by subtraction of the sCOD from TCOD. An assumed fraction of 33% was initially attributed to the unbiodegradable particulate COD so that an initial estimate of Sbpi (influent biodegradable particulate substrate) could be made (Ristow et al., 2005). In the case of WAS this value was significantly higher since it is expected that WAS contains less biodegradable material than primary sludges. To determine Sbp in the effluent, the particulate COD was estimated by subtraction. If the unbiodegradable effluent particulate was not transformed in the bioreactor (i.e., Supi=Sup), then the Sbp in the effluent was equal to the effluent particulate COD minus the unbiodegradable fraction.

$$\boldsymbol{rate_{hydrolysis} = \frac{Q}{V}\left(S_{bpi} - S_{bp}\right) + b_{ad} \times Z_{ad}} \qquad \textbf{Eq. 4.5}$$

With the calculated first estimate of the rate of hydrolysis, Eq. 4.4 was solved for the acidogenic biomass. This value was then substituted in Eq. 4.3 to calculate a revised rate of hydrolysis based on surface reaction kinetics. The resulting hydrolysis rates and the corresponding first-order constants are summarized in table 4.5. Literature suggested that the anaerobic hydrolysis constant is 0.5 so the experimental values fall in the lower range if calculated this way. Also, note that WAS had negative values for the rates, this is due to the small amounts of VFAs obtained as well as due to the high variability in feed values.

Table 4.5 Calculated rates of hydrolysis via first order and surface reaction kinetics

		First-order		Surface Reaction	
		Avg	St.dev	Avg	St.dev
PS	R_{hydr}	156.5	511.3	213.2	68.5
	k_h	0.04	0.1	0.03	0.01
ML	R_{hydr}	18.22	379.42	24.09	10.54
	k_h	0.01	0.05	0.004	0.002
WAS	R_{hydr}	-13.41	124.04	-5.65	6.23
	k_h	-0.0003	0.04	-0.002	0.003

4.2 BioWin simulations

The use of models that simulate anaerobic fermentation may assist with process control and optimization. The following section describes how BioWin's Activated Sludge and Anaerobic Digestion Model (ASDM) was tested with the objective of evaluating the ability of the model to predict experimental results and identifying areas where the model may be improved. A discussion of how the model was set up is initially presented. Then, a critical evaluation of the model performance is presented to identify the areas where the model could be improved. Lastly, alternate methods to improve the ASDM model performance are evaluated.

4.2.1 Model Design and influent considerations

As previously discussed in the Literature Review, the ASDM model is an integrated model that can predict the performance of full-scale WWTPs. BioWin has two elements that model anaerobic digestion; the anaerobic digester unit (AD) and the variable volume Activated Sludge reactor (VVR). In BioWin, the same kinetic formulation for hydrolysis is used in both the anaerobic digestion and activated sludge units. However, different reduction factors (η_{fe}) for hydrolysis are applied in the anaerobic zone of activated sludge (0.04), and anaerobic digester units (0.5). These (η_{fe}) factors represent an empirical reduction to the hydrolysis rate and are meant to capture the effect of the anaerobic environment on the breakdown process. The default values have been previously determined to describe experimental data, but the evaluation of the two applications has historically been conducted separately. It is, unclear why the values of these factors are so different. The main physical difference between the two systems is the closed versus open headspace that impacts upon liquid-gas transfer. The AD includes the headspace, which causes a small effect in pH because of CO_2 accumulation. In the upcoming results, the AD unit was focused on since it most closely reflected the experimental set up employed in this study.

The BioWin simulator includes the viable heterotrophic biomass content as a state variable in all streams since it has been found to affect fermenter process performance (Dold et al., 2010). Traditionally this fraction in raw wastewaters has been assumed to be relatively small, (default value in BioWin is 2% of the total COD as heterotrophic biomass in raw wastewater). However, oxygen uptake rate (OUR) studies performed by EnviroSim on the Elmira influent in 2013 showed that the biomass concentration fluctuated from 6%-12% (Dold, 2013). Hence, in this modeling exercise, a biomass concentration of 7% of influent COD was assumed as it was within the range reported by Dold (2013).

Another important change in the default values for the influent element in BioWin was the ammonia fraction of the influent element. This fraction describes the fraction of ammonia and therefore the fraction of soluble organic nitrogen in the influent TKN concentration. The ammonia fraction of the influent was found to average 0.45 g NH3/g TKN, which was lower than the default value used in BioWin of 0.66 g NH3/g TKN.

With these preliminary estimates of OHO fraction in the influent and the ammonia fraction of TKN, an initial model was developed. Feed values to the bench scale reactors were initially calibrated, and then the ASDM model was tested to determine the hydrolysis rate constants that best matched the test data.

4.2.2 Model Calibration

4.2.2.1 Feed calibration

The ASDM model was initially configured to reflect the experimental feed values. The PS model in BioWin consisted of the influent element and a primary clarifier and was employed to characterize the feed to the PS reactor. The underflow of the clarifier was fed to the AD unit according to the experimental feeding schedule. An SRT of 6 days was maintained in the reactor unit, and the temperature of the model was set to 20˚C.

The model predictions for the PS feed in terms of pH, solids, and COD are compared to the experimental values in Figure 4.8. A parameter that was relatively easy to fit for the feed was pH since the operation of the primary clarifier was not expected to cause substantial changes in pH and was one of the input values for the influent element. Increasing in complexity, COD was another input value for the influent element. However, its concentration depended on how the primary clarifier was operated. The clarifier had a sludge blanket of 10% of the settler height and was set to operate at 60% TSS removal which resulted in 40% COD removal. However, these removal values fluctuated slightly through the dynamic runs. On a similar note, suspended solids were also dependent on primary clarifier operation, and the influent element did not specify this value, so it was challenging to achieve a good fit of the feed VSS. While pH has an almost perfect fit, the solids and COD were manipulated until the predicted values reflected the overall trend of the experimental results.

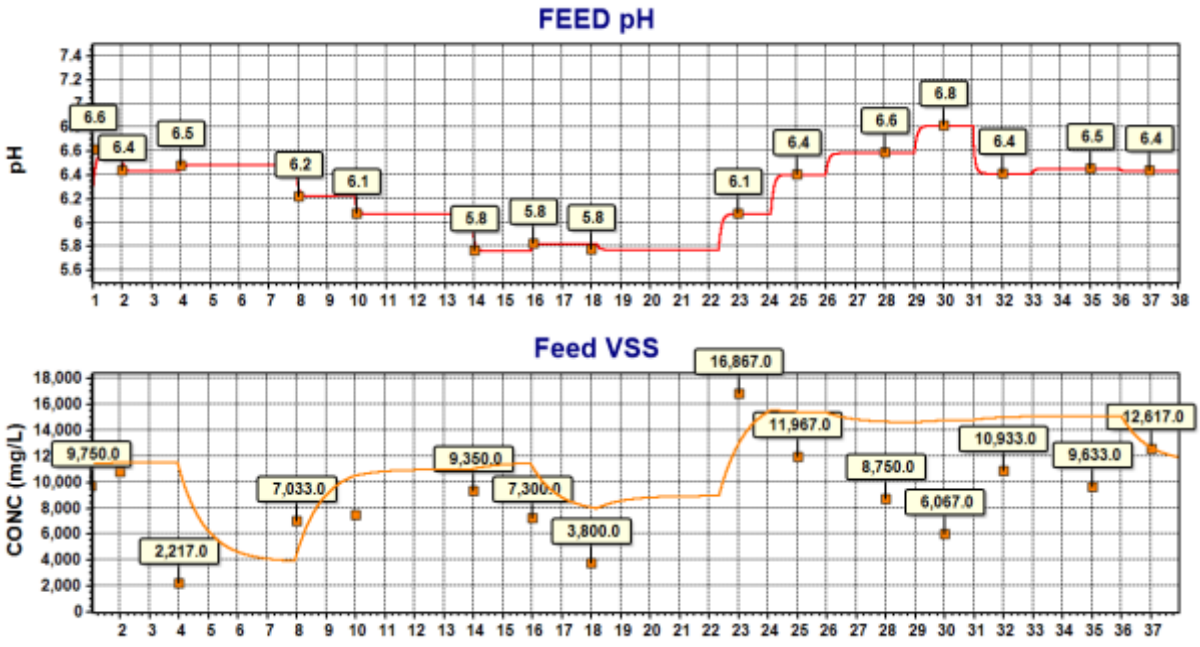

Figure 4.8: Calibration results for PS feed in terms of pH, VSS, and TCOD (Cont'd)

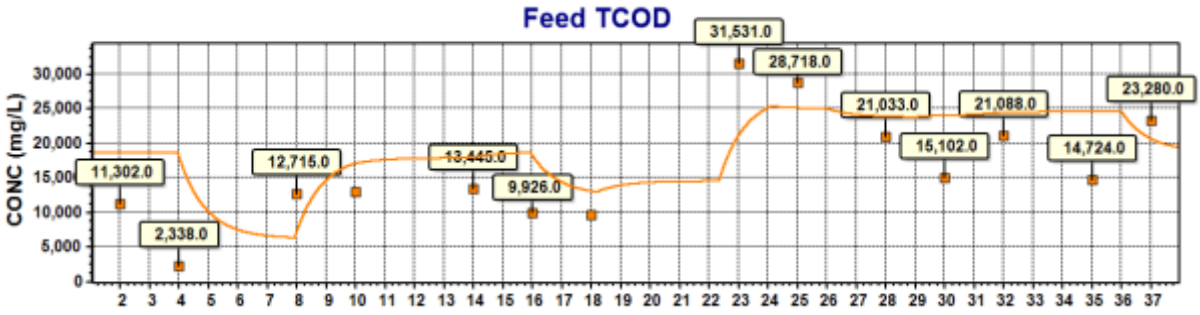

Figure 4.8: Calibration results for PS feed in terms of pH, VSS, and TCOD

Once the PS feed calibration was deemed to reflect the experimental PS feed values appropriately, a 5-stage BNR process was added to the model to generate a representative characterization of the WAS collected at the plant. A primary fermenter operating under default conditions was included in the model to provide rbCOD to the anaerobic zone in a similar way that the Elmira plant is configured. Internal recycles were set so that P removal and nitrification-denitrification were active at 2.6Q (where Q is the flow into the process train) and the recycle activated sludge (RAS) was set to 60% of the flow from the feed.

Figure 4.9 below shows the WAS feed model fit with the experimental values in terms of pH, TCOD, and VSS. With respect to pH, the feed values fit the test data well. Additionally, despite a few outliers the predicted total COD and VSS concentrations followed the experimental trend. Although, it is apparent that the model tended to under predict VSS loading. It is evident that the further downstream into the process, the variability in feed concentrations had less effect, resulting in less unpredictable behavior.

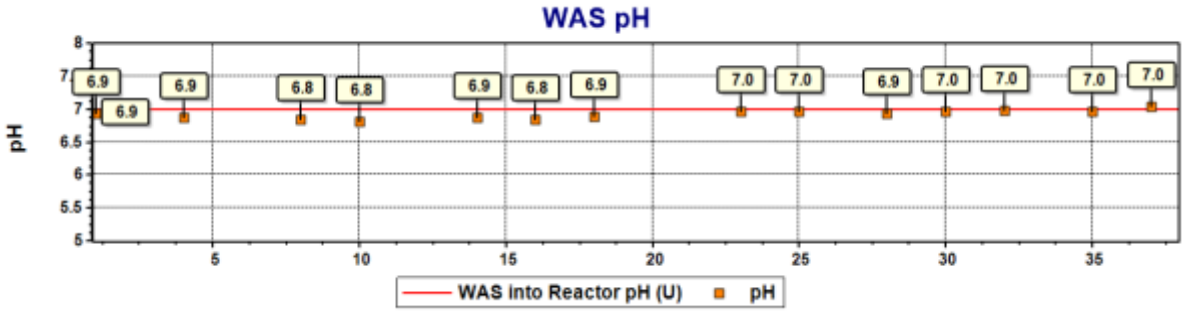

Figure 4.9: Calibration results for WAS (Cont'd)

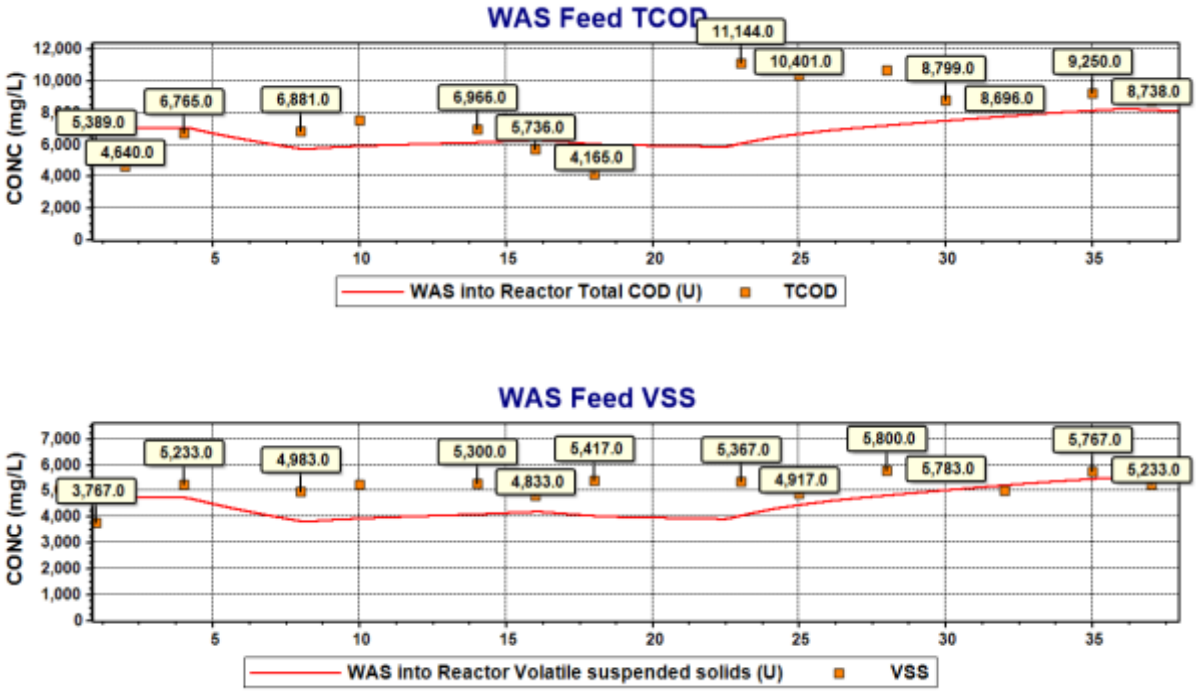

Figure 4.9: Calibration results for WAS

Once the primary and secondary models were established, a mixer was added to the third model to blend the two streams together as per the experimental rationale to fit the model to experimental values. Figure 4.10 shows the calibration results for ML in terms of pH, TCOD, and VSS. From this figure it can be observed how the trends for both previous reactors compounded. pH again fit well while the solids and TCOD had some outliers that the model was not able to capture, but the overall trends were reflected well.

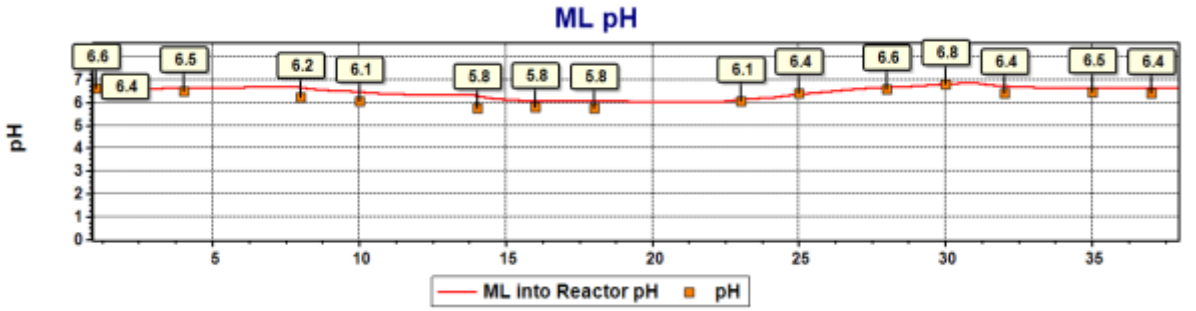

Figure 4.10: Calibration results for ML (Cont'd)

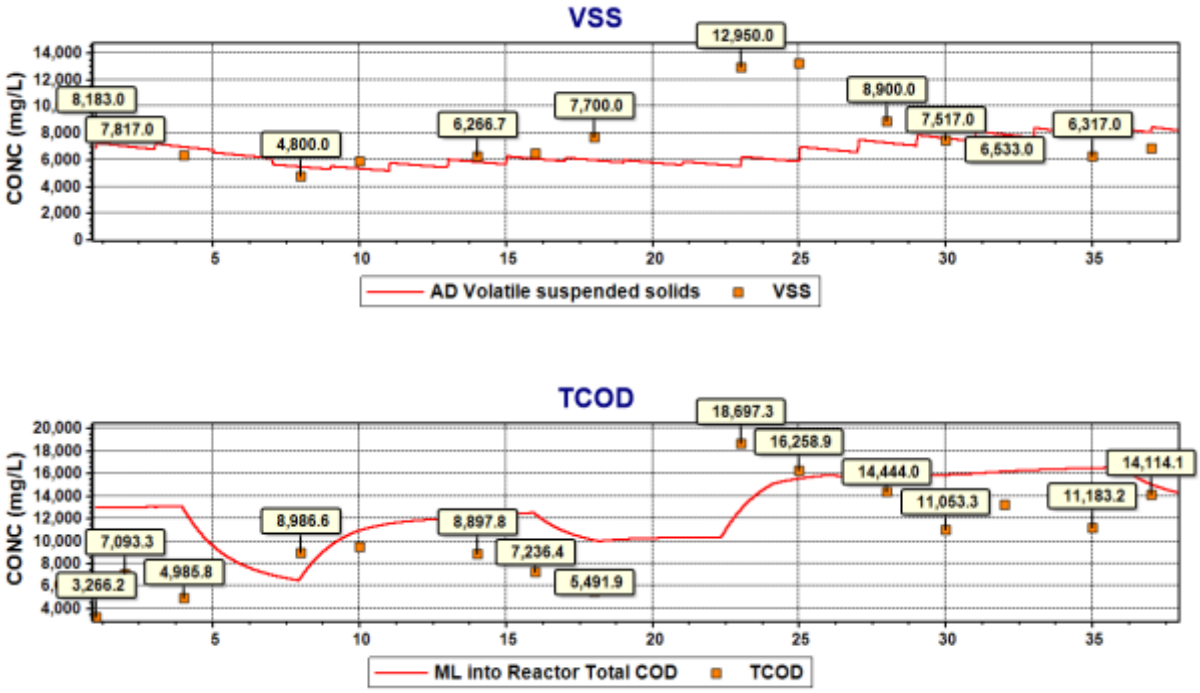

Figure 4.10: Calibration results for ML

4.2.2.2 Model Predictions and parameter estimation

Once the feed values were established to reflect the experimental results, the ASDM anaerobic digester was added to the models to carry out modeling of the acid-phase fermentation of the sludges. The hydrolysis expressions employed in BioWin's ASDM are shown in table 4.6. Note that the (η_{fe}) factor reduced the rate of hydrolysis in anaerobic conditions as previously discussed. The default hydrolysis rate correction factor (η_{fe}) of 0.5 was modified until the model predictions best fit with the experimental results. The method of least squares was used to determine the appropriate fit, with the goal of determining the (η_{fe}) factor that yielded the lowest sum of squares. The fitting was conducted separately for multiple responses that were measured in the fermenters with the goal of determining the values that best fit each of the responses.

Table 4.6 Hydrolysis expressions in the Activated Sludge and Anaerobic Digestion Model (ASDM) from BioWin

Process	Stoichiometry								Process Rate
	XSP	Xsc	Xon	Xop	Sbsc	NH3-N	Nos	PO4P	
Hydrolysis of XSCOD	- 1				1				$k_h \times \eta_{fe} \times \frac{k_o}{k_o + D_o} \times \frac{k_{no}}{k_{no} + NO3N} \times \frac{\frac{X_{sp}}{Z_{bh}}}{k_x + \frac{X_{sp}}{Z_{bh}}} \times Z_{bh}$
Hydrolysis of XON			-1				1		$k_h \times \eta_{fe} \times \frac{k_o}{k_o + D_o} \times \frac{k_{no}}{k_{no} + NO3N} \times \frac{\frac{X_{sp}}{Z_{bh}}}{k_x + \frac{X_{sp}}{Z_{bh}}} \times Z_{bh} \times \frac{X_{on}}{X_{sp}}$
Hydrolysis of XOP				-1				1	$k_h \times \eta_{fe} \times \frac{k_o}{k_o + D_o} \times \frac{k_{no}}{k_{no} + NO3N} \times \frac{\frac{X_{sp}}{Z_{bh}}}{k_x + \frac{X_{sp}}{Z_{bh}}} \times Z_{bh} \times \frac{X_{op}}{X_{sp}}$
Adsorption of Colloidal COD	1	-1							$K_{ads} \times X_{sc}$
Ammonification						1	-1		$K_{amm} \times N_{os} \times (Z_{bh} + Z_{bp})$

In the case of PS, the (η_{fe}) factor was tested across a range of values. In Table 4. 7 the results from the least squares are presented. It can be observed that the range of values were on the lower end of the typical range of values as the soluble substrates produced were predicted better. However, note that there was an inconsistency when all species are looked at together. The higher end of the scale better predicted the solids concentrations in the reactor, while the lower end better described the soluble species. In the case of PS, a factor of 0.2 was found to result in the best fit of predicted and observed VFA, sCOD, and NH3 production. This factor however also fit the TCOD and Solids responses when compared to the other tested values.

Table 4.7 Least Squares comparison for An. Factor in PS reactor

(η_{fe})	0.04	0.1	0.15	0.2	0.25	0.3	0.4	0.5	0.8	0.9
TSS	16151	14816	38498	14195	27783	17560	13254	7938	6950	7439
VSS	15869	14157	40571	13013	28842	16413	12792	7268	8788	9518
TCOD	25021	24798	89318	25380	89633	25160	88903	88647	89300	89291
sCOD	204222	30275	24942	6448	52456	22297	97948	128257	171349	174637
NH3	942	245	56	30	194	216	764	1252	489	508
VFA	270039	44897	29147	10223	56625	22066	32972	95284	72918	73222

The calibrated model predictions for a (η_{fe}) value of 0.2 are presented in Figure 4.11 in term of TCOD, NH3, and VFA. The TCOD responses had a closer fit at the beginning of the test and as time passed the fit worsens. The fit with regards to the ammonia concentrations was the closest of the responses. With respect to VFA, the model still achieved a good job fit of this response despite the outliers on day 14 and 16. Additionally, it can be observed that at the very start and at the end of the study period the fit decreased in quality. It can be observed that 15-20% of TCOD converted to VFAs in the models for PS. Moreover, the reactor generated up to 3000 mg/L of VFAs, which was consistent with the experimental data. The short-term variation observed in the figures for ammonia and VFAs was due to the feeding schedule. After feeding, the concentrations of soluble species were expected to increase as hydrolysis proceeded.

PS

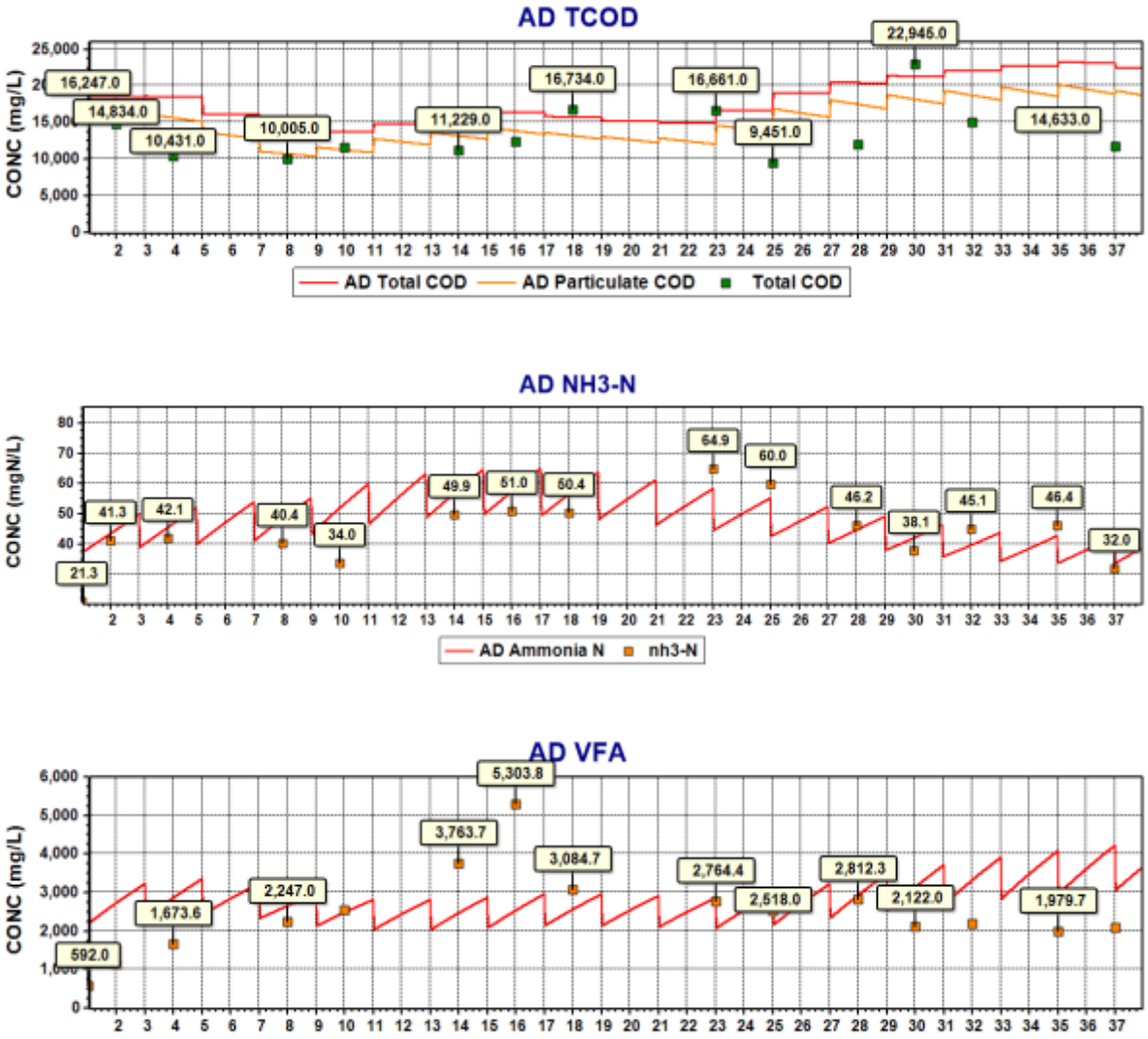

Figure 4.11: PS baseline model predictions with respect to TCOD, NH3, and VFA

In the case of WAS, the (η_{fe}) factor was also tested across a range of values. However, in this case the model configuration was set up to represent a full-scale plant so that the model could produce a WAS that was representative of that collected experimentally. Therefore, it was necessary to include an additional PS fermenter that fed into the BNR process. Hence, the model had a configuration with two anaerobic digesters, one for primary sludge that fed into the process train, and a second one that was the reactor meant to study the WAS

fermentation. This "primary" fermenter was different from the test reactor used to investigate the hydrolysis of WAS and was set up based on the PS calibrated model since it seemed to provide a better fit than the default value used in BioWin. Hence, the primary digester was operating with a factor of 0.2, while the range of values was tested for the secondary digester receiving WAS.

Table 4. 8 presents the results from the least squares analysis of the WAS fermentation simulations. It can be observed that the range of best fit values focused more on the lower end of the range tested. However, note that the most promising factor was 0.04. Simulations with values of 0.03 and 0.05 were attempted however the model could not find a solution with these values. In the case of WAS, it was deemed that a factor of 0.04 was the best fit of predicted and observed VFA, sCOD, and NH3 production. This factor however also fits relatively well with the TCOD and Solids errors when compared to the other tested values.

Table 4.8 Least Squares comparison for An. Factor in WAS reactor

(η_{fe})	0.04	0.1	0.2	0.3	0.4	0.45	0.5
TSS	5690	6956	126474	7200	7274	7281	7286
VSS	4056	5439	24556	5708	5789	5797	5803
TCOD	17923	19721	20050	20050	20138	20144	20148
sCOD	1849	2394	2550	2550	2604	2610	2615
NH3	111	246	278	278	288	289	289
VFA	2956	4403	4678	4678	4769	4779	4788

The model predictions for a (η_{fe}) value of 0.04 are presented in Figure 4.12 in terms of TCOD, NH3, and VFAs. With regards to TCOD, the figure shows that this species was mostly underpredicted, with a better fit at the beginning of the study rather than at the end where most outliers were located. In terms of effluent ammonia, the model also has a good fit. However, discrepancies in the first half of the study were noticeable while the fit improved towards the end of the experiment. For the WAS sample, the amount of VFA generated was extremely small, and this data was considered suspect as it was within the lower limit range

of the GC apparatus used to measure this constituent. Figure 4.12 demonstrates that the model largely over predicted the concentration of VFAs produced.

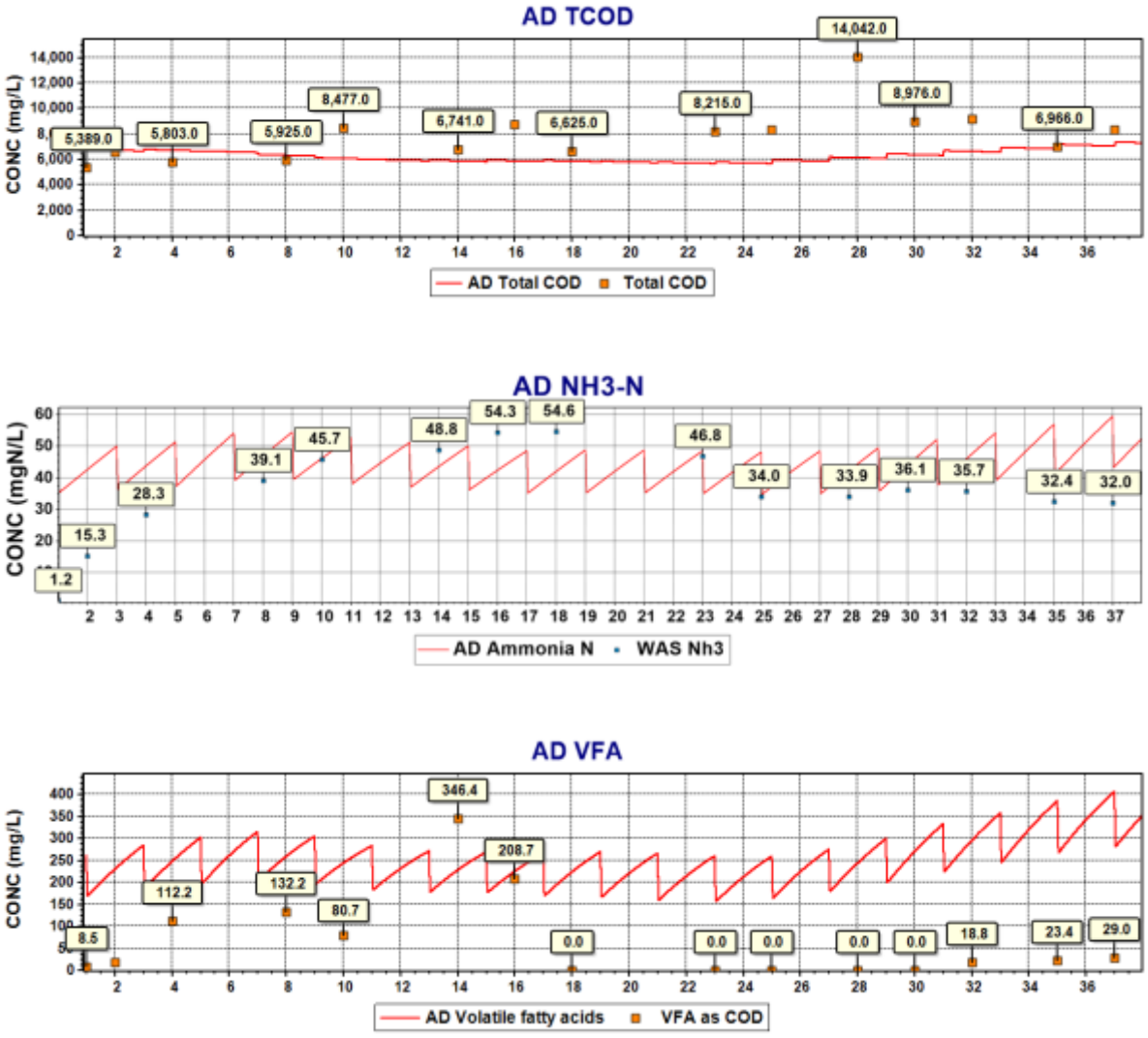

Figure 4.12: WAS baseline model predictions with respect to TCOD, NH3, and VFA

In the case of ML, the (η_{fe}) factor was tested across a range of values and Table 4. 9 presents the best fit results from the least squares. From Table 4.9 it can be seen that the lower the factor, the lower the hydrolysis rate and therefore the solids data fit better when tested at the lowest factors. However, slightly increasing the factor yielded much better results for the soluble species while still confirming that hydrolysis was happening. In the case of ML, a factor of 0.1 was the found to result in the best fit of predicted and observed VFA, sCOD, and

NH3 production. This factor however also fit the TCOD and Solids concentrations well when compared to the other tested values.

Table 4.9 Least Squares comparison for An. Factor in ML reactor

(η_{fe})	0.04	0.1	0.2	0.3	0.4	0.5
TSS	19958	24676	44599	71422	78526	81517
VSS	16756	21398	44299	78763	88290	92397
TCOD	16151	15844	15806	15987	15994	15992
sCOD	60203	4268	20491	41699	47771	50395
NH3	592	36	278	661	778	829
VFA	85849	10500	23686	42024	45501	46300

With regards to the ML reactor with a (η_{fe}) value of 0.1, the COD balance also matched closely particularly in the first half of the study. Ammonia effluent concentrations were also better fit in the first half of the study with most outliers happening between day 16 and day 25. The VFA production fit was also improved. Although it appears that the model predicted a more stable operation than the one measured experimentally, the model predicted the generation of about 1500 mg/L of VFA as COD, which represents about 12% of the influent COD, which somewhat agreed with the experimental results.

ML

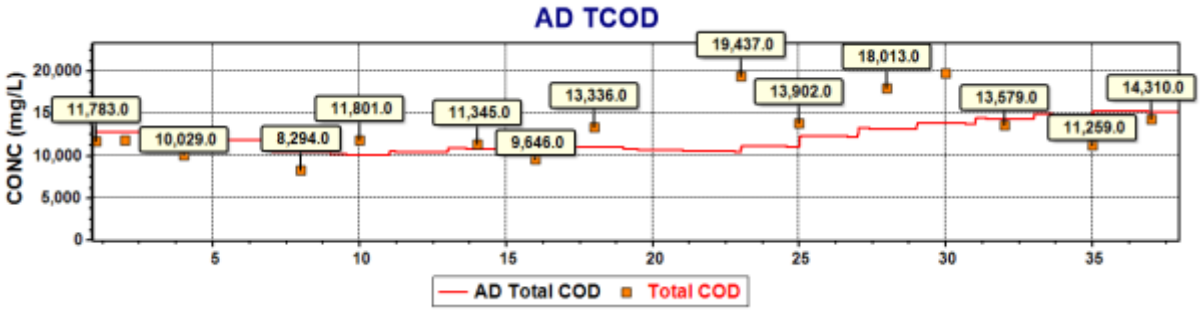

Figure 4.13: ML baseline model predictions with respect to TCOD, NH3, and VFA (Cont'd)

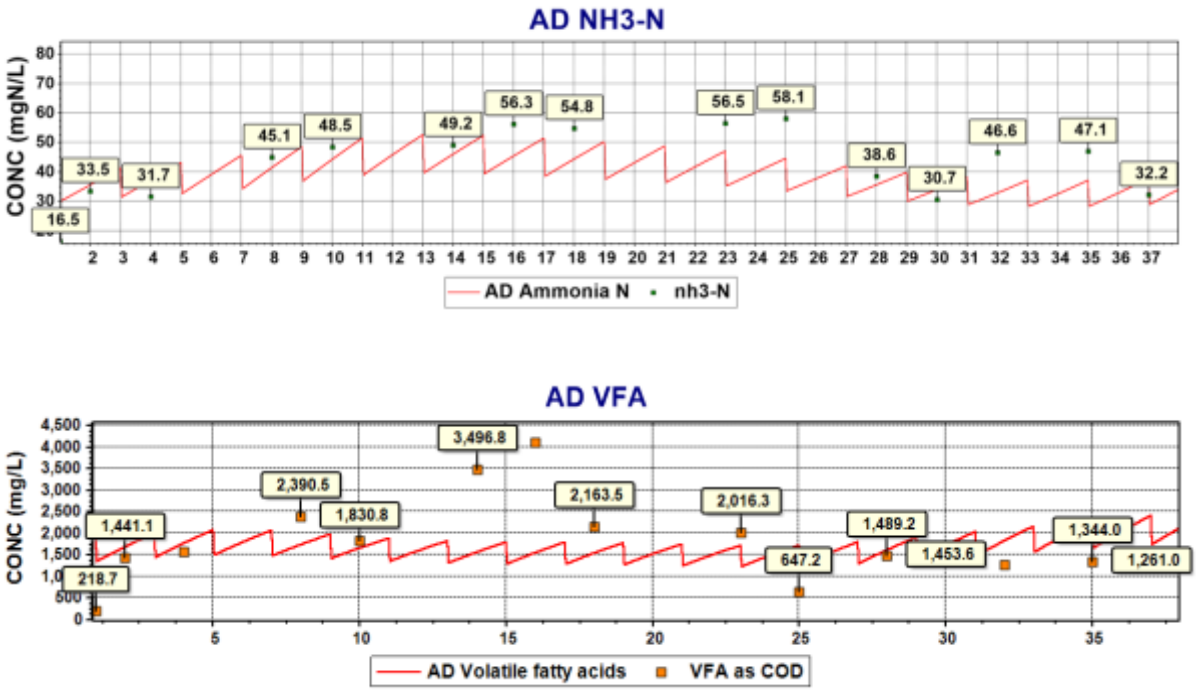

Figure 4.13: ML baseline model predictions with respect to TCOD, NH3, and VFA

In summary, the model calibration of the fermentation reactors found different hydrolysis rate constants provided the best match of measured VFA production and COD removal. From the summary in Table 4.10 it can be seen that the rate constants ranged from 0.04 to 0.2, while the default value is 0.5, across the samples suggesting that the sludge composition and resulting reactor conditions played an important role in the fermentation reactions.

Table 4.10: Summary of An. Factors used for hydrolysis

Parameters	Defaults	PS	WAS	ML
Hydrolysis rate [1/d]		2.1		
An Hydr Factor AD [-]	0.5	0.2	0.04	0.1

4.3 Evaluation of acid-phase anaerobic digestion models

As previously demonstrated, it was found that different (η_{fe}) factors were required to provide the best fit of the experimental data for the various

fermenters. The need for differing (η_{fe}) factors in this regard poses challenges for predictive use of the models. This section addresses efforts that were carried out to extend the ASDM model to improve the universality of the hydrolysis expression. From the literature review, it was found two major aspects of hydrolysis that the ASDM model is missing are product inhibition and the role of enzyme availability on the hydrolysis rate.

4.3.1 Product Inhibition

Product inhibition was evaluated through the incorporation of the terms described in Eq. 4.6 (where Ksb is the inhibition constant, and Sbsc is the soluble substrate produced by the hydrolysis reaction) into the hydrolysis process. The rationale for using such an expression was that at high Sbsc concentrations, the factor would be reduced while a smaller amount of soluble product would result in a smaller inhibitory effect:

$$\frac{\boldsymbol{Ksb}}{\boldsymbol{Ksb}+\boldsymbol{Sbsc}} \qquad \textbf{Eq. 4.6}$$

In this implementation Eq .4.6 replaced the (η_{fe}) factor that is used by default in BioWin in the hydrolysis rate expression, thereby creating a more dynamic expression that responds to environmental conditions rather than requiring fitting of the (η_{fe}) factor itself. It would be useful for increasing the universality of the model if the same Ksb improved the model for all three reactors. To implement this function in the hydrolysis expression, the model builder functionality of BioWin was employed. In this regard, the entire anaerobic digestion model was not needed since only the hydrolysis processes were the focus of this study. The extension consisted of five processes that replace the same five processes in BioWin's ASDM. Table 4.11 summarizes the proposed extension to the current form of ASDM:

Table 4.11: Product inhibition extension for ASDM

Process	Stoichiometry								Process Rate
	XSP	Xsc	Xon	Xop	Sbsc	NH3-N	Nos	PO4P	
Hydrolysis of XSCOD	- 1				1				$k_h \times \frac{k_o}{k_o + D_o} \times \frac{k_{no}}{k_{no} + NO3N} \times \frac{\frac{X_{sp}}{Z_{bh}}}{k_x + \frac{X_{sp}}{Z_{bh}}} \times Z_{bh} \times \frac{K_{sb}}{K_{sb} + S_{bsc}}$
Hydrolysis of XON			-1				1		$k_h \times \frac{k_o}{k_o + D_o} \times \frac{k_{no}}{k_{no} + NO3N} \times \frac{\frac{X_{sp}}{Z_{bh}}}{k_x + \frac{X_{sp}}{Z_{bh}}} \times Z_{bh} \times \frac{K_{sb}}{K_{sb} + S_{bsc}} \times \frac{X_{on}}{X_{sp}}$
Hydrolysis of XOP				-1				1	$k_h \times \frac{k_o}{k_o + D_o} \times \frac{k_{no}}{k_{no} + NO3N} \times \frac{\frac{X_{sp}}{Z_{bh}}}{k_x + \frac{X_{sp}}{Z_{bh}}} \times Z_{bh} \times \frac{K_{sb}}{K_{sb} + S_{bsc}} \times \frac{X_{op}}{X_{sp}}$
Adsorption of Colloidal COD	1	-1							$K_{ads} \times X_{sc}$
Ammonification						1	-1		$K_{amm} \times N_{os} \times (Z_{bh} + Z_{bp})$

This model initially calibrated Ksb to the experimental data for all reactors. In the case for PS, the initial guess values for Ksb chosen for the model come from the Sbsc concentration output from the closest prediction using the native BioWin model. For WAS and ML, the Ksb factor to be tested was the same chosen for PS since the objective of this section is to investigate the universality of these new process rate expressions. Observe how the slope varies with time, each peak would represent a feeding, and the slopes show the production of rbCOD at each SRT. Observe that the concentrations kept in the reactor are quite low. However, they are not constant as the anaerobic factor would suggest. If this process is indeed subject to product inhibition, then this graph might be proof that using a single factor to describe the inhibition is insufficient. Moreover, since the Sbsc concentration is in the range of 2 – 18 mg COD/L, it was deemed appropriate to analyze a range of K_{sb} values in increasing order of magnitude 1,10, 50, and 500. Since it was found that the model errors were smaller values on the lower side of the range, the values were expanded to consider finer values from 0 to 1.

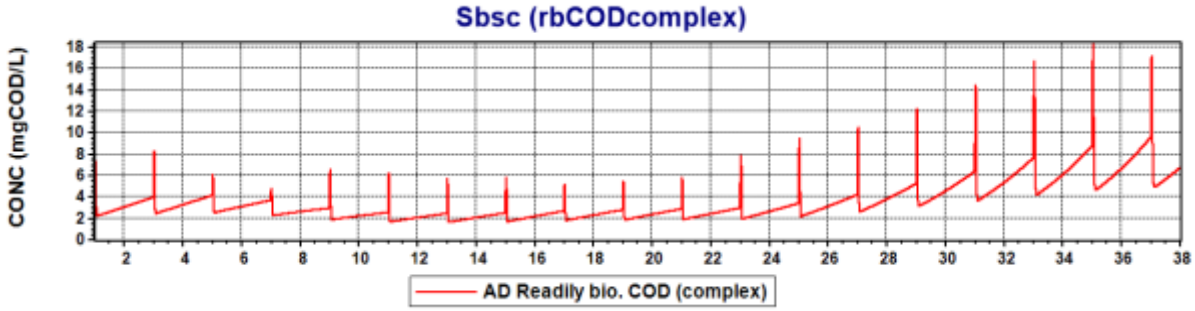

Figure 4.14: rbCOD produced in PS inhibition model

The best fit value for Ksb was found to be 0.5 since the higher magnitude values decreased the quality of fit as per the squared errors methodology. Table 4.12 below shows the error comparison between the product inhibition model and the default BioWin model., In general the errors appear to have a minimum with a Ksb of 0.35. When these errors are compared to the ones obtained by the original ASDM model (nfe) they also perform better for all species. The prediction errors

were similar with respect to solids and TCOD responses. The inhibition model had slightly better predictions of NH3, sCOD, and VFA production.

Table 4.12: PS inhibition model squared errors

Ksb	0.05	0.1	0.2	0.3	0.35	0.4	0.5	0.6	0.7	nfe = 0.2
TSS	14941	14709	14612	14672	14726	14789	14930	15081	15235	14195
VSS	14242	13881	13648	13633	13660	13702	13810	13940	14080	13013
TCOD	24834	25003	25217	25330	25359	25380	25399	25404	25401	25380
sCOD	21475	10676	5447	4565	4585	4739	5249	5872	6523	6448
NH3	191	94	39	26	24	25	29	35	41	30
VFA	33487	18688	10658	8562	8195	8043	8096	8384	8776	10223

For a Ksb value of 0.35, Figure 4.15 shows the residual errors plotted against the species of interest. In this case, the plots for ammonia, VFA, and sCOD were analyzed since the low errors in these species were considered when choosing the Ksb value. The raw residuals plots indicate that although the data set was small the residuals were mostly randomly distributed for soluble species. In the case for the outliers of the ammonia and VFA residuals these belonged to specific points. For example, in the case of VFAs the model was not able to capture the concentrations around day 15. Without these, the plot seems randomly distributed. Likewise, for sCOD the inability of the model to capture the concentrations in the initial week of the run suggests a trend to overpredict values but the model predictions improved for the latter part of the dataset.

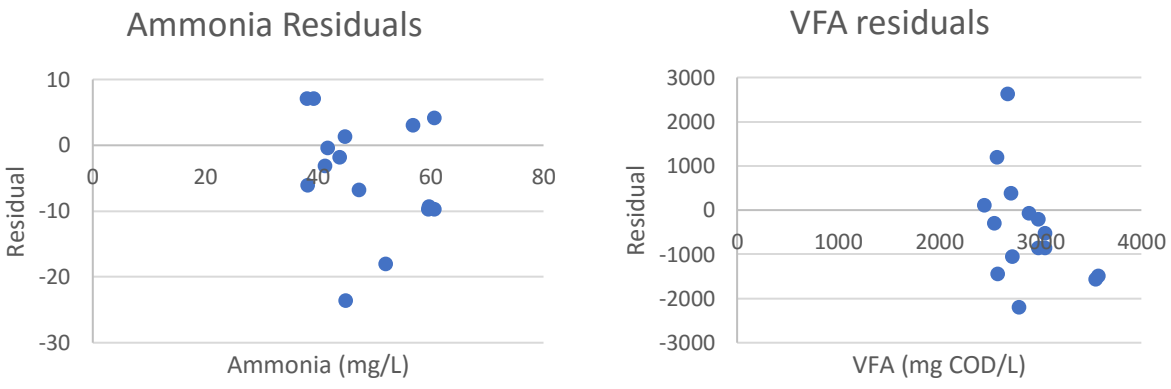

Figure 4.15: Residual plot for PS inhibition model (Cont'd)

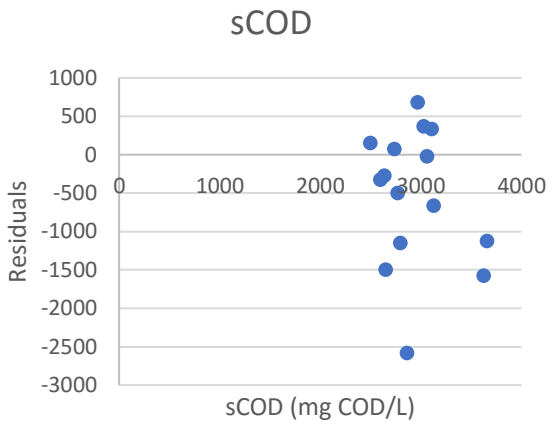

Figure 4.15: Residual plot for PS inhibition model

Additionally, Figure 4.16 shows the model predictions with respect to VSS, TCOD, sCOD, Ammonia, and VFAs compared to the experimental results. It can be seen that there was a good fit with most results. However, some outliers in solids and VFA indicated the potential for improvement.

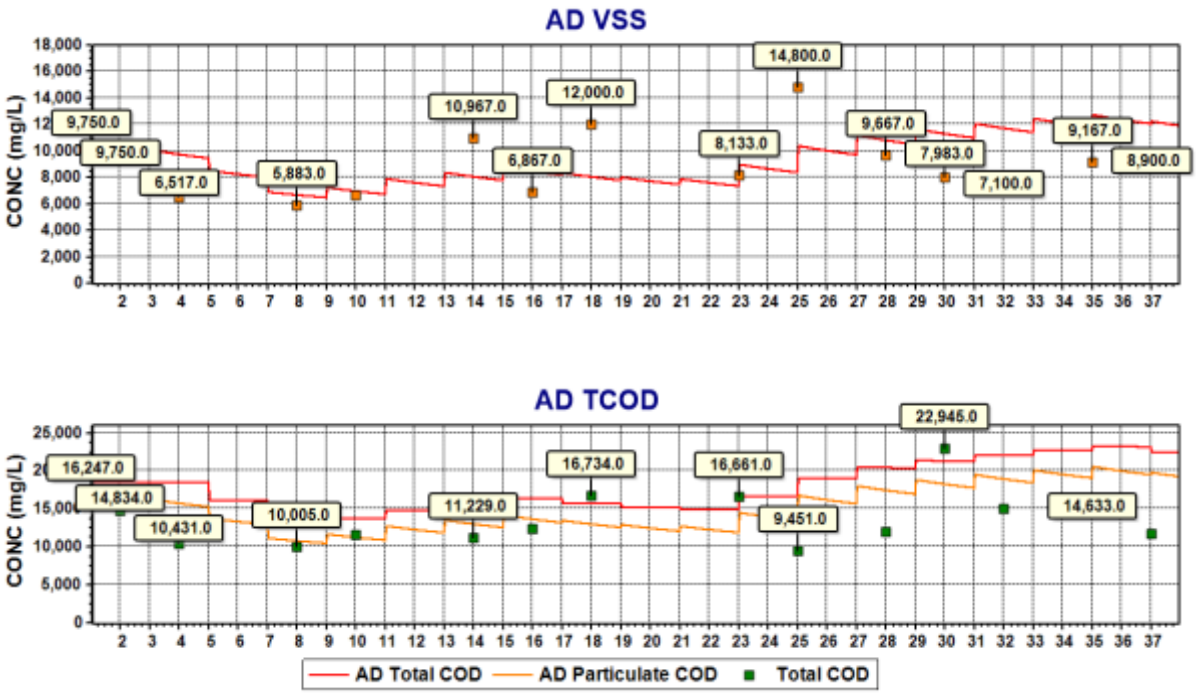

Figure 4.16: Results from PS inhibition model(Cont'd)

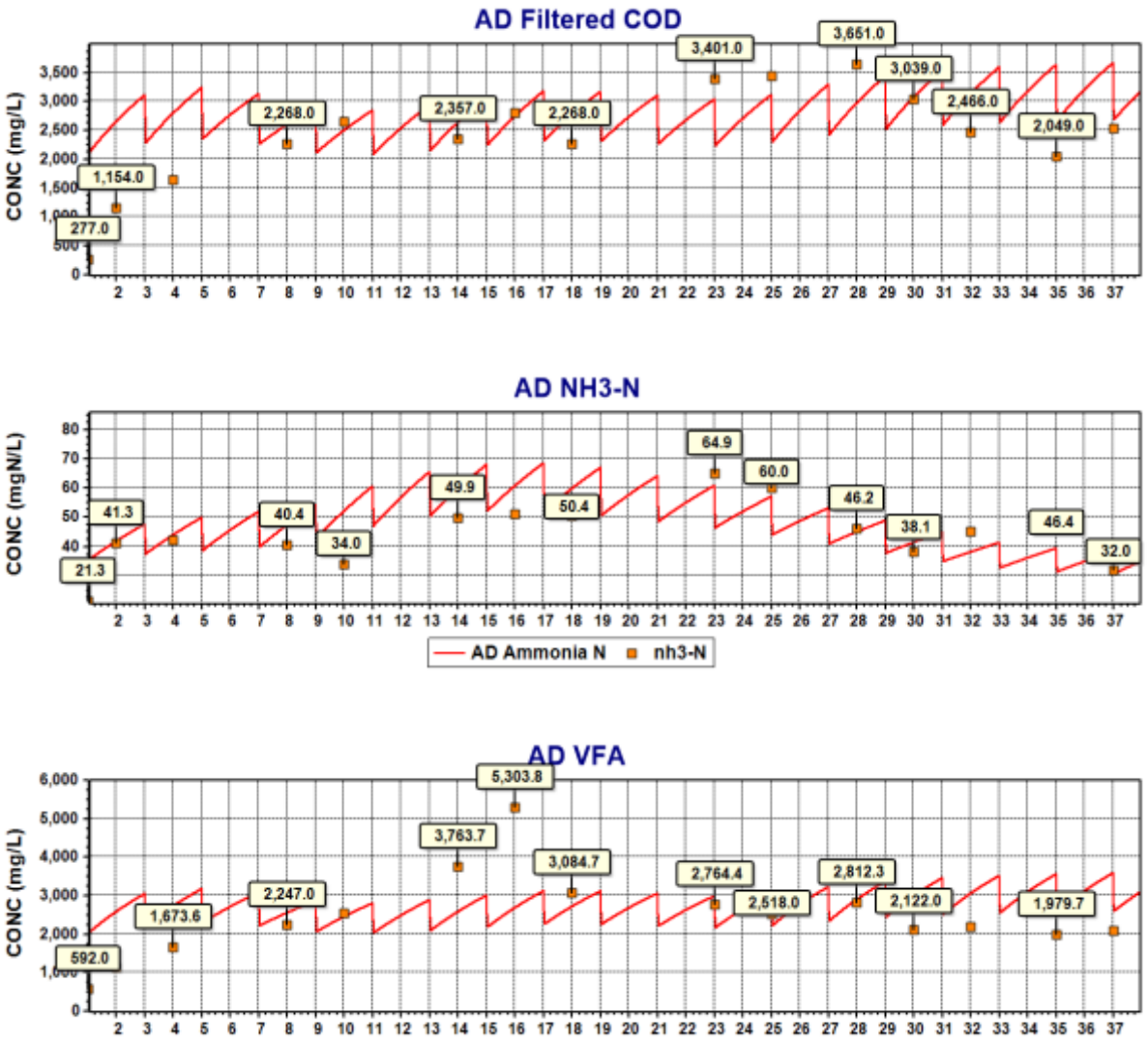

Figure 4.16: Results from PS inhibition model

For the WAS results, a Ksb of 0.35 was also used to predict the behavior of the fermenter. This was done to investigate the universality of the product inhibition expression. Table 4.13 shows the error comparison between the product inhibition and default BioWin models. From the table, it can be seen that errors were similar for both models. However, the inhibition model had a slightly better prediction concerning TCOD. The error differences were largest for sCOD, and

VFA concentration responses and the inhibition model performed worse for most of WAS species.

Table 4.13: WAS inhibition model squared errors

Parameter (WAS)	Baseline AD=0.04	Ksb=0.35
TSS	5690	7186
VSS	4056	4425
TCOD	17923	12776
sCOD	1849	5274
NH3	111	282
VFA	2956	8022

The residuals plots with regards to the soluble species for the WAS reactor are presented in Figure 4.17. Even though the data set was relatively small, the residuals show that the model consistently overpredicted the amount of soluble substrate generated. The errors were more prominent when concentrations were high, particularly for VFAs.

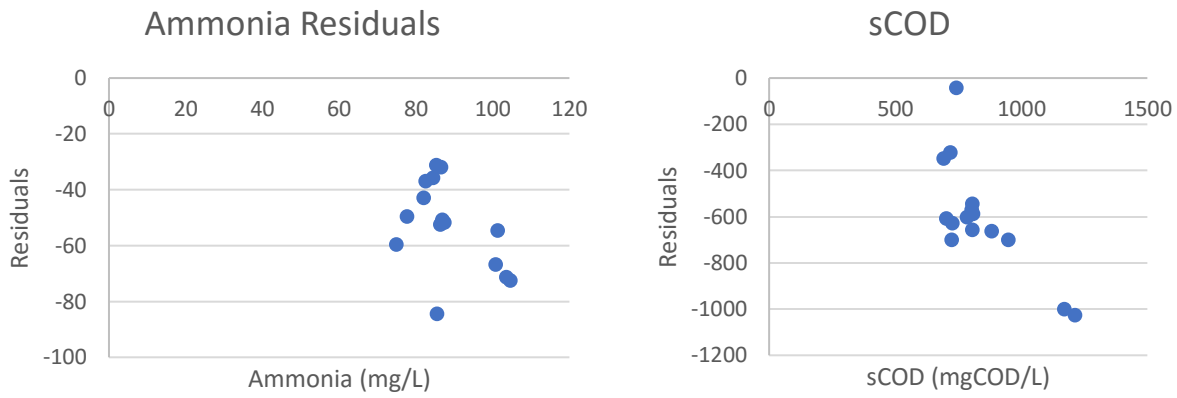

Figure 4.17: Residual plots for WAS inhibition model (Cont'd)

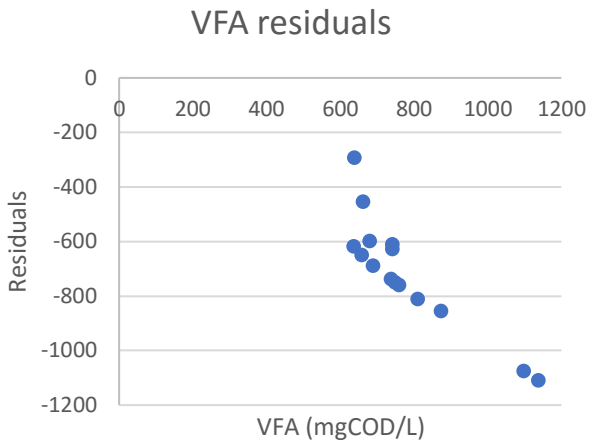

Figure 4.17: Residual plots for WAS inhibition model

The model predictions are compared with the observed responses in Figure 4.18. It can be seen that the model over-predicted the production of soluble substrates while under predicting the solids concentrations. This overprediction indicates that hydrolysis was happening at a reduced rate in the experimental setup than the one this model described. In the case of WAS VFAs, there was a gap because the generated VFAs were too close to the detection limit of the GC apparatus and hence some error was expected.

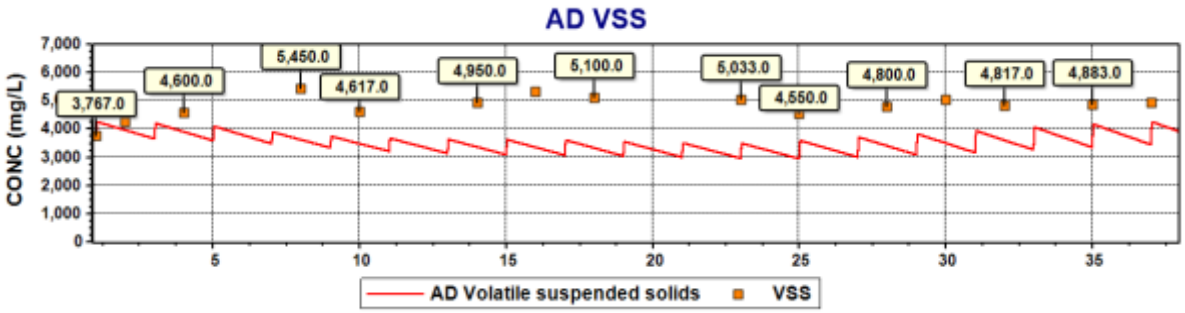

Figure 4.18: Results of WAS inhibition model (Cont'd)

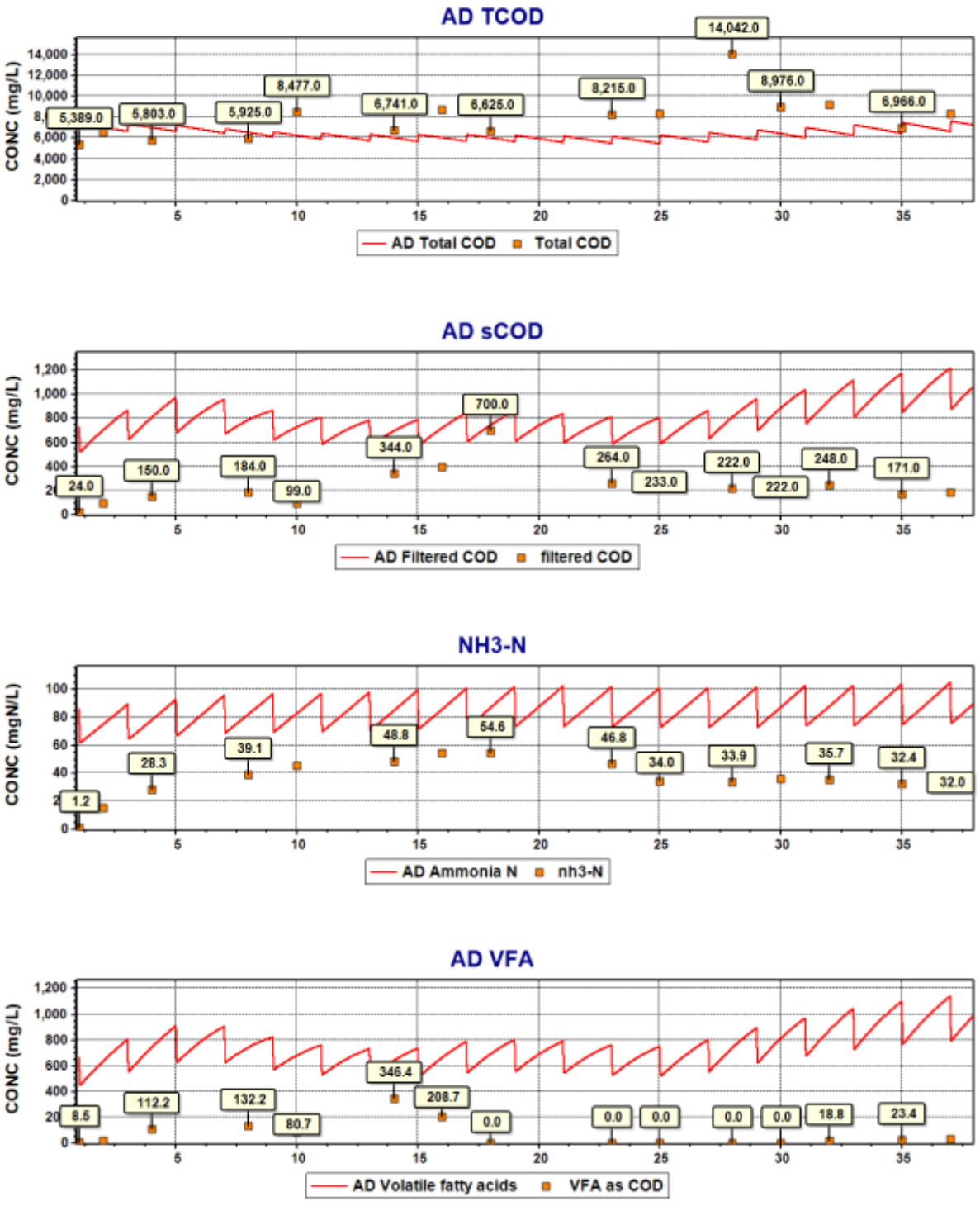

Figure 4.18: Results of WAS inhibition model

The third data set to fit was the ML reactor. The Ksb value chosen was 0.35 and Table 4.14 shows the error comparison between the original ASDM from BioWin

and the proposed inhibition model. From Table 4.14 it can be seen that the inhibition model better-predicted solids and COD data. Concerning ammonia and VFA, the errors were similar. This would suggest that for the case of ML the inhibition model improved the overall predictions of the experimental hydrolysis data.

Table 4.14: ML inhibition model squared errors

Parameter (ML)	Baseline AD=0.1	Inhibition model Ksb=0.35
TSS	24676	18382
VSS	21398	15234
TCOD	15844	14472
sCOD	4268	3497
NH3	36	38
VFA	10500	10097

The residual errors for the model predictions concerning the soluble species in the ML reactor are shown in Figure 4.19. The figures indicate that the model underpredicted ammonia and sCOD concentrations suggesting a bias in response. For the case of the VFA residuals, it seems that there might be a trend to under predict at higher concentrations while it over predicted at lower concentrations.

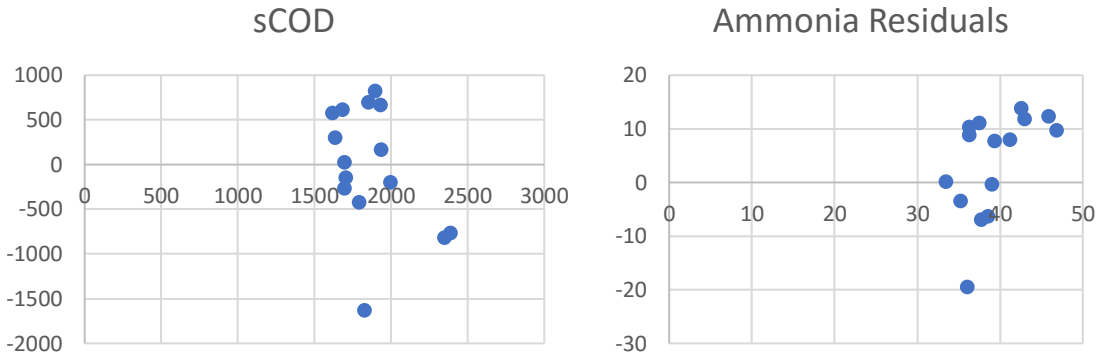

Figure 4.19: Residual plots for ML inhibition model (Cont'd)

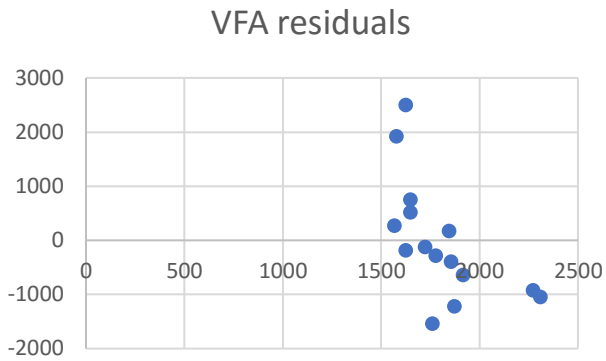

Figure 4.19: Residual plots for ML inhibition model

These results were further corroborated in Figure 4.20 that presents the model predictions for the ML reactor with respect to the species of interest. The inhibition model seemed to fit well with the experimental results. However, note that the period between days 20 and 30 seems to be the most problematic to fit possibly due to the increased solids loading for most species. Additionally, there was an initial outlier for VFA concentrations that would explain the higher points in the previously discussed VFA residuals plots:

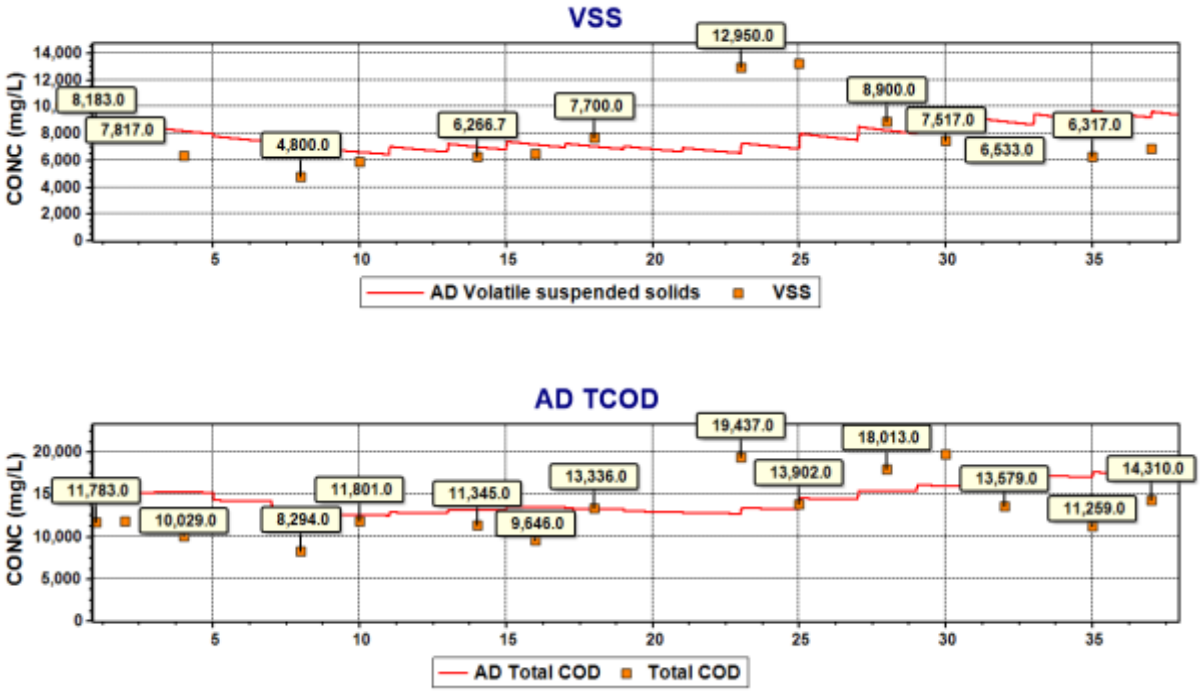

Figure 4.20: Results from ML inhibition model (Cont'd)

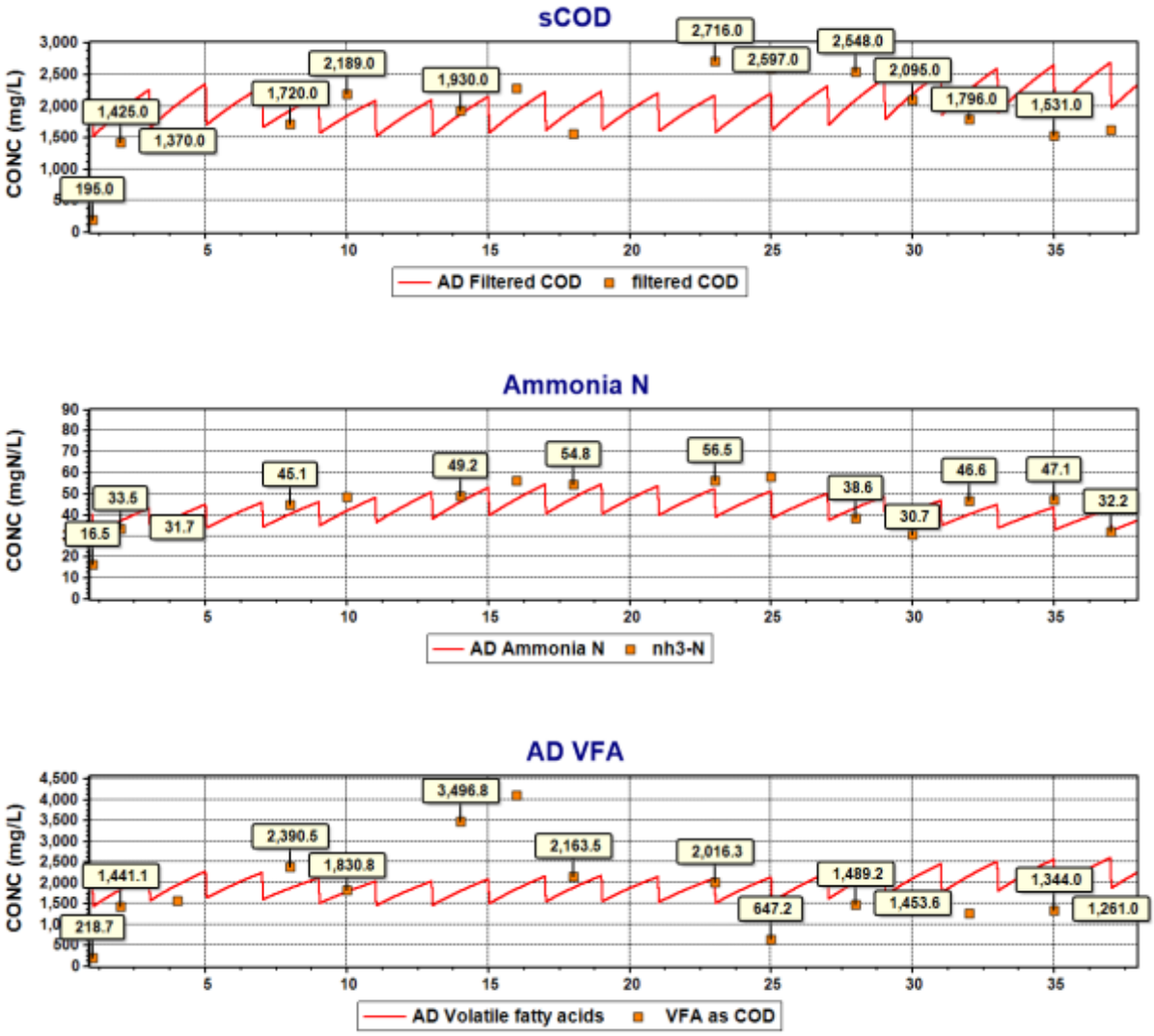

Figure 4.20: Results from ML inhibition model

The results suggest that the inhibition model better predicted the experimental results as compared to the anaerobic factor approach for the PS and ML reactors only. The WAS reactor behavior was, however, less well described by the inhibition model. It is important to note that that the errors associated with the inhibition model were still significant. The models did not successfully pass a chi-squared statistic test, as all of them have rejected the fit. To further refine the model in pursuit of a better fit with the data and a proper distribution of residuals, an enzyme function was evaluated.

4.3.2 Enzyme model

Considering the scope of this study, an approach to understanding the enzymatic behavior was chosen because it seems that the literature agrees that the effect of enzymes is important and that it has been overlooked so far. Dold and Marias (1986) expressed the rate of hydrolysis using a surface reaction expression via Eq. 2.13. Vavilin et al. (1996) developed a hydrolysis model that included kinetics describing the process via which a particle attaches to an organism and consequentially undergoes surface degradation because of secreted enzymes. Additionally, it has been suggested that in a batch reactor there wouldn't be initially enough bacteria and enzyme to colonize every available surface but that in a shorter than fermentation time bacteria will grow and eventually be able to cover all surfaces. Hobson (1987) proposed that all particles would be uniformly degraded if they underwent such a process. Furthermore, Sanders (2001) concluded that hydrolytic enzymes are typically present in excess and that the amount of surface available for hydrolysis is the most important factor for describing the rate of hydrolysis. However, the effect that hydrolytic enzymes have in the process has not yet been elucidated.

Since there are various bacterial groups in action during anaerobic digestion, simulating each group and their produced enzymes would be unnecessarily complicated. It is an accepted approach to simplify the breakdown of organics into either carbohydrates, proteins, and lipids (Batstone et al. 2000); however, for model implementation in BioWin models, the enzymes should be described relative to XSCOD, XON, and XOP. The model builder in BioWin allows for the addition of two soluble user-defined state variables. Since municipal sludges do not exclusively consist of either carbohydrates, proteins or lipids but a mixture of these (Batstone et al., 2000) it was deemed practical to employ grouped parameters. Hence one enzyme rate equation that describes the overall rate of enzyme production was employed in the hydrolysis rate equation for all species. It is recognized that the three processes would undergo slightly different

enzymatic kinetics, but due to this study's scope, an effort was made to simplify the analysis further.

Philip et al. (1993) measured the activity of different enzymes in a septic tank sludge and found that phosphatase and lipase activities were in the same order of magnitude as cellulase and protease activity. Moreover, they concluded that all enzymatic activity was bound to the solid part of the sludge. Furthermore, studies have agreed that using cellulose as a substitute for enzymatic analysis is suitable since it is very likely that cellulose is the most abundant carbohydrate in sludges. It is commonly the primary polymer in many organic wastes, and its degradation depends on enzymatic activity. Cellulose is easily biodegradable, and there is widely available data regarding its breakdown kinetics (Sanders, 2001).

The production of cellulose was also found to have similarities with the generation of protease, particularly with the inhibition by high glucose levels. There are however some differences with other hydrolytic enzymes. Protease was found to be inhibited by the production of free amino acids while ammonia can inhibit the hydrolysis of cellulose (Sanders, 2001). Table 4.15 contains the modified hydrolysis expression and the additional enzyme production rate for the previously developed product inhibition model. This process would consume the soluble substrate and produce the hydrolytic enzyme. In the enzyme production expression, there is a product inhibition factor for when Sbsc concentrations are too high. The produced enzyme will then play a role in a factor within the hydrolysis process rates, where the overall rate would be reduced at reduced enzyme concentrations.

Table 4.15: Enzyme model extension for ASDM

Process	Stoichiometry									Process Rate
	XSP	Xsc	Xon	Xop	Sbsc	NH3-N	Nos	PO4P	$\lvert E_Q \rvert$	
Hydrolysis of XSCOD	-1				1					$k_h \times \frac{k_o}{k_o + D_o} \times \frac{k_{no}}{k_{no} + NO3N} \times \frac{\frac{X_{sp}}{Z_{bh}}}{k_x + \frac{X_{sp}}{Z_{bh}}} \times Z_{bh} \times \frac{K_{sb}}{K_{sb} + S_{bsc}} \times \frac{\lvert E_Q \rvert}{\propto_Q + \lvert E_Q \rvert}$
Hydrolysis of XON			-1				1			$k_h \times \frac{k_o}{k_o + D_o} \times \frac{k_{no}}{k_{no} + NO3N} \times \frac{\frac{X_{sp}}{Z_{bh}}}{k_x + \frac{X_{sp}}{Z_{bh}}} \times Z_{bh} \times \frac{K_{sb}}{K_{sb} + S_{bsc}} \times \frac{X_{on}}{X_{sp}} \times \frac{\lvert E_Q \rvert}{\propto_Q + \lvert E_Q \rvert}$
Hydrolysis of XOP				-1				1		$k_h \times \frac{k_o}{k_o + D_o} \times \frac{k_{no}}{k_{no} + NO3N} \times \frac{\frac{X_{sp}}{Z_{bh}}}{k_x + \frac{X_{sp}}{Z_{bh}}} \times Z_{bh} \times \frac{K_{sb}}{K_{sb} + S_{bsc}} \times \frac{X_{op}}{X_{sp}} \times \frac{\lvert E_Q \rvert}{\propto_Q + \lvert E_Q \rvert}$
Adsorption of Colloidal COD	1	-1								$K_{ads} \times X_{sc}$
Ammonification						1	-1			$\mathrm{K_{amm} \times N_{os} \times (Z_{bh} + Z_{bp})}$
Enzyme Production					-1				1	$\mathrm{Y_{E/X} \times \left(\frac{K_{E/S}}{S_{bsc} + K_{E/S}}\right) \times \frac{u_{max} \times S_{bsc} \times X_{sp}}{K_s + S_{bsc}}}$

This model with the enzyme extension was run following the previously described methodology for the product inhibition model. Since the expression for product inhibition was maintained in this new model, K_{sb} had the previously fit value of 0.35 for all three reactors. Additionally, the rate constants for the enzyme formulation were taken from Humphrey (1979). The study focused on cellulose fermentation and their shrinking site model and provided the basis for the new design. These constants are summarized in Table 4.16:

Table 4.16: Enzyme rate constants for new model based on Humphrey (1979)

Parameter	Model	Magnitude	Units
Enzyme yield	$Y_{E/X}$	0.01	g/g
Substrate IC50 in enzyme growth	$K_{E/S}$	0.01	g/l
Enzyme half-saturation constant	α_Q	0.3	g/l
Half-saturation	K_s	0.1	g/l
Max specific growth rate	U_{max}	0.25	l/hr

For the case of PS, Figure 4.21 shows the prediction of enzyme concentration throughout the study period. Note that the production remained stable within a range of values for PS. Unfortunately, this study did not measure or classify any enzymes, but the graph below serves to confirm that the model was predicting the production of enzyme species that would affect the hydrolysis rate.

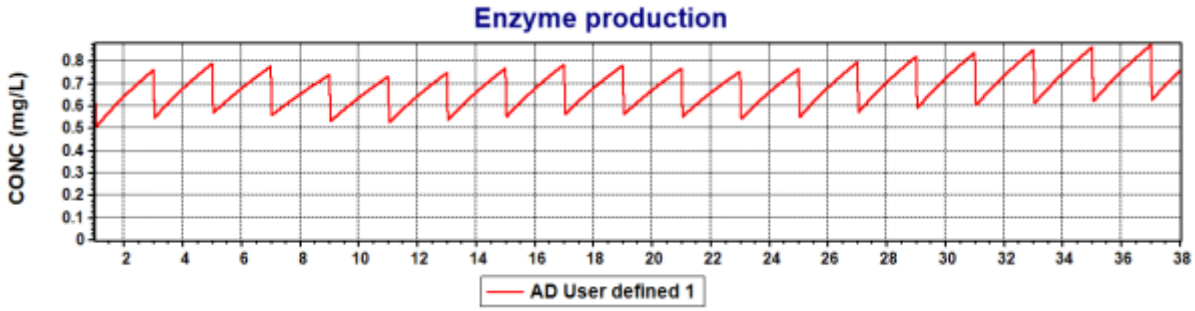

Figure 4.21: Enzyme production from PS

The error comparison with the previously developed models was done following the methodology for squared errors and visually analyzing the plots of residuals. Table 4.17 shows the errors for the PS reactor compared to the previously discussed models. It can be seen that this model describes ammonia and soluble species well like the previous models; however, there were still some significant errors regarding solids and TCOD, but overall the model behaved similarly to the product inhibition model.

Table 4.17: PS enzyme model squared errors

Parameter (PS)	Baseline AD=0.2	Inhibition model Ksb=0.35	Enzymatic model
TSS	14195	14726	14652
VSS	13013	13660	13597
TCOD	25380	25359	25338
sCOD	6448	4585	4627
NH3	30	24	25
VFA	10223	8195	8563

The residuals plots for the PS reactor for the soluble species are shown in Figure 4.22. This Figure shows that most errors were randomly distributed, except for VFAs and this was possibly due to the outliers around day 16 of the test.

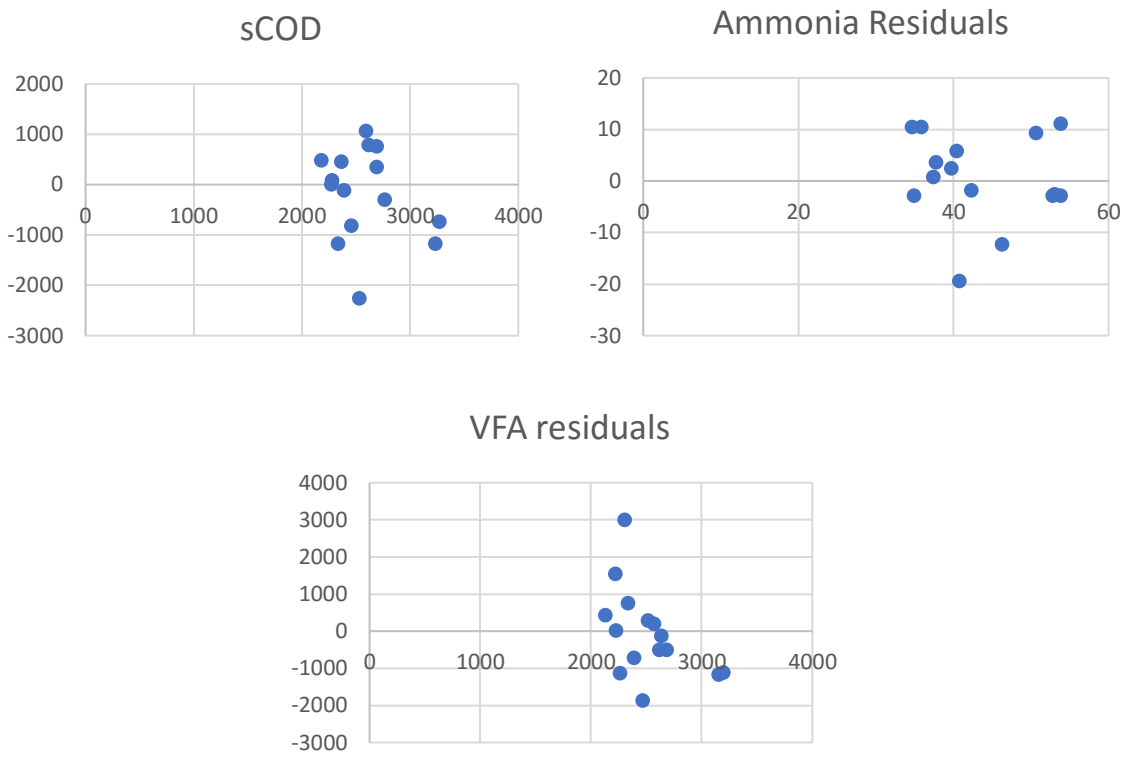

Figure 4.22: Residual plots for PS enzyme model

The predictions of the model were compared with the data in Figure 4.23. From this figure, it can be seen that the model tended to underpredict values especially in the middle of the study period when compared to experimental values. This has been a common result throughout this study. The variability in feed concentrations was the most likely explanation for such behavior.

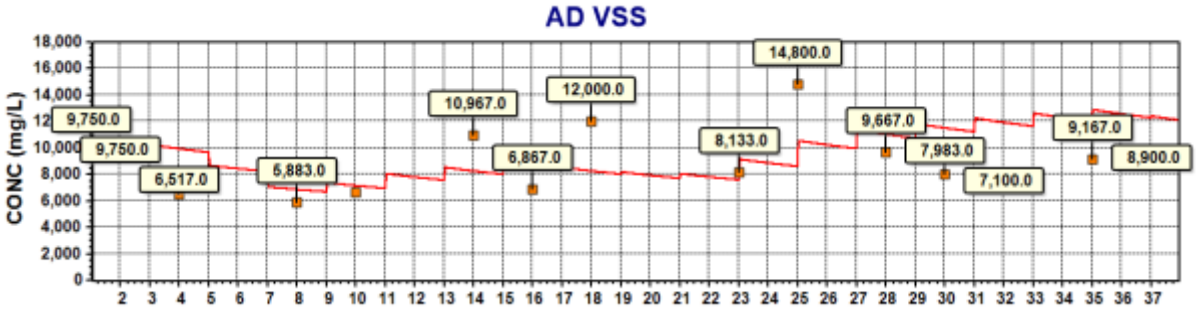

Figure 4.23: Results for PS enzyme mode (Cont'd)

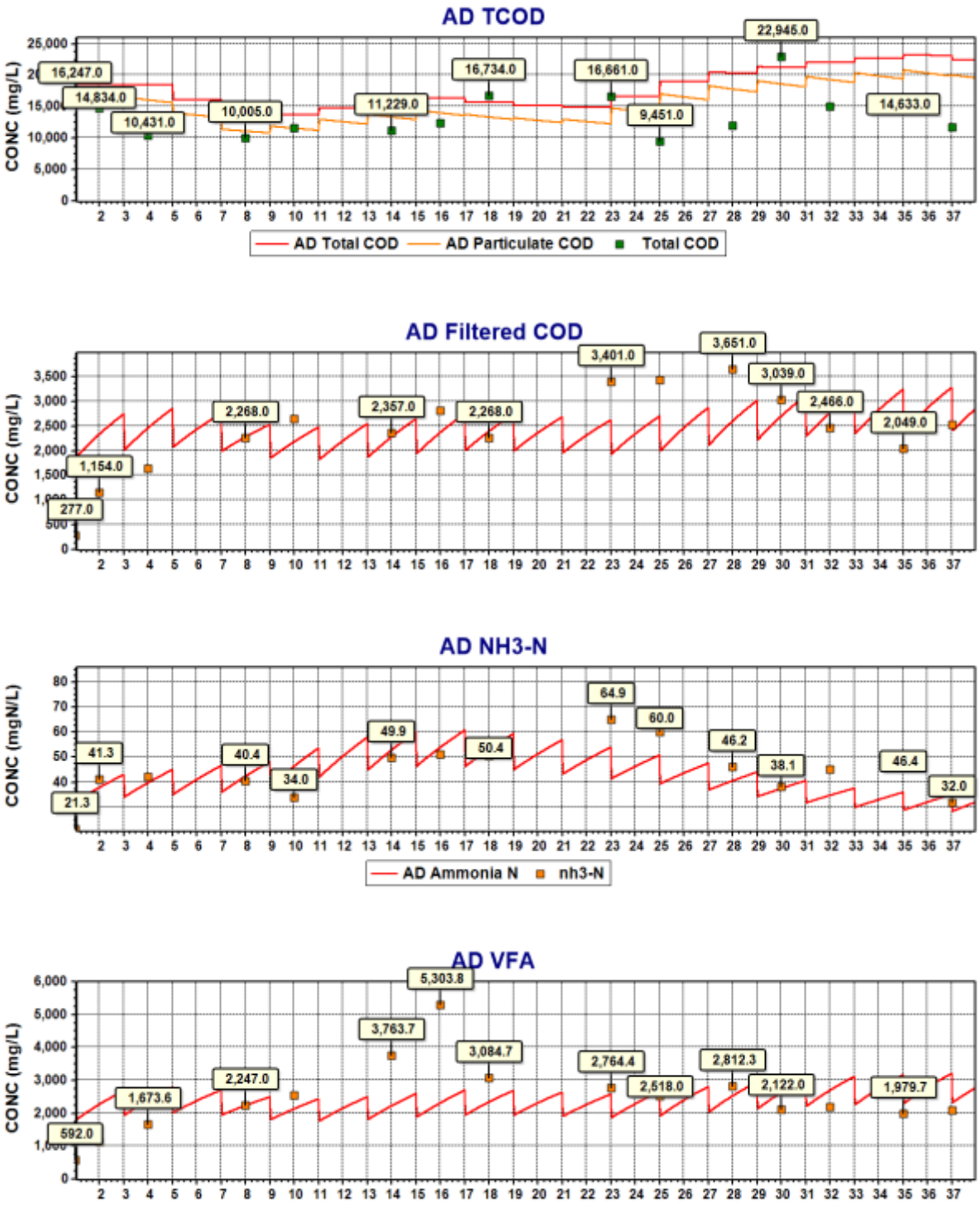

Figure 4.23: Results for PS enzyme model

Table 4. 18 presents a comparison between the least squares errors for all three models for WAS. From Table 4.18 it can be seen that the model improved in

comparison to the inhibition model for all species. When compared to the baseline case, the predictions from the enzyme model had less error with regards to solids and COD values, but it fails to improve predictions of the soluble species concentrations:

Table 4.18: WAS enzyme model squared errors

Parameter (WAS)	Baseline AD=0.04	Inhibition model Ksb=0.35	Enzymatic model
TSS	5690	7186	4496
VSS	4056	4425	2177
TCOD	17923	12776	10188
sCOD	1849	5274	4754
NH3	111	282	184
VFA	2956	8022	7417

Figure 4.24 presents the enzyme production for WAS, and it can be seen that the predicted values were larger than that for PS. This was due to the smaller values of Sbsc that the WAS reactor produced.

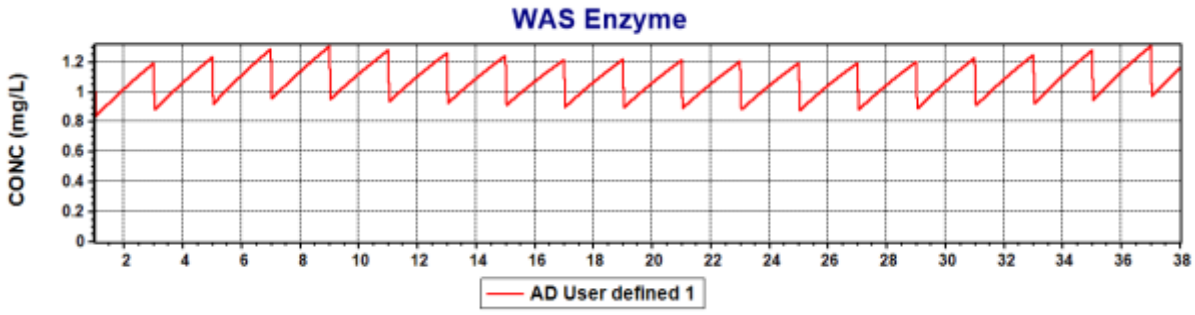

Figure 4.24: Enzyme produced in WAS Enzyme model

The residual plots are shown in Figure 4.25 for the WAS reactor for the soluble species. The model consistently over-predicted soluble species but this was expected due to the insufficient concentrations found experimentally in the entire dynamic run, but particularly after the third week. In the case of VFA there

wasn't sufficient information to assess from experimental results whether the model was accurately predicting VFA production:

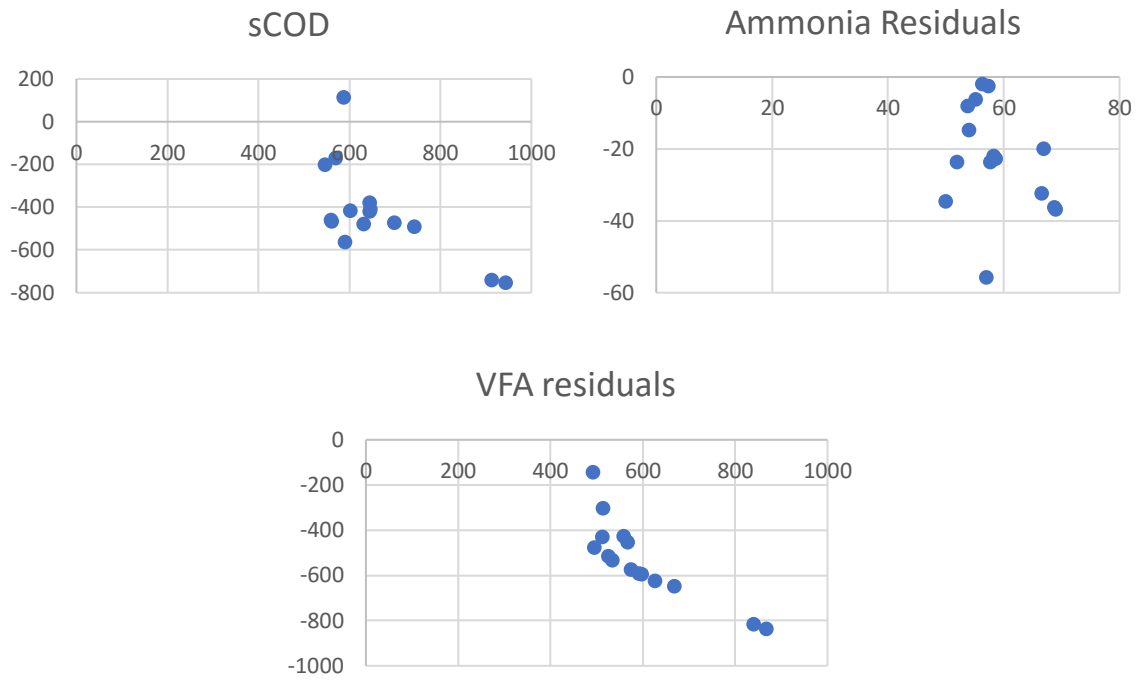

Figure 4.25: Residual plots for WAS enzyme model

Figure 4.26 shows the WAS enzyme model predictions compared to experimental values. The previously discussed over-prediction can be observed in the model outputs, especially considering soluble substrates generation. Additionally, for Solids and TCOD, the effect was reversed, as these species were underpredicted. These results were similar to those obtained in previous WAS analysis throughout this study and are a good example of how challenging it is to fit a hydrolysis model, particularly when the rates are very low. The main obstacle to overcome in the WAS model was that this model had the lowest hydrolysis rate of all experiments. This is because even though the model fit is not perfect and the model overpredicts the extent of hydrolysis, lowering the rate even further would halt hydrolysis altogether.

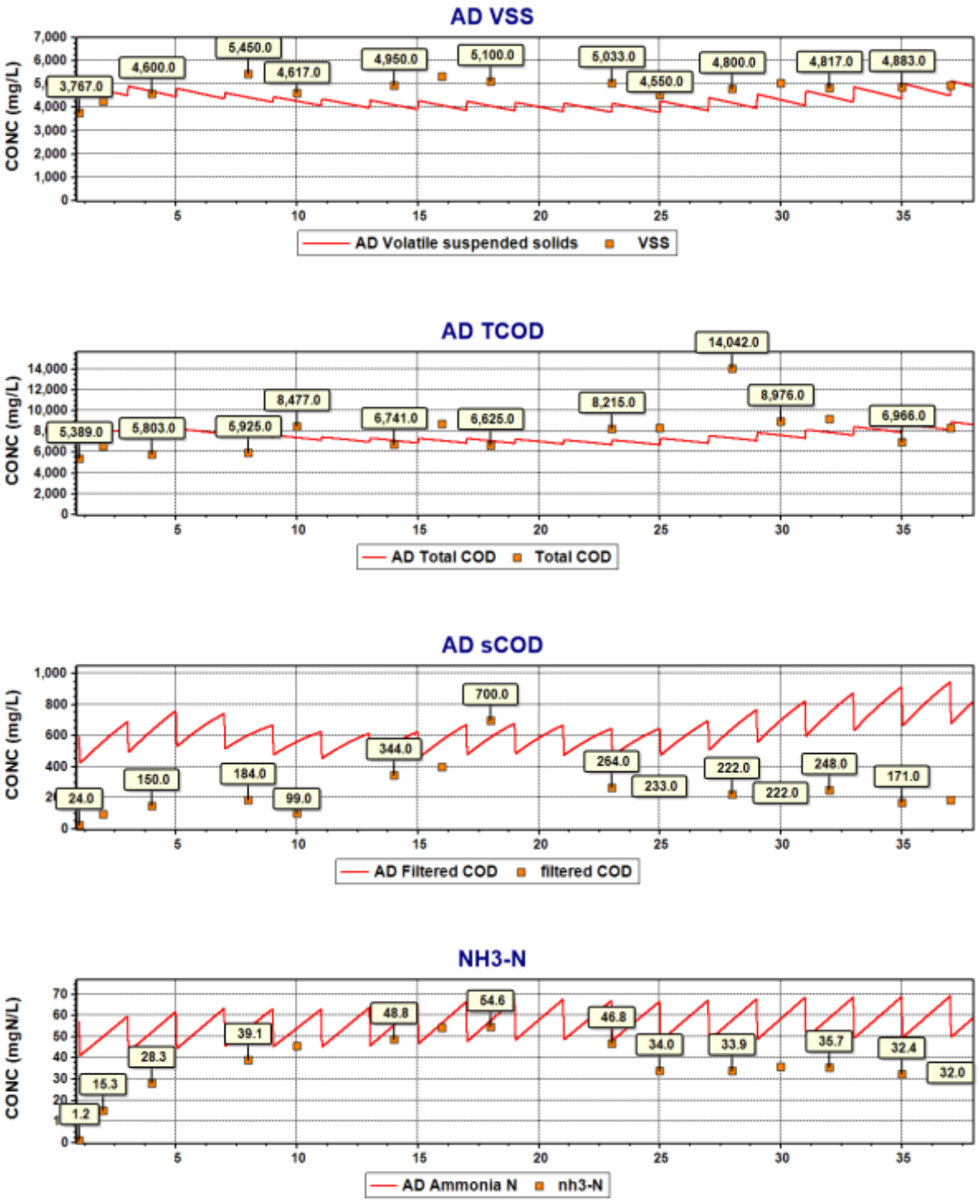

Figure 4.26: Results for WAS enzyme model (Cont'd)

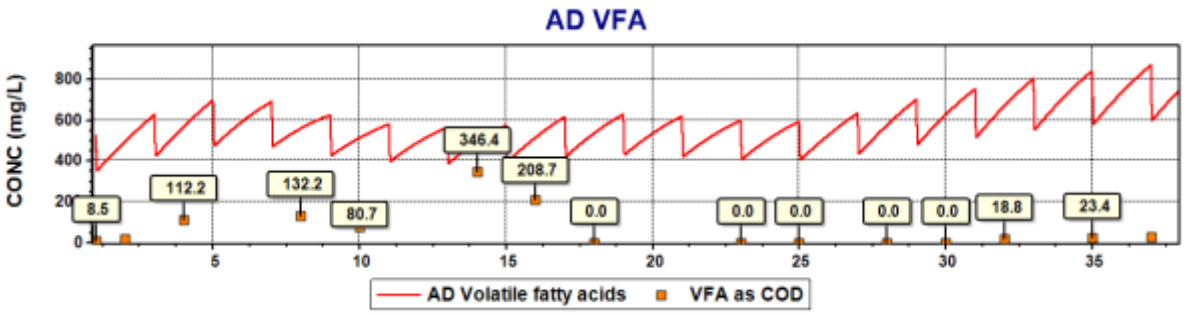

Figure 4.26: Results for WAS enzyme model

The ML reactor was also evaluated using the enzyme model. Figure 4.27 shows the predicted enzyme production for this reactor. Note that these predictions lie between the levels predicted for PS and WAS.

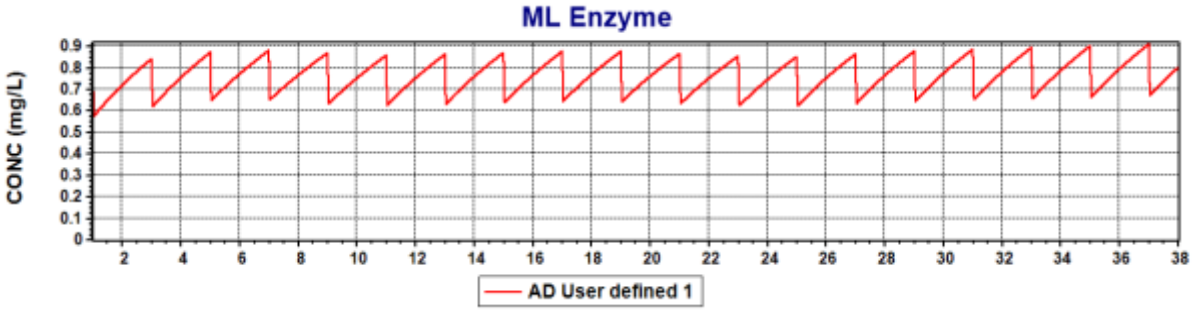

Figure 4.27: Enzyme produced in ML enzyme model

The errors in model predictions are summarized in Table 4.19 are compared to previous models. From Table 4.19 it can be observed that there was little difference between the inhibition and enzymatic models. The enzyme model predictions were marginally better at describing solids while the inhibition model was better for soluble species. Both models had similar errors, so it was not possible to differentiate between there performance. It is clear, however, that both models performed better than the baseline case using only the BioWin native model.

Table 4.19: ML squared errors for Enzyme model

Parameter (ML)	Baseline AD=0.1	Inhibition model Ksb=0.5	Enzymatic model
TSS	24676	18382	18220
VSS	21398	15234	15137
TCOD	15844	14472	14594
sCOD	4268	3497	3649
NH3	36	38	43
VFA	10500	10097	10503

Figure 4.28 presents the residual plots for the soluble species for the ML reactor running the enzyme model. These plots show a slight trend to under predict values for ammonia and sCOD. The trend for VFAs was maintained, as the model seemed to under predict values at high concentrations and over predict at lower ones. It would be apparent that the model predicts a smaller rate of hydrolysis when calculated this way.

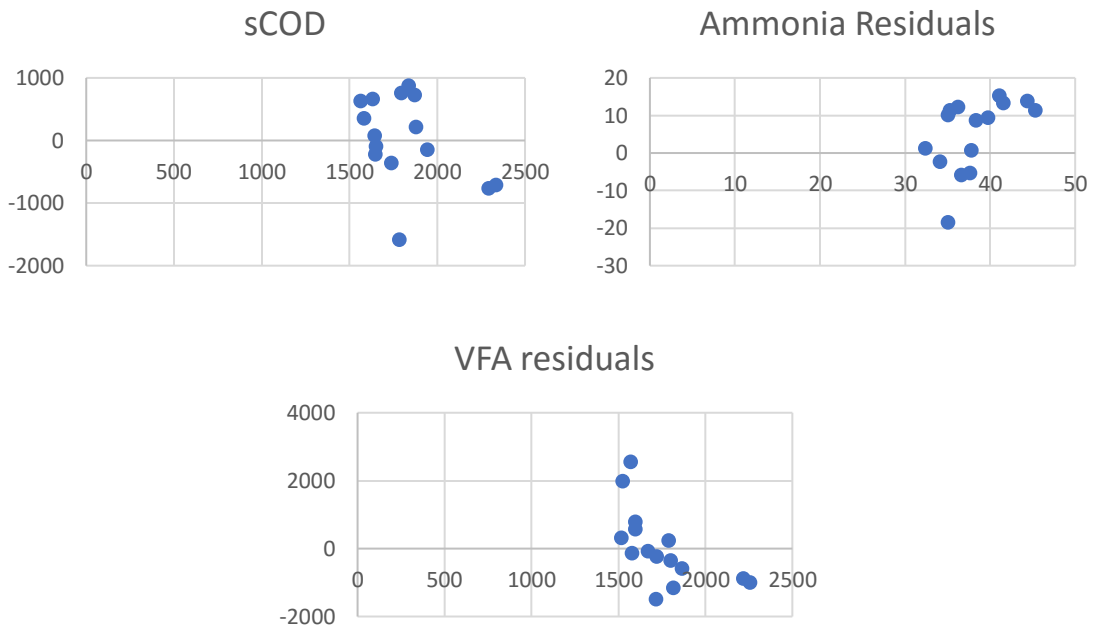

Figure 4.28: Residual plots for ML enzyme model

Figure 4.29 presents the model predictions along with the experimental data. From Figure 4.29 it can be observed that the model tended to underpredict

values. This confirmed the observations made in the residual plots. However, the fit with experimental values was deemed to be reasonable.

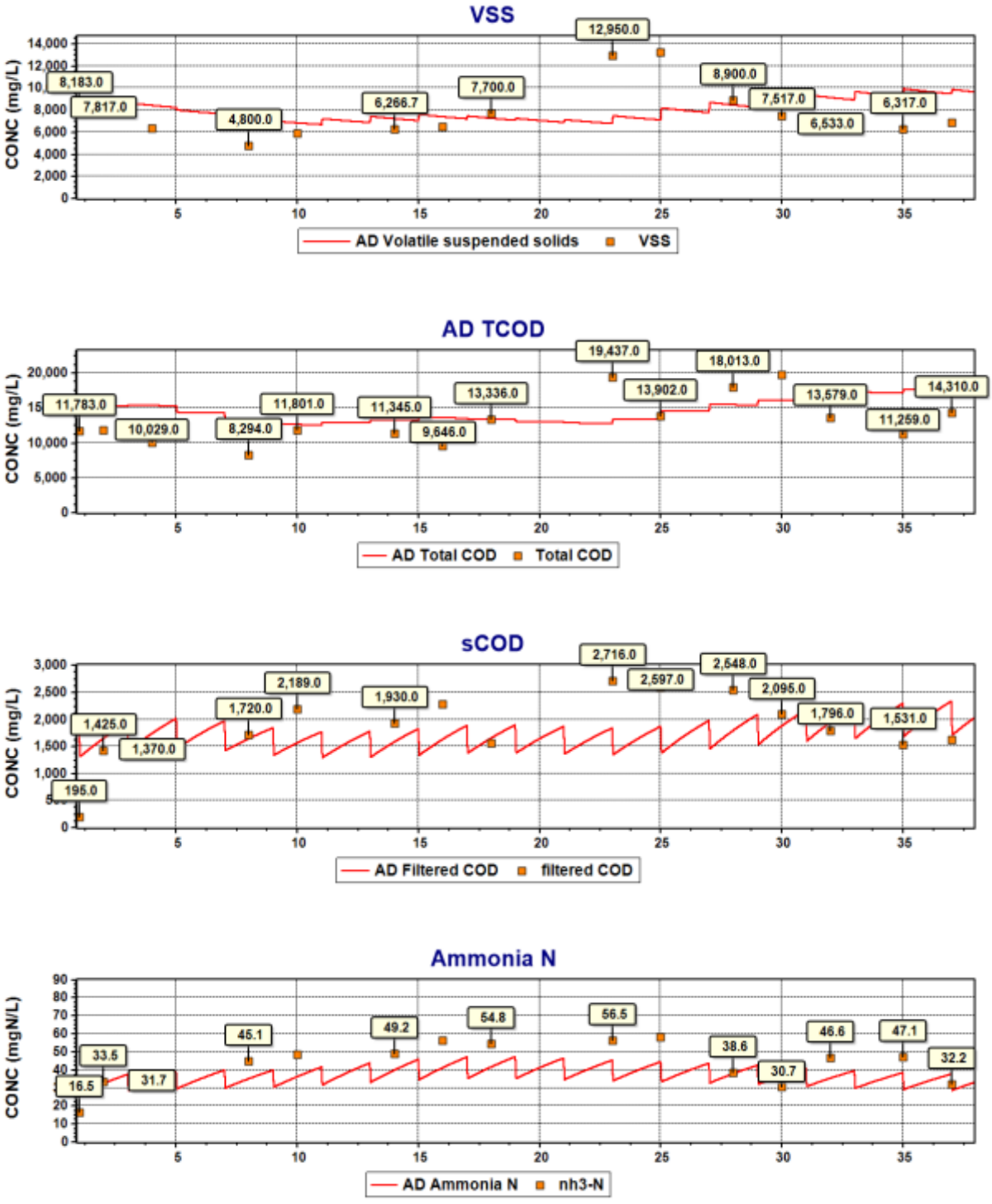

Figure 4.29: ML Enzyme model predictions (Cont'd)

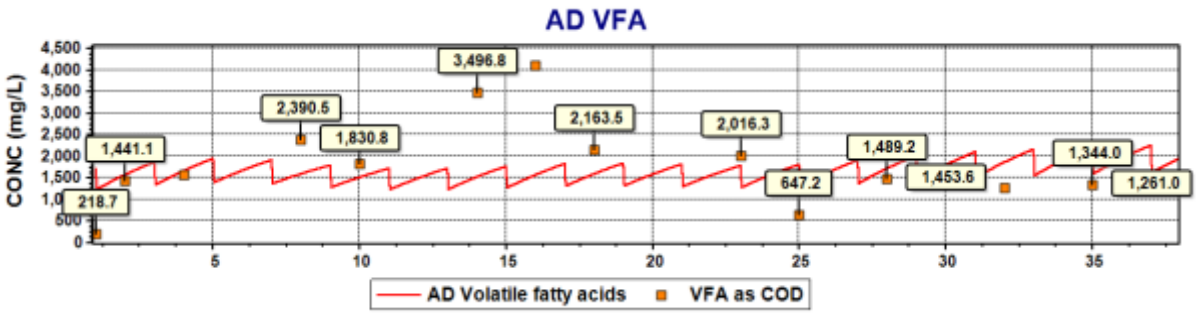

Figure 4.29: ML Enzyme model predictions

To conclude, the enzymatic model provided an improved prediction of the dynamic hydrolysis of PS, WAS and ML samples with the same parameters without the need for extensive calibration. The inhibition model also provided improved predictions and was in some cases better than the enzyme model. The inhibition expressions were much simpler than enzymatic ones, which are inherently an oversimplification of the process. However, the parameters needed to be fit accordingly which reduces the universality of the expression. Both models improve the model fit when compared to the baseline ASDM model native to BioWin. This was concluded after observing smaller values for the least squared errors on the difference between model predictions and experimental values. This study suggests that future research should give close attention to the enzyme species produced and the dependence of the rate of hydrolysis on constituents affected by the various enzymes that this process produces. Perhaps a better calibration of the parameters in the enzyme model would improve the model ability to predict results. This study also highlights the importance of a good feed characterization when considering consistent VFA production in support of BNR; the better characterized the feed is, the better predictions the models will make.

5. Conclusions

During this study, a 40-day bench-scale fermentation of PS, WAS, and ML provided experimental data to analyze the prediction capabilities of acid-phase anaerobic digestion models. The 4L reactors operated at a 6-day SRT, and 21˚C. The ML reactor was composed of 38% WAS and 62% PS by volume.

The experimental VFA yield values were 0.21 mg VFA/mg TCOD for PS, 0.014 mg VFA/mg TCOD for WAS, and 0.20 mg VFA/mg TCOD for ML. It was found that adding WAS to the PS increased the hydrolysis of PS solids by at least 10% (±27) based on VFA produced by influent VSS and 19% (±29) based on VFA produced by influent TCOD. Note that the standard deviation values were significant, and it is suggested that further research controls for sludge composition in dynamic studies to avoid high variability in results.

The composition of the VFAs produced indicated the metabolic pathways that govern the reaction. In the case of PS, a propionate-type fermentation appeared to be the dominant process. For WAS the acetate-ethanol pathway seemed to describe the process better. For ML, it appears that the addition of WAS shifted the fermentation from a propionate-type to an acetate-ethanol type. ML showed an ideal composition of VFAs, made up almost entirely of propionate and acetate. These are the most useful acids for downstream BNR, so the composition of VFAs was deemed appropriate for this study.

When the original BioWin ASDM model simulated the experiments, the anaerobic factor chosen for each sludge was different. For PS, WAS and ML it was 0.2, 0.04 and 0.1 respectively, although the default used in BioWin is 0.5. The model seemed to predict the overall trends of the reaction, but it was deemed that there was room for improvement.

The first extension to the model was a product inhibition function. This function helped reduce the uncertainty of choosing an anaerobic factor since only one

factor was found to provide a reasonable fit in all three reactors. The best fit parameter (Ksb) was found to have a value of 0.35. This factor improved the ability of the model to predict the behavior of the PS and ML reactors, but it failed to enhance prediction of the WAS results.

The second extension to the model was an enzyme surface-limited function, which the literature suggested was an important consideration that has been overlooked so far. This new model performed similarly to the inhibition model, by improving the predictions for the PS and ML reactors. However, results for the WAS reactor were not improved significantly. In fact, the main obstacle to overcome in the WAS model was that this model had the least amount of hydrolysis happening out of all the experiments. Hence, even though the model fit is not very good and the models overpredict the extent of hydrolysis, lowering the rate even further would halt hydrolysis altogether. This extension was based on enzymes produced in cellulose fermentation because of similarities to the experimental substrate. However, it was deemed that model fitting or the addition of other enzymes might improve the model predictions.

Hence, it is suggested that future research expands on characterizing the enzymatic behavior of the hydrolytic bacteria. Additionally, this study showed that the inhibitory effects of soluble products could also be a simple extension to improve acid-phase anaerobic digestion models, so it is recommended to include inhibition in future enzyme models. Moreover, for studies considering the effect of WAS addition to improving PS hydrolysis; it is suggested to experimentally control for solids and COD content since it seems hydrolysis rates are most sensitive to these parameters, particularly the biodegradable particulate COD. Lastly, for subsequent research on dynamic modeling, particularly PS hydrolysis in a full-scale plant setting, it is recommended to investigate on a longer term whether the addition of other sludges like WAS could improve the effective VFA yield for the plant.

6. References:

Andreasen, K., Petersen, G., Thomsen, H., and Strube, R. (1997). Reduction of Nutrient Emission by Sludge Hydrolysis. Wat. Sci. Tech., 35 (10), 79.

APHA (1998) Standard Methods for the examination of water and waste water American Public Health Association.

Banister, S. S., Pitman, A. R., & Pretorius, W. A. (1998). The solubilisation of N and P during primary sludge acid fermentation and precipitation of the resultant P. *Water SA*, *24*(4), 337–342.

Banister, S. S., & Pretorius, W. A. (1998). Optimisation of primary sludge acidogenic fermentation for biological nutrient removal. *Water SA*, *24*(1), 35–41.

Barnard, J., Kobylinski, E., Rabinowitz, B., Debarbadillo, C., Stevens, G., & Schauer, P. (2014). Highlights From The Most Popular Session at WEFTEC The Complete Guideline to Fermenters in Biological Nutrient Removal, (1986).

Barnard, J. L. (1984). Activated primary tanks for phosphate removal. *Water SA*, *3*(10), 121–126. Retrieved from http://www.wrc.org.za/Knowledge Hub Documents/Water SA Journals/Manuscripts/1984/WaterSA_1984_10_0336.PDF

Batstone, D. J., Keller, J., Angelidaki, I., Kalyuzhnyi, S. V., Pavlostathis, S. G., Rozzi, A., … Vavilin, V. A. (2002). The IWA Anaerobic Digestion Model No 1 (ADM1). *Water Science and Technology*, *45*(10), 65–73. https://doi.org/10.2166/wst.2008.678

Batstone, D. J., Keller, J., Newell, R. B., & Newland, M. (2000). Modelling anaerobic degradation of complex wastewater. I: Model development. *Bioresource Technology*, *75*(1), 67–74. https://doi.org/10.1016/S0960-8524(00)00018-3

Batstone, D. J., Puyol, D., Flores-Alsina, X., & Rodríguez, J. (2015). Mathematical modelling of anaerobic digestion processes: applications and future needs. *Reviews in Environmental Science and Biotechnology*, *14*(4), 595–613. https://doi.org/10.1007/s11157-015-9376-4

Chen, Y., Jiang, X., Xiao, K., Shen, N., Zeng, R. J., & Zhou, Y. (2017). Enhanced volatile fatty acids (VFAs) production in a thermophilic fermenter with stepwise pH increase – Investigation on dissolved organic matter transformation and microbial community shift. *Water Research*, *112*, 261–268. https://doi.org/10.1016/j.watres.2017.01.067

Chen, Y., Li, X., Zheng, X., & Wang, D. (2013). Enhancement of propionic acid fraction in volatile fatty acids produced from sludge fermentation by the use of food waste and Propionibacterium acidipropionici. *Water Research*, *47*(2), 615–622. https://doi.org/10.1016/j.watres.2012.10.035

Comeau, Y., Hall, K., Hancock, R., & Oldham, W. (1986). Biochemical model for enhanced biological phosphorus removal. *Water Research*, *20*(12), 1511–1521. https://doi.org/10.1016/0043-1354(86)90115-6

Deinema, M. H., Habets, L. H. A., Scholten, J., Turkstra, E., & Webers, H. A. A. M. (1980). The accumulation of polyphosphate in Acinetobacter spp. *FEMS Microbiology Letters*, *9*(4), 275–279. https://doi.org/10.1111/j.1574-6968.1980.tb05652.x

Dold, P., Al-Omari, a., Mokhayeri, Y., Awobamise, M., Stinson, B., Bodniewicz, B., … Murthy, S. (2010). Measuring Influent Heterotrophic Biomass Content for Modeling and Design. *Proceedings of the Water Environment Federation*, *2010*(18), 95–111. https://doi.org/10.2175/193864710798130454

Dold, P. L., & Marais, G. R. (1986). Evaluation of the general activated sludge model proposed by the IAWPRC task group. *Water Science and Technology*, *18*(6), 63–89.

Eastman, J.A. and Ferguson, J.F. (1981) Solubilization of Particulate Organics Carbon during the Acid Phase of Anaerobic Digestion. Journal Water Pollution Control Federation, 53, 352-366.

Elefsiniotis, P. (1993). The effect of operational and environmental parameters on the acid-phase anaerobic digestion of primary sludge. *PhD Thesis National Technical University of Athens, Greece M.A.Sc.University of Toronto*, (January), 206.

Elefsiniotis, P., & Oldham, W. K. (1994). Anaerobic acidogenesis of primary sludge: The role of solids retention time. *Biotechnology and Bioengineering*, *44*(1), 7–13. https://doi.org/10.1002/bit.260440103

Fang, H. H. P., & Liu, H. (2002). Effect of pH on hydrogen production from glucose by a mixed culture. *Bioresource Technology*, *82*(1), 87–93. https://doi.org/10.1016/S0960-8524(01)00110-9

Ferreiro, N., & Soto, M. (2003). Anaerobic hydrolysis of primary sludge: Influence of sludge concentration and temperature. *Water Science and Technology*, *47*(12), 239–246.

Gebremariam, S. Y., Beutel, M. W., Christian, D., & Hess, T. F. (2011). Research advances and challenges in the microbiology of enhanced biological phosphorus removal--a critical review. *Water Environment Research : A*

Research Publication of the Water Environment Federation, *83*(3), 195–219. https://doi.org/10.2175/106143010X12780288628534

Ghosh, S. (1981). Kinetics of acid-phase fermentation in anaerobic digestion. Biotechnology and bioengineering Symposium No. 11: 301-313

Henze, M., Gujer, W., Mino, T., & van Loosdrecht, M. C. M. (2000). Activated Sludge Models ASM1, ASM2, ASM2d and ASM3. *IWA Publishing*, 121. https://doi.org/10.1007/s13398-014-0173-7.2

Hobson, P. N. (1987). A model of some aspects of microbial degradation of particulate substrates. *Journal of Fermentation Technology*, *65*(4), 431–439. https://doi.org/10.1016/0385-6380(87)90140-3

Hu, Z. R., Wentzel, M. C., & Ekama, G. A. (2002). Anoxic growth of phosphate-accumulating organisms (PAOs) in biological nutrient removal activated sludge systems. *Water Research*, *36*(19), 4927–4937. https://doi.org/10.1016/S0043-1354(02)00186-0

Humphrey, 1979. The hydrolysis of cellulosic materials to useful products. In: Brown, R.D., Jurasek,L. (Eds.), Hydrolysis of Cellulose: Mechanisms of Enzymatic and Acid Catalysis. American Chemical Society, Washington, DC, pp 25-53

Ji, Z., Chen, G., & Chen, Y. (2010). Effects of waste activated sludge and surfactant addition on primary sludge hydrolysis and short-chain fatty acids accumulation. *Bioresource Technology*, *101*(10), 3457–3462. https://doi.org/10.1016/j.biortech.2009.12.117

Jones, R. M. (1992). Dynamic modelling for control of high rate anaerobic wastewater treatment processes. *McMaster University Phd Thesis*.

Lee, W. S., Chua, A. S. M., Yeoh, H. K., & Ngoh, G. C. (2014). A review of the production and applications of waste-derived volatile fatty acids. *Chemical Engineering Journal*, *235*, 83–99. https://doi.org/10.1016/j.cej.2013.09.002

Lilley, Wentzel, Loewenthal, & Marais. (1990). Acid Fermentation of Primary Sludge at 20C. *University of Cape Town*, (February). Retrieved from https://open.uct.ac.za/bitstream/handle/11427/8295/thesis_ebe_1990_lilley_id.pdf?sequence=1

Maharaj, I., & Elefsiniotis, P. (2001). The role of HRT and low temperature on the acid-phase anaerobic digestion of municipal and industrial wastewaters. *Bioresource Technology*, *76*(3), 191–197. https://doi.org/10.1016/S0960-8524(00)00128-0

Metcalf, E., & Eddy, H. (2003). Wastewater engineering: treatment and reuse. *Tata McGraw-Hill Publishing Company Limited, 4th Edition. New Delhi, India*. https://doi.org/10.1016/0309-1708(80)90067-6

Münch, E. v., Keller, J., Lant, P., & Newell, R. (1999). Mathematical Modelling of Prefermentersði . Model Development and Verification. *Water Research*, *33*(12), 2752–2768. https://doi.org/10.1016/S0043-1354(98)00516-8

Pavlostathis, S. G., & Giraldo-Gomez, E. (1991). Kinetics of anaerobic treatment. *Water Science and Technology*, *24*(8), 35–59.

Philip, H., Maunoir, S., Rambaud, A., & Philippi, L. S. (1993). Septic tank sludges: Accumulation rate and biochemical characteristics. *Water Science and Technology*, *28*(10), 57–64.

Pratt, S., Liew, D., Batstone, D. J., Werker, A. G., Morgan-Sagastume, F., & Lant, P. A. (2012). Inhibition by fatty acids during fermentation of pre-treated waste activated sludge. *Journal of Biotechnology*, *159*(1–2), 38–43. https://doi.org/10.1016/j.jbiotec.2012.02.001

Rabinowitz, B., & Fries, M. K. (2010). Primary Sludge Fermenters in BNR Plants : Are they Cost-Effective for Meeting Effluent Phosphorus Limits ?, (October 2008), 83–94.

Ristow, N., Sötemann, S., Loewenthal, R., Wentzel, M., & Ekama, G. (2005). Hydrolysis of Primary Sewage Sludge under Methanogenic, Acidogenic and Sulfate-reducing Conditions, (1216).

Sanders, W. (2001). *Anaerobic hydrolysis digestion of complex substrates*.

Smolders, G. J. F., van der Meij, J., van Loosdrecht, M. C. M., & Heijnen, J. J. (1995). A structured metabolic model for the anaerobic and aerobic stoichiometry of the biological phosphorus removal process. Biotechnology and Bioengineering. *Biotechnology and Bioengineering*, *47*(3), 277–287. https://doi.org/10.1002/bit.260470302

Thomas, M., Wright, P., Blackall, L., Urbain, V., & Keller, J. (2003). Optimisation of Noosa BNR plant of improve performance and reduce operating costs. *Water Science and Technology*, *47*(12), 141–148.

Ucisik, A. S., & Henze, M. (2008). Biological hydrolysis and acidification of sludge under anaerobic conditions: The effect of sludge type and origin on the production and composition of volatile fatty acids. *Water Research*, *42*(14), 3729–3738. https://doi.org/10.1016/j.watres.2008.06.010

Vavilin, V. A., Rytov, S. ., & Lokshina, L. Y. (1996). A description of hydrolysis kinetics in anerobic degradation of particulate organic matter. *Bioresource*

Technology, *56*, 229–237.

Wentzel, M., Dold, P., Ekama, G., & Marais, G. (1989). Enhanced polyphosphate organism cultures in activated sludge systems: Part 3 Kinetic Model. *Water SA*, *15*(2), 89.

Wu, H., Yang, D., Zhou, Q., & Song, Z. (2009). The effect of pH on anaerobic fermentation of primary sludge at room temperature. *Journal of Hazardous Materials*, *172*(1), 196–201. https://doi.org/10.1016/j.jhazmat.2009.06.146

Yeoman, S., Stephenson, T., Lester, J. N., & Perry, R. (1988). The removal of phosphorus during wastewater treatment: A review. *Environmental Pollution*, *49*(3), 183–233. https://doi.org/10.1016/0269-7491(88)90209-6

Yuan, Q., Sparling, R., & Oleszkiewicz, J. A. (2011). VFA generation from waste activated sludge: Effect of temperature and mixing. *Chemosphere*, *82*(4), 603–607. https://doi.org/10.1016/j.chemosphere.2010.10.084

Zoetemeyer, R. J., van den Heuvel, J. C., & Cohen, A. (1982). pH influence on acidogenic dissimilation of glucose in an anaerobic digestor. *Water Research*, *16*(3), 303–311. https://doi.org/10.1016/0043-1354(82)90190-7

7. Appendix A: Hydrolysis rate calculations for PS, ML and WAS

Primary Sludge Reactor Hydrolysis rate Calculations

	SRT	6	days			Feeding Vol	1.3	L	Yad	0.22	kg/kg							
	Q	0.66	L/d			After Wasted	2.7	L	bad	0.2	1/d		Kh	2.2	mgCOD/mg Zad as COD.d			
	V	4	L						Rh	6	days		Kx	0.15	mgCOD/mg Zad as COD			
									Supi=	33.00%	= Sup'							

Day	PS FEED TCODin	PS FEED sCODin	FEED pCOD	PS TCODout	PS sCODout	PS pCODout	Reactor initial pCOD	Reactor initi Sbpi	Reactor fina Sbp	First Estimate Rhydr	kH	PS VFA out	Ratio VFA/sCOD	Zad estimate	Rhydr New	Error	Hydr Constant
	Sti = Supi + Sbpi + Ssi	Ssi = Susi +Sbsfi +	Supi +Sbpi					67%									
0	16247	277.08	15969.5				15969.5	10700	9166	253.1	0.03	591.95					
2	11302	520.66	10781.4	14833.9	1154.0	13679.9	12737.9	8534	5889	436.4	0.07	1130.09	0.98	91.9	201.77	-234.65	0.03
4	2338	204.01	2134.4	10431.2	1641.1	8790.1	6627.0	4440	5184	-122.7	-0.02	1673.62	1.02	95.7	210.03	332.70	0.04
8	12715	755.10	11959.7	10005.0	2268.3	7736.7	9109.1	6103	6051	8.7	0.00	2247.04	0.99	93.0	204.11	195.43	0.03
10	13080	1126.55	11953.5	11679.6	2648.9	9030.7	9980.6	6687	5944	122.5	0.02	2555.72	0.96	90.6	198.80	76.28	0.03
14	13445	1175.27	12270.2	11228.9	2356.6	8872.3	9976.6	6684	6467	35.9	0.01	3763.66	1.60	149.9	328.68	292.76	0.05
16	9926	1251.38	8674.4	12465.1	2813.3	9651.8	9334.1	6254	9692	-567.3	-0.06	5303.80	1.89	177.0	388.27	955.54	0.04
18	8148	2773.73	5374.0	16733.7	2268.3	14465.4	11510.7	7712	8884	-193.4	-0.02	3084.74	1.36	127.7	280.24	473.60	0.03
23	31531	1132.64	30398.3	16660.7	3400.9	13259.7	18829.8	12616	4027	1417.2	0.35	2764.45	0.81	76.3	167.39	-1249.80	0.04
25	28718	675.94	28041.7	9450.8	3440.5	6010.3	13170.5	8824	5616	529.4	0.09	2518.00	0.73	68.7	150.87	-378.49	0.03
28	21033	438.45	20594.4	12032.8	3650.6	8382.1	12351.1	8275	13337	-835.2	-0.06	2812.33	0.77	72.3	158.97	994.19	0.01
30	15102	481.08	14620.7	22944.9	3038.6	19906.3	18188.5	12186	8433	619.3	0.07	2121.96	0.70	65.6	144.05	-475.21	0.02
32	21088	706.38	20381.3	15053.1	2466.2	12586.8	15120.0	10130	8431	280.4	0.03	2184.63	0.89	83.2	182.67	-97.71	0.02
35	14724	185.74	14538.5	14632.9	2049.1	12583.8	13219.1	8857	6214	436.1	0.07	1979.67	0.97	90.7	199.08	-237.02	0.03
37	23280	551.10	22728.7	11807.4	2533.2	9274.2	13646.9	9143	9590	-73.7	-0.01	2081.10	0.82	77.1	169.45	243.11	0.02
39	8793	511.52	8281.7	16989.5	2676.3	14313.2	12352.9	8276				2196.16	0.82	77.0			
average	15681.5	832.6	14848.9	13796.6	2560.4	11236.2	12410.3	8314.9	7411.3	156.5	0.04	2561.1	1.0	95.8	213.2	63.6	0.03
st dev	7716.3	614.0	7807.3	3450.3	647.6	3457.1	3175.5	2127.6	2354.4	511.3	0.10	1061.2	0.3	31.3	68.5	561.9	0.01

		First-order		Surface Reaction	
		Avg	St.dev	Avg	St.dev
PS	Rhydr	156.5	511.3	213.2	68.5
	Kh	0.04	0.1	0.03	0.01

Mixed Liquor Sludge Reactor Hydrolysis rate Calculations

	SRT	6	days		Feeding Vol	1.3	L	Yad	0.22	kg/kg							
	Q	0.66	L/d		After Wasted	2.7	L	bad	0.2	1/d		Kh	2.2	mgCOD/mg Zad as COD.d			
	V	4	L					Rh	6	days		Kx	0.15	mgCOD/mg Zad as COD			
								Supi=	33.00%	= Sup'							

Day	ML FEED TCODin	ML FEED sCODin	FEED pCOD	ML TCODout	ML sCODout	ML pCODout	Reactor initial pCOD	Reactor initi Sbpi	Reactor final Sbp	First Estimate Rhydr	kh	ML VFA out	Ratio VFA/sCOD	Zad estimate	Rhydr New	Error	Hydr Constant
	Sti = Supi + Sbpi + Ssi	Ssi = Susi +Sbsfi +	Supi +Sbpi					67%									
0	12121	181.05	11939.7				11939.7	7999.6	6952	172.8	0.02	218.7					
2	8771	333.45	8437.1	11801.3	1424.9	10376.4	9746.1	6529.9	5802	120.2	0.02	1441.1	1.01	11.1	24.32	-95.84	0.00
4	4021	136.90	3883.8	10029.3	1370.1	8659.2	7107.2	4761.8	4404	59.0	0.01	1592.9	1.16	12.7	27.95	-31.04	0.01
8	10498	482.51	10015.5	8293.9	1720.3	6573.6	7692.2	5153.8	6440	-212.3	-0.03	2390.5	1.39	15.2	33.41	245.67	0.01
10	10984	727.62	10256.0	11801.3	2189.2	9612.2	9821.4	6580.4	6308	45.0	0.01	1830.8	0.84	9.1	20.11	-24.90	0.00
14	10983	746.02	10237.4	11344.6	1930.4	9414.3	9681.8	6486.8	4927	257.4	0.05	3496.8	1.81	19.8	43.54	-213.90	0.01
16	8334	812.88	7520.9	9645.7	2292.7	7353.0	7407.6	4963.1	7891	-483.0	-0.06	4116.0	1.80	19.6	43.16	526.20	0.01
18	6634	1770.85	4863.5	13335.9	1558.9	11777.0	9530.1	6385.2	11203	-795.0	-0.07	2163.5	1.39	15.2	33.37	828.39	0.00
23	23784	720.75	23063.0	19437.5	2715.9	16721.6	18782.5	12584.3	7574	826.6	0.11	2016.3	0.74	8.1	17.85	-808.78	0.00
25	21757	438.06	21319.2	13902.2	2597.1	11305.0	14559.6	9755.0	10361	-100.0	-0.01	647.2	0.25	2.7	5.99	105.98	0.00
28	17101	310.71	16790.7	18012.5	2548.4	15464.1	15895.2	10649.8	11840	-196.4	-0.02	1489.1	0.58	6.4	14.05	210.42	0.00
30	12707	322.33	12384.5	19766.3	2094.8	17671.5	15953.2	10688.7	7895	461.0	0.06	1453.6	0.69	7.6	16.69	-444.32	0.00
32	16379	463.64	15915.1	13579.4	1796.4	11783.1	13126.0	8794.4	6518	375.7	0.06	1269.9	0.71	7.7	17.00	-358.66	0.00
35	12644	115.16	12528.8	11259.4	1531.5	9727.9	10638.2	7127.6	8501	-226.5	-0.03	1344.0	0.88	9.6	21.10	247.64	0.00
37	17754	352.33	17401.7	14310.2	1622.8	12687.3	14219.5	9527.1	9716	-31.2	0.00	1261.0	0.78	8.5	18.69	49.91	0.00
39	9180	328.95	8850.6	16234.4	1732.4	14502.0	12665.3	8485.7				1313.7	0.76	8.3			
average	12768.7	537.5	12231.2	13516.9	1941.7	11575.2	11788.4	7898.2	7812.8	18.2	0.01	1855.1	1.0	10.8	24.1	16.9	0.004
st dev	5372.9	390.3	5452.1	3392.6	426.6	3198.5	3426.0	2295.4	2207.0	379.4	0.05	957.9	0.4	4.8	10.5	394.2	0.002

	First-order		Surface Reaction	
	Avg	St.dev	Avg	St.dev
Rhydr	18.2	379.417972	24.09	10.54
Kh	0.01	0.05	0.004	0.002

Waste Activated Sludge Reactor Hydrolysis rate Calculations

SRT	6	days		Feeding Vol	0.325	L	Yad	0.22	kg/kg							
Q	0.167	L/d		After Wasted	0.675	L	bad	0.2	1/d		Kh	2.2	mgCOD/mg Zad as COD.d			
V	1	L					Rh	6	days		Kx	0.15	mgCOD/mg Zad as COD			
							Supi=	65.00%	= Sup'							

Day	WAS FEED TCODin	WAS FEED sCODin	FEED pCOD	WAS TCODout	WAS sCODout	WAS pCODout	Reactor initial pCOD	Reactor initi Sbpi	Reactor final Sbp	First Estimate Rhydr	kh	WAS VFA out	Ratio VFA/sCOD	Zad estimate	Rhydr New	Error	Hydr Constant
	Sti = Supi + Sbpi + Ssi	Ssi = Susi +Sbsfi +	Supi +Sbpi					35%									
0	5389	24.36	5364.8				5364.8	1877.7	2271	-65.7	-0.03	8.47					
2	4640	28.01	4612.2	6582.7	94.4	6488.3	5878.6	2057.5	1978	13.2	0.01	17.75	0.19	-2.3	-5.15	-18.35	0.00
4	6765	27.41	6738.0	5803.3	150.4	5652.9	6005.5	2101.9	2009	15.5	0.01	112.18	0.75	-6.0	-13.21	-28.66	-0.01
8	6881	37.76	6843.3	5925.0	183.9	5741.1	6099.4	2134.8	2932	-133.1	-0.05	132.19	0.72	-5.8	-12.73	120.42	0.00
10	7563	76.73	7486.4	8476.5	99.3	8377.2	8087.7	2830.7	2239	98.8	0.04	80.74	0.81	-6.5	-14.40	-113.23	-0.01
14	6966	45.67	6920.6	6741.0	344.1	6397.0	6567.2	2298.5	2928	-105.1	-0.04	346.39	1.01	-8.1	-17.83	87.26	-0.01
16	5736	97.43	5638.8	8762.7	397.6	8365.1	7479.0	2617.7	2074	90.8	0.04	208.72	0.52	-4.2	-9.29	-100.13	0.00
18	4165	134.58	4030.6	6625.3	700.3	5925.0	5309.4	1858.3	2783	-154.4	-0.06	0.00	0.00	0.0	0.00	154.40	0.00
23	11144	48.72	11095.0	8214.7	263.7	7951.0	8972.8	3140.5	2845	49.4	0.02	0.00	0.00	0.0	0.00	-49.40	0.00
25	10401	49.94	10350.8	8360.8	233.2	8127.6	8850.1	3097.5	4837	-290.5	-0.06	0.00	0.00	0.0	0.00	290.49	0.00
28	10687	102.30	10584.6	14042.2	222.3	13819.9	12768.5	4469.0	3064	234.7	0.08	0.00	0.00	0.0	0.00	-234.67	0.00
30	8799	63.33	8735.9	8975.8	222.3	8753.6	8747.8	3061.7	3125	-10.6	0.00	0.00	0.00	0.0	0.00	10.59	0.00
32	8696	67.60	8628.1	9176.8	247.8	8928.9	8831.2	3090.9	2379	119.0	0.05	18.75	0.08	-0.6	-1.34	-120.30	0.00
35	9250	0.00	9249.8	6966.3	170.5	6795.8	7593.4	2657.7	2848	-31.8	-0.01	23.39	0.14	-1.1	-2.43	29.33	0.00
37	8738	28.01	8710.3	8324.3	187.6	8136.7	8323.1	2913.1	3101	-31.4	-0.01	29.04	0.15	-1.2	-2.74	28.61	0.00
39	9810	31.06	9779.0	9079.4	219.8	8859.5	9158.4	3205.4				0.00	0.00	0			
average	8016.1	55.9	7960.2	8137.1	249.1	7888.0	7911.5	2769.0	2795.8	-13.4	-0.0003	64.6	0.3	-2.4	-5.7	4.0	-0.002
st dev	2074.0	34.0	2083.2	1940.8	143.2	1956.0	1804.0	631.4	695.5	124.0	0.0398	96.1	0.4	2.8	6.2	127.6	0.003

	First-order		Surface Reaction	
	Avg	St.dev	Avg	St.dev
Rhydr	-13.4	124.044145	-5.65	6.23
Kh	0.00	0.04	0.00	0.00

8. Appendix B: BioWin Model Configurations

Primary Sludge

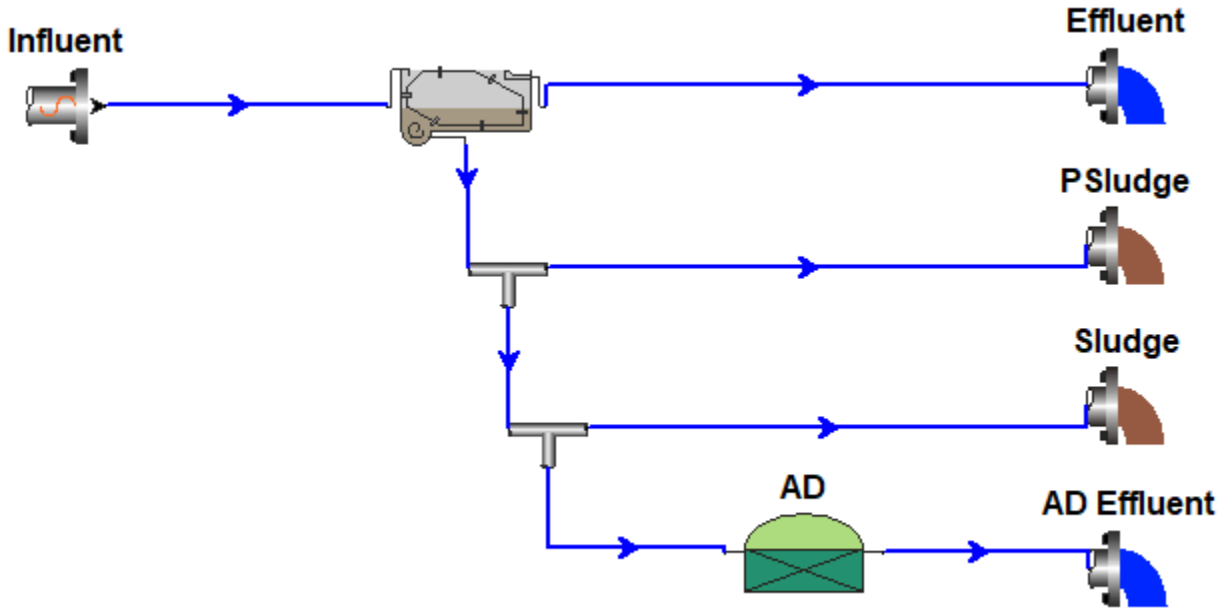

Waste Activated Sludge

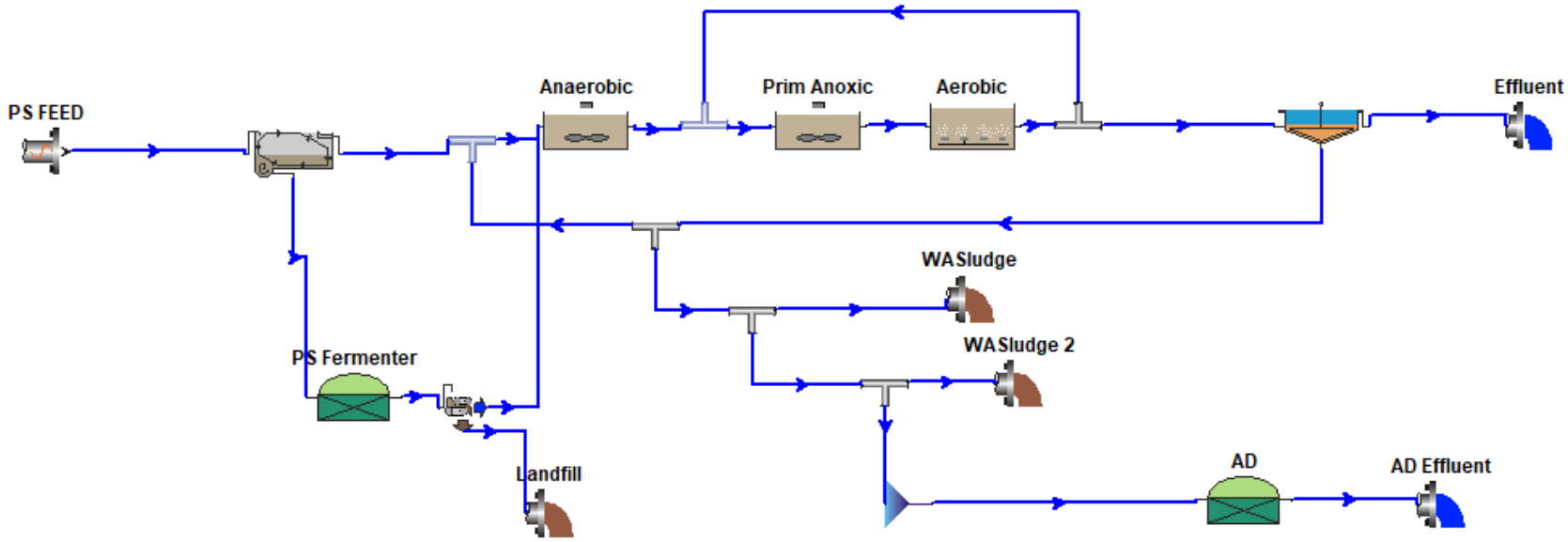

Mixed Liquor Model

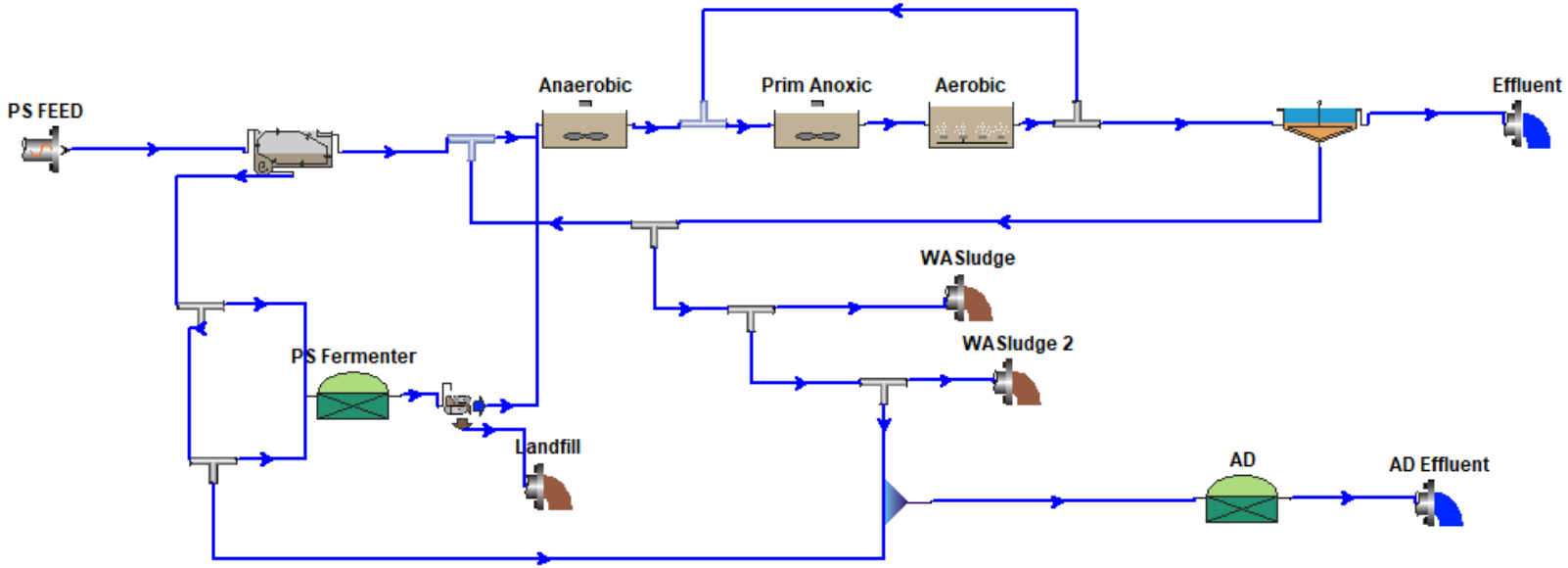

9. Appendix C: Raw Data

pH and Temperature Summary

No. of Test	Days	PS	PS+AS	WAS	PS Feed	WAS Feed	Temperature (°C)
1	0	6.62	6.71	6.94	6.62	6.94	18
2	2	5.59	5.71	6.90	6.44	6.93	19
3	4	5.61	5.71	6.87	6.49	6.87	24
4	8	4.99	5.44	6.79	6.23	6.84	22
5	10	4.88	5.31	6.84	6.08	6.81	23
6	14	4.80	5.17	6.69	5.77	6.87	20
7	16	4.67	5.06	6.75	5.83	6.85	23
8	18	4.55	4.97	6.77	5.78	6.89	23
8	23	4.72	5.03	6.65	6.08	6.97	23
8	25	4.93	5.42	6.84	6.41	6.97	21
9	28	5.05	5.37	6.85	6.59	6.93	23
10	30	4.71	5.34	6.80	6.82	6.97	21
11	32	5.30	5.79	5.84	6.42	6.98	22
12	35	5.24	5.63	6.76	6.46	6.96	21
13	37	5.02	5.55	6.84	6.44	7.04	22
14	39	4.57	5.44	6.78	6.87	6.94	23
15	51	5.22	5.27	6.84	6.68	7.03	21
16	53	5.28	5.83	6.81	7.73	6.90	21
17	56	5.89	6.38	6.61	7.08	7.06	21
18	58	6.13	6.52	6.51	6.86	7.00	22
19	60	5.63	6.14	6.81	6.32	7.00	21

TSS and VSS Summary Table

mg/L

Day	PS		ML		WAS		PS Feed		WAS Feed		ML FEED	
	TSS	VSS	TSS	VSS	TSS	VSS	TSS	VSS	TSS	VSS	TSS	VSS
0	11150	9750	9483	8183	4783	3767	11150	9750	4783	3767	9113	7835
2	11150	9750	9183	7817	5633	4267	12433	10850	6350	4750	10487	8898
4	7683	6517	7300	6333	6017	4600	2583	2217	6967	5233	3986	3182
8	6683	5883	5733	4800	7133	5450	8067	7033	6383	4983	7528	6377
10	7667	6683	7050	5883	5983	4617	8517	7467	6850	5267	7983	6763
14	12633	10967	7400	6267	6600	4950	10567	9350	6917	5300	9399	8054
16	8200	6867	7717	6500	7000	5317	8267	7300	6367	4833	7659	6511
18	13400	12000	8900	7700	6300	5100	4183	3800	6867	5417	5042	4317
23	9433	8133	15467	12950	6517	5033	19433	16867	6883	5367	15417	13187
25	18000	14800	15967	13250	5733	4550	14167	11967	6400	4917	11681	9711
28	11267	9667	10533	8900	5967	4800	10650	8750	7433	5800	9621	7806
30	9200	7983	9067	7517	6700	5033	7400	6067	8033	5783	7603	5976
32	9000	7100	8117	6533	5883	4817	12900	10933	6650	5017	10900	9040
35	10667	9167	7283	6317	4400	4883	11100	9633	6967	5767	9777	8396
37	10467	8900	8100	6883	6317	4950	14617	12617	6867	5233	12137	10254
39	7967	6717	6283	5150	5867	4583	3933	3450	8700	6833	5459	4533
51	14167	11533	11333	9367	5833	4433	6433	5400	5583	4217	6161	5021
53	10500	8917	8067	6567	6450	4950	4250	3683	4017	2833	4175	3411
56	5333	4333	5517	4383	5900	4200	2283	1883	7000	5533	3793	3051
58	3933	3100	4117	3250	6400	5050	6617	5767	6317	4850	6521	5473
60	3617	3167	3650	3150	5150	4183	10300	9217	6317	5133	9025	7910

COD Summary Table

mg COD/L

Day	PS			PS+AS			WAS		
	TCOD	sCOD	ffCOD	TCOD	sCOD	ffCOD	TCOD	sCOD	ffCOD
0	16247	277	250	11783	195	155	5389	24	19
2	14834	1154	810	11801	1425	1075	6583	94	88
4	10431	1641	1297	10029	1370	1227	5803	150	146
8	10005	2268	1927	8294	1720	1434	5925	184	127
10	11680	2649	2302	11801	2189	1720	8477	99	76
14	11229	2357	1912	11345	1930	1522	6741	344	249
16	12465	2813	2031	9646	2293	1879	8763	398	296
18	16734	2268	3176	13336	1559	2180	6625	700	523
23	16661	3401	2862	19437	2716	2143	8215	264	201
25	9451	3441	2521	13902	2597	1894	8361	233	166
28	12033	3651	2722	18013	2548	1879	14042	222	152
30	22945	3039	2445	19766	2095	1748	8976	222	151
32	15053	2466	2010	13579	1796	1422	9177	248	165
35	14633	2049	1665	11259	1531	856	6966	171	55
37	11807	2533	1918	14310	1623	1388	8324	188	124
39	16989	2676	2147	16234	1732	1510	9079	220	129
51	26355	3017	2299	20978	1906	1474	6985	194	144
53	22799	2612	1985	13299	1531	1455	6790	197	219
56	8811	1866	1346	6430	798	786	8215	242	166
58	5097	1075	920	6577	344	350	7807	187	132
60	6571	1340	1221	5931	600	612	7399	219	175

COD Summary Table

mg COD/L

Day	PS Feed			WAS Feed		
	TCOD	**sCOD**	**ffCOD**	**TCOD**	**sCOD**	**ffCOD**
0	16247	277	250	5389	24	19
2	11302	521	441	4640	28	35
4	2338	204	219	6765	27	21
8	12715	755	673	6881	38	26
10	13080	1127	923	7563	77	88
14	13445	1175	950	6966	46	41
16	9926	1251	1233	5736	97	84
18	8148	2774	1069	4165	135	423
23	31531	1133	889	11144	49	38
25	28718	676	445	10401	50	26
28	21033	438	314	10687	102	54
30	15102	481	481	8799	63	58
32	21088	706	822	8696	68	76
35	14724	186	110	9250	0	0
37	23280	551	521	8738	28	76
39	8793	512	408	9810	31	46
51	11978	697	518	5980	44	30
53	6376	773	795	4695	79	85
56	2838	332	353	9603	52	79
58	10991	457	326	7076	36	36
60	18384	1203	953	7782	69	60

VFA production Summary Table

mg VFA
as COD /L

	Acetate			Propionate			Iso-Butyrate			n-Butyrate		
Days	**PS**	**PS+AS**	**WAS**	**PS**	**PS+AS**	**WAS**	**PS**	**PS+AS**	**WAS**	**PS**	**PS+AS**	**WAS**
0	220.61	127.27	8.47	167.29	72.16	0.00	71.63	0.00	0.00	132.42	19.24	0.00
2	493.48	569.59	14.38	374.15	488.23	0.00	40.10	56.89	0.00	147.95	216.90	0.00
4	691.52	695.66	75.87	540.33	505.33	0.00	51.80	42.30	11.99	268.46	242.58	0.00
8	806.04	822.00	51.01	754.29	557.34	21.67	60.69	169.86	16.53	380.63	393.68	12.15
10	915.65	566.87	22.15	866.29	578.63	12.08	78.74	98.96	12.78	403.70	287.82	12.08
14	677.75	1047.80	108.39	690.81	670.72	35.34	167.82	93.67	41.88	1241.25	922.06	30.46
16	1288.07	1041.02	0.00	888.66	711.54	43.81	447.33	198.69	43.42	1322.43	923.56	26.78
18	1062.96	776.87	0.00	726.90	521.85	0.00	123.27	90.54	0.00	704.47	433.85	0.00
23	994.30	878.43	0.00	675.39	456.16	0.00	102.47	84.75	0.00	629.35	311.81	0.00
25	935.99	190.04	0.00	631.27	146.96	0.00	90.33	71.52	0.00	564.08	66.37	0.00
28	1028.86	622.99	0.00	710.61	359.33	0.00	95.23	71.02	0.00	635.07	233.31	0.00
30	784.45	675.54	0.00	501.94	349.03	0.00	76.23	50.91	0.00	491.72	216.15	0.00
32	702.73	610.89	18.75	442.47	244.21	0.00	108.08	71.96	0.00	505.83	146.97	0.00
35	764.13	658.74	17.61	485.83	289.65	5.78	82.04	68.07	0.00	414.04	146.45	0.00
37	909.30	615.34	21.24	491.98	301.14	7.80	61.85	56.07	0.00	419.94	158.64	0.00
39	989.44	668.60	0.00	534.78	306.55	0.00	58.40	49.39	0.00	443.86	161.43	0.00
51	0.00	0.00	18.10	0.00	0.00	8.70	0.00	0.00	1.47	0.00	0.00	0.00
53	796.96	569.12	13.04	531.86	306.20	0.00	90.50	85.39	0.00	480.07	194.87	0.00
56	0.00	80.96	0.00	0.00	51.90	0.00	27.20	67.36	0.00	22.95	31.96	0.00
58	0.00	89.14	0.00	0.00	43.90	0.00	0.00	0.00	0.00	0.00	0.00	0.00
60	989.44	668.60	0.00	0.00	0.00	0.00	0.00	0.00	0.00	0.00	0.00	0.00

VFA production Summary Table (Cont'd)

mg VFA as COD /L

	Iso-Valarate			n-Valarate			TOTAL VFA as COD		
Days	**PS**	**PS+AS**	**WAS**	**PS**	**PS+AS**	**WAS**	**PS**	**PS+AS**	**WAS**
0	0.00	0.00	0.00	0.00	0.00	0.00	591.95	218.67	8.47
2	29.88	43.22	3.36	44.52	66.24	0.00	1130.09	1441.06	17.75
4	33.57	32.14	24.32	87.93	74.90	0.00	1673.62	1592.91	112.18
8	108.32	227.59	22.65	137.08	219.99	8.19	2247.04	2390.46	132.19
10	109.95	135.83	18.91	181.40	162.70	2.75	2555.72	1830.82	80.74
14	421.38	356.99	95.54	564.63	405.57	34.77	3763.66	3496.81	346.39
16	651.96	313.94	72.68	705.35	927.24	22.03	5303.80	4115.99	208.72
18	125.97	94.49	0.00	341.18	245.87	0.00	3084.74	2163.48	0.00
23	103.76	87.00	0.00	259.17	198.13	0.00	2764.45	2016.29	0.00
25	80.81	80.79	0.00	215.52	91.57	0.00	2518.00	647.24	0.00
28	71.35	60.49	0.00	271.21	142.01	0.00	2812.33	1489.15	0.00
30	32.57	31.50	0.00	235.06	130.43	0.00	2121.96	1453.56	0.00
32	127.37	88.08	0.00	298.15	107.78	0.00	2184.63	1269.88	18.75
35	72.23	81.70	0.00	161.40	99.44	0.00	1979.67	1344.03	23.39
37	28.56	38.71	0.00	169.47	91.12	0.00	2081.10	1261.04	29.04
39	0.00	34.17	0.00	169.68	93.51	0.00	2196.16	1313.65	0.00
51	0.00	0.00	0.00	0.00	0.00	0.00	0.00	0.00	28.27
53	105.33	128.83	0.00	225.07	91.04	0.00	2229.79	1375.45	13.04
56	41.42	22.00	0.00	0.00	0.00	0.00	91.57	254.17	0.00
58	0.00	0.00	0.00	0.00	0.00	0.00	0.00	133.05	0.00
60	0.00	0.00	0.00	0.00	0.00	0.00	989.44	668.60	0.00

Ammonia Concentration

mg N/ L

Day	PS	PS+AS	WAS	PS Feed	WAS Feed		PS Feed NH3/TKN ratio
0	21.25	16.51	1.22	20.63	1.22		
2	41.34	33.52	15.25	27.55	5.05		0.43
4	42.08	31.71	28.25	24.23	7.39		0.37
8	40.44	45.09	39.12	44.55	11.69		0.43
10	34.01	48.46	45.71	47.93	14.00		0.64
14	49.91	49.16	48.75	56.58	16.68		1.01
16	50.98	56.29	54.27	56.33	18.61		1.23
18	50.40	54.76	54.60	63.25	21.33		1.25
23	64.89	56.54	46.78	35.37	1.24		0.64
25	59.95	58.14	34.01	18.69	1.16		0.33
28	46.20	38.58	33.93	19.31	0.26		0.13
30	38.13	30.72	36.07	26.85	0.32		0.71
32	45.13	46.61	35.66	27.30	0.20		0.20
35	46.36	47.06	32.36	29.03	0.50		0.06
37	32.04	32.24	32.04	28.29	0.64		0.12
39	35.91	35.95	41.92	24.42	0.00		0.15
51	59.54	47.19	33.68	29.24	0.04		0.07
53	79.31	81.12	43.32	50.85	1.09		0.32
56	78.32	50.32	33.76	23.26	0.00		0.16
58	60.04	39.78	34.42	23.26	0.00		
60	58.80	35.95	35.25	34.30	0.46	Avg	0.46

TKN and sTKN Summary Table

mg N/L

Days	PS		PS+AS		WAS		PS Feed		WAS Feed	
	TKN	sTKN	TKN	sTKN	TKN	sTKN	TKN	sTKN	TKN	sTKN
0	118.65	35.69	102.52	27.5	124.76	3.9	-	-	-	-
2	65.13	51.38	311.97	89.7	75.79	10.2	64.76	52.5	395.00	8.8
4	80.79	137.64	87.37	150.9	102.59	50.4	66.29	124.7	138.98	26.3
8	236.72	118.86	357.65	84.0	325.09	59.6	102.44	95.9	67.39	13.6
10	291.98	62.10	66.09	164.6	327.33	15.7	74.43	25.2	96.55	17.4
14	288.78	46.34	298.32	40.7	437.28	24.5	55.94	28.7	77.18	29.5
16	61.04	18.07	263.13	45.1	52.74	22.7	45.76	69.6	66.63	27.5
18	41.49	116.58	45.46	119.7	62.88	29.3	50.53	115.7	74.27	20.5
23	58.68	118.83	52.39	127.4	44.56	51.4	55.67	90.5	46.11	21.8
25	56.57	107.80	67.83	94.0	73.02	55.0	56.03	98.4	70.52	16.0
28	64.20	91.50	79.17	112.7	38.42	57.8	143.36	127.0	8.61	18.7
30	101.27	132.37	72.28	159.0	40.31	61.7	37.71	88.9	41.95	17.3
32	303.75	124.04	278.79	146.2	331.89	51.6	135.51	992.9	383.56	10.0
35	152.62	97.96	182.17	110.2	461.14	49.5	461.14	70.1	535.82	14.2
37	483.94	123.44	245.09	118.0	489.65	32.3	237.83	113.7	557.47	17.5
39	272.80	200.08	328.60	100.9	489.64	63.6	167.90	-3.5	94.21	40.4
51	735.81	138.27	0.00	0.0	424.12	82.4	429.62	82.1	129.04	10.4
53	494.64	383.12	126.90	635.7	477.35	85.0	160.46	101.4	252.22	13.8
56	372.79	309.31	312.56	531.2	506.27	64.1	144.14	4.4	676.89	7.4

Phosphorus Summary Table

mg P/L

Day	PS	ML	WAS	PS Feed	WAS Feed
0	28.05	27.35	0.05	28.05	0.05
2	93.30	107.95	34.30	62.85	0.43
4	120.50	112.50	39.50	37.40	5.84
8	139.35	153.00	47.25	84.15	5.00
10	139.35	152.50	18.07	21.33	14.93
14	151.10	154.00	57.30	80.30	10.43
16	156.30	157.75	55.35	79.85	16.68
18	159.20	169.60	55.30	78.55	16.85
23	173.40	180.00	36.70	67.35	0.00
25	193.85	165.45	55.80	40.38	0.00
28	208.60	160.65	62.50	56.75	0.00
30	271.80	197.30	72.00	28.80	0.00
32	203.40	155.10	69.00	45.90	0.00
35	160.55	134.75	78.05	46.40	0.00
37	184.80	130.25	86.40	43.95	0.00
39	177.30	145.90	108.95	22.68	0.00
51	262.10	190.50	104.80	46.25	0.00
53	205.20	171.00	115.80	18.73	0.00
56	108.55	102.35	128.45	23.75	0.00
58	73.37	78.31	131.90	19.12	0.00
60	74.28	90.15	137.95	47.55	0.00

Glossary

ADM1 = Anaerobic digestion model No. 1
ASDM = Activated sludge and anaerobic digestion model
BNR= Biological nutrient removal
bpCOD = biodegradable particulate COD
bVSS = biodegradable VSS
C_a= concentration of acidogenic biomass
C_e= concentration of hydrolytic enzyme
C_e= concentration of hydrolytic enzymes
C_{mo}= concentration of monomer species
$C_{NH4\text{-}N}$= concentration of ammonia nitrogen
CO2 = Carbon dioxide gas
COD = Chemical oxygen demand
C_p= concentration of particulate substrate
C_{VFA}= concentration of VFA
$C_{x,a}$= concentration of acidogenic bacteria
$C_{x,m}$= concentration of methanogenic bacteria
d_e= denaturation rate constant for hydrolytic enzymes
D_o= dissolved oxygen concentration
EBPR = Enhanced biological phosphorus removal
E_Q = Enzyme concentration
H2 = Hydrogen gas
I_1= Inhibition function
k = first-order constant
K_a= half-saturation coefficient for monomer species
K_{ads}= adsorption of colloidal COD rate constant
k_{ALK}= saturation coefficient for alkalinity
K_{amm}= ammonification rate constant
k_{dis}= first-order disintegration constant
$K_{E/S}$ = Substrate IC50 in enzyme growth
k_{fe}= saturation coefficient for fermentation of S_f
k_h= first-order hydrolysis rate constant
K_h= hydrolysis rate constant
$k_{hydr,ch}$= first-order carbohydrate hydrolysis constant
$k_{hydr,li}$= first-order lipids hydrolysis constant
$k_{hydr,pr}$= first-order protein hydrolysis constant
k_{hydr}= first order hydrolysis rate constant

$k_{m,aa}$= specific Monod maximum uptake rate constant for amino acids
$k_{m,fa}$= specific Monod maximum uptake rate constant for fatty acids
$k_{m,su}$= specific Monod maximum uptake rate constant for sugars
K_m= half-saturation coefficient for VFA
k_{max}= maximum specific substrate uptake utilization rate constant for stored particulate substrate
K_n= half-saturation coefficient for ammonia nitrogen
K_{NH4-N}= saturation coefficient for ammonia nitrogen
K_{NO}= saturation coefficient for nitrate
K_{NO3}= half-saturation coefficient for nitrate
k_o= saturation coefficient for dissolved oxygen
k_{O2}= half-saturation coefficient for dissolved oxygen
K_p=saturation coefficient for phosphorus species
K_s= Monod half-saturation constant
k_x= saturation coefficient for particulate COD
LCFA = Long-chain fatty acids
ML= Mixed liquor sludge
nbpCOD = non-biodegradable particulate COD
nbVSS = non-biodegradable VSS
NH3 = Ammonia
NH3-N= Ammonia N
NO3N= nitrate concentration
Nos = soluble biodegradable organic nitrogen
NOS = Soluble organic nitrogen
OHO = Ordinary heterotrophic organism
PHA = poly-hydroxy-alkanoates
pH_{LL}= lower pH limit
pH_{UL}= upper pH limit
PO4P = phosphate
PS = primary sludge
q_{fe}= maximum rate for fermentation
r_{aa}= rate of amino acids uptake
rbCOD = readily biodegradable COD
$r_{d,e}$= denaturation reaction rate
r_{dis}= rate of disintegration
r_{fa}= rate of fatty acids uptake
r_{fe}= rate of fermentation
R_h = Hydraulic retention time
$R_{hydr,an}$= rate of anaerobic hydrolysis
$r_{hydr,ch}$= rate of carbohydrate hydrolysis

$r_{hydr,li}$= rate of lipids hydrolysis
$r_{hydr,p}$= rate of particulate hydrolysis
$r_{hydr,pr}$= rate of protein hydrolysis
r_{hydr}= rate of hydrolysis
r_{su}= rate of sugars uptake
$r_{x,a}$= reaction rate for acidogenic biomass growth
$r_{x,m}$= reaction rate for methanogenic biomass growth
$r_{xh,growth}$= rate of heterotrophic growth
S_A= fermentation products, acetate
S_{aa}= amino acids concentration
S_{ALK}= Alkalinity concentration
Sbp = biodegradable particulate substrate (as COD)
Sbpi = initial Sbp
Sbsa = Acetic acid
Sbsc = Soluble (readily) biodegradable COD
Sbsp = Propionic acid
S_f= fermentable, readily biodegradable substrates
S_{fa}= fatty acids concentration
S_{NH4-N}= ammonia nitrogen concentration
S_{NO3}= nitrate concentration
S_{O2}= dissolved oxygen concentration
S_{PO4}= inorganic soluble phosphorus, primarily ortho-phosphates
SRT = Solids Retention Time
SS = Suspended solids
S_{su}= Sugar concentration
TCODi = Total COD influent
TKN = Total Kjeldahl Nitrogen
TSS = Total Suspended Solids
u_h= maximum growth rate on substrate of heterotrophic organisms
$u_{max,a}$= maximum specific growth rate for acidogens
VFA = Volatile fatty acids
VFA'_{ovo}= initial concentration mg of VFA as COD per mg of initial VSS
VFA'_{pvo}= potential in mg of VFA as COD per mg of initial VSS
VFA'_{tvo}= concentration in mg of VFA as COD per mg of initial VSS at any time t
VSS = Volatile Suspended Solids
WAS = Waste activated sludge
WWTP = Wastewater treatment plant
X_{aa}= amino acids degraders
X_{ch}= carbohydrate concentration
$X_{composite}$= composite waste material

X_{fa}= Long chain fatty acid degraders
X_h= heterotrophic organisms
X_{li}= lipids concentration
X_{ON}= particulate biodegradable organic nitrogen
X_{OP}= particulate biodegradable organic phosphorus
X_{pr}= protein concentration
X_s= slowly biodegradable substrates
X_{sc}= slowly biodegradable COD (Colloidal)
X_{sp}= slowly biodegradable COD (particulate)
X_{su}= sugar degraders
Y_a= acidogenic biomass yield
$Y_{E/X}$= Enzyme yield
Y_e= yield for hydrolytic enzymes on insoluble or soluble substrate
Z_{ad}= acidogenic biomass concentration
Z_{bh}= heterotrophic biomass concentration
Z_{bp}= PAO organisms
α_Q = Enzyme half-saturation constant
η_{fe}= correction factor for anaerobic hydrolysis